

MODELING OF LINEAR INDUCTION MACHINES  
FOR ANALYSIS AND CONTROL

by

Armando José Sinisterra

A Thesis Submitted to the Faculty of  
The College of Engineering and Computer Science  
in Partial Fulfillment of the Requirements for the Degree of  
Master of Science

Florida Atlantic University

Boca Raton, Florida

April 2011

MODELING OF LINEAR INDUCTION MACHINES  
FOR ANALYSIS AND CONTROL

by

Armando José Sinisterra

This thesis was prepared under the direction of the candidate's thesis advisors, Dr. Manhar Dhanak, Department of Ocean and Mechanical Engineering and Dr. Nikolaos Xiros, Virginia Tech, and has been approved by the members of his supervisory committee. It was submitted to the faculty of the College of Engineering and Computer Science and was accepted in partial fulfillment of the requirements for the degree of Master of Science.

SUPERVISORY COMMITTEE:

  
Manhar Dhanak, Ph.D.

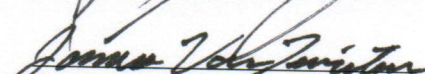
Thesis Co-Advisor



Nikolaos Xiros, Ph.D.

Thesis Co-Advisor

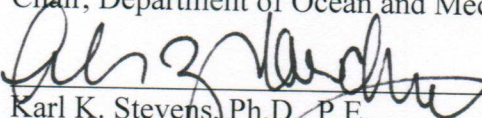
  
Pierre-Philippe Beaujean, Ph.D.

  
James VanZwieten, Ph.D.



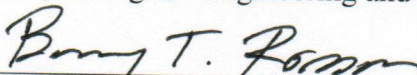
Mohammad Ilyas, Ph.D.

Chair, Department of Ocean and Mechanical Engineering



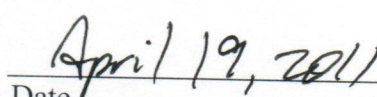
Karl K. Stevens, Ph.D., P.E.

Dean, College of Engineering and Computer Science



Barry T. Rosson, Ph.D.

Dean, Graduate College

  
Date

## ACKNOWLEDGEMENTS

The author wishes to express his most profound gratitude and appreciation to God for giving him the strength in difficult times; to his parents Teresita Molina and Gustavo Sinisterra and his sister Maria Mercedes Sinisterra for their unconditional love and support; to Julian Guerra, Dimitrios Psarrou, and all of his friends from the AUV Lab for their friendship and for helping him so many times; to Dr. Nikolaos Xiros for giving him the opportunity to work on this project; to Mr. William Laing and all the people of the Center for Ocean Energy Technology for their support and kindness; and to the love of his life, Lina Fernanda Garcia, for becoming just that and much more.

## ABSTRACT

Author: Armando José Sinisterra  
Title: Modeling of Linear Induction Machines for Analysis and Control  
Institution: Florida Atlantic University  
Thesis Advisor: Dr. Manhar Dhanak and Dr. Nikolaos Xiros  
Degree: Master of Science  
Year: 2011

In this thesis, the analysis of the dynamic response of a Linear Induction Motor as an electromechanical system is done, accounting for all the governing equations implied in the process which are used to develop the corresponding simulation models. Once this model is presented, a feedback control system is implemented in order to analyze the controlled response of the motor, considering the applications and conditions analogue to aircraft launcher systems. Also a comparison between the Linear and Rotary induction motors describing the differences, similarities and equivalences will be developed.

MODELING OF LINEAR INDUCTION MACHINES  
FOR ANALYSIS AND CONTROL

LIST OF TABLES.....	vii
TABLE OF FIGURES.....	ix
1 INTRODUCTION .....	1
2 PROBLEM STATEMENT.....	4
3 LITERATURE REVIEW .....	5
3.1 Overview.....	5
3.2 The Equivalent Circuit of a Real Transformer .....	6
3.3 The Equivalent Circuit of a Rotary Induction Motor.....	8
3.4 Linear Induction Motor (LIM).....	9
4 LIM EQUIVALENT CIRCUIT ANALYSIS.....	18
4.1 Overview.....	18
4.2 Dynamic Analysis and State-Space Equation.....	18
4.3 Equivalence Analysis of the Corresponding Parameters Between LIM and RIM.....	21
5 DYNAMIC ANALYSIS AND MATLAB SIMULATION FOR A LIM .....	29
5.1 Overview.....	29
5.2 Simulation of a LIM with a Constant Velocity of the Rotor. ....	30
5.3 Simulation of a LIM with a Linear Velocity of the Rotor. ....	32
5.4 Setting the Desired Thrust by Using Lookup Tables.....	34
5.5 Analysis and Simulation of the LIM as an Electromechanical System .....	45
5.6 Setting the Desired Speed by Using Lookup Tables .....	52
5.7 Calibration of a PID Controller.....	60
5.8 PI Controller.....	64
6 METHODOLOGY AND PROCEDURES.....	74
6.1 Overview.....	74
6.2 Test Bench: General Specifications.....	74
6.3 Motor parameters identification.....	75
6.4 Actual Tests .....	79
6.5 Equivalences of Parameters between the actual RIM motor and a corresponding LIM.....	94
7 CONCLUSIONS.....	107

8	APPENDIXES .....	109
8.1	Matlab Script from Section 5.4.1, page 38 (interp3.m).....	109
8.2	Matlab Script from Section 6.4.3.3, page 93, (MotorParam.m and myfunk.m).....	110
8.3	TEST BENCH PROCEDURES .....	112
9	BIBLIOGRAPHY .....	138

## LIST OF TABLES

Table 4.1. Cases of analysis corresponding to different configurations of LIM. ....	27
Table 4.2. Approximated equivalent set of parameters of a RIM.....	28
Table 5.1. Parameters for simulation case 2. ....	31
Table 5.2. Values of $V_s$ , $V_r$ and $V_{ol}$ for which the thrust needs to be defined. ....	36
Table 5.3. Thrust for each combination $V_s$ , $V_r$ , $V_{ol}$ . ....	37
Table 5.4. Voltage amplitude for each combination $V_s$ , $V_r$ and $Th$ . ....	41
Table 5.5. System response verification by using 3D-Lookup table. ....	42
Table 5.6. Parameters and quantities for the LIM. ....	47
Table 5.7. Rotor speed values for each $f$ , $V_{ol}$ combination.....	54
Table 5.8. Ziegler-Nichols calibration parameters. ....	63
Table 6.1. General specifications for the motors in the Test Bench. ....	74
Table 6.2. General specifications for the controlling drives. ....	74
Table 6.3. Parameters obtained from CTSOft software.....	76
Table 6.4. Reactances proportions for the Locked Rotor Test. ....	79
Table 6.5. No-Load Tests measurements and results for the motor. ....	82
Table 6.6. No-Load Tests measurements and results for the generator. ....	83
Table 6.7. Values of inductance for the motor and the generator.....	85
Table 6.8. Measurements and results for the 15 Hz tests for three different loads on the motor. ....	88
Table 6.9. Measurements and results for the 15 Hz tests for five different loads on the generator. ....	88
Table 6.10. Physical parameters for the motor and the generator from the Test Bench..	89
Table 6.11. Variation of Thevenin quantities with the frequency for the actual RIM motor from the Test Bench. ....	97
Table 6.12. Equivalent LIM in steady state. ....	97

Table 6.13. . Equivalent LIM parameters. ....	99
Table 6.14. Actual RIM parameters.....	99
Table 6.15. Equivalent LIM (new model). ....	102
Table 6.16. Previous model . ....	102
Table 8.1. Serial mode. ....	118
Table 8.2. Serial Mode parameters. ....	118
Table 8.3. Serial communication baud rate. ....	119
Table 8.4. Serial communications address.....	119
Table 8.5. Estimated motor speed.....	122
Table 8.6. Motor speed. ....	123
Table 8.7. Drive output frequency. ....	123
Table 8.8. Drive encoder position.....	123
Table 8.9. Number of motor poles. ....	124
Table 8.10. Motor rated power factor. ....	125
Table 8.11. Encoder phase angle. ....	126
Table 8.12. Motor rated voltage.....	127
Table 8.13. Motor rated full load speed (RPM).....	127
Table 8.14. Motor rated current. ....	128
Table 8.15. Rated frequency. ....	129
Table 8.16. Operating mode selector. ....	129
Table 8.17. Operating mode selector settings.....	129
Table 8.18. Min. connection requirements for each control mode. ....	130
Table 8.19. Min. connection requirements for each mode of operation. ....	130
Table 8.20. Autotune.....	131
Table 8.21. Minimum reference clamp.....	134
Table 8.22. Maximum reference clamp. ....	134
Table 8.23. Catch a spinning motor. ....	135
Table 8.24. Catch a spinning motor settings.....	135
Table 8.25. Rated rpm autotune.....	136

## TABLE OF FIGURES

Figure 3.1. Per-phase Equivalent Circuit of a Real Transformer. ....	6
Figure 3.2. Per-phase Equivalent Circuit of a Rotary Induction Motor.....	8
Figure 3.3. representation of a single-sided Linear Induction Motor (SLIM). ....	10
Figure 3.4. Side view of a Linear Induction Motor (LIM). ....	11
Figure 3.5. Distribution of effective MMF at velocity $> 0$ (Duncan, 1983). ....	13
Figure 3.6. Per-phase Equivalent circuit of a Linear Induction Motor (LIM). ....	15
Figure 3.7. Vertical (transverse) forces and thrust on a LIM. ....	17
Figure 4.1. Per-phase Equivalent Circuit of a Rotary Induction Motor.....	21
Figure 4.2. Per-phase Equivalent circuits for a LIM (up) and a RIM (down) in steady- state. ....	22
Figure 5.1. Simulink model for simulation case 1: constant velocity of the rotor.....	31
Figure 5.2. From top to bottom: primary current ( $I_1$ ), secondary current ( $I_2$ ) and thrust (Th). ....	31
Figure 5.3. Simulink model for simulation case 2: linear velocity of the rotor. ....	32
Figure 5.4. From top to bottom: primary current ( $I_1$ ), secondary current ( $I_2$ ) and thrust (Th). ....	33
Figure 5.5 Simulink model: Setting the desired thrust using Lookup tables.....	35
Figure 5.6. Thrust matrix with dimensions $5 \times 5 \times 5$ . ....	39
Figure 5.7. Voltage amplitude matrix with dimensions $5 \times 5 \times 5$ . ....	40
Figure 5.8. 3-D Lookup Table Simulink block with.....	42
Figure 5.9. Actual RMS value of Thrust for a reference thrust of 360.7 N. ....	43
Figure 5.10. Actual RMS value of Thrust for a reference thrust of 550 N. ....	43
Figure 5.11. Actual RMS value of Thrust for a reference thrust of 1200 N. ....	43
Figure 5.12. Actual RMS value of Thrust for a reference thrust of 1800 N. ....	44
Figure 5.13. Actual RMS value of Thrust for a reference thrust of 2254 N. ....	44

Figure 5.14. Simulink Model for the Electromechanical System .....	46
Figure 5.15. Stator and rotor currents response in time of the LIM. ....	49
Figure 5.16. Thrust response in time of the LIM.....	50
Figure 5.17. Acceleration, speed and position response in time, of the rotor.....	51
Figure 5.18. Mean thrust Versus rotor speed response of the LIM. ....	52
Figure 5.19. Simulink Model of the LIM Using Lookup Tables to Set a Desired Rotor Speed.....	53
Figure 5.20. Frequency demultiplexer block. ....	55
Figure 5.21. Voltage amplitude, demultiplexer block. ....	56
Figure 5.22. Stator and rotor currents response using Lookup Tables. ....	57
Figure 5.23. Thrust response in time of the LIM using Lookup Tables. ....	58
Figure 5.24. Acceleration, speed and position response of the rotor.....	59
Figure 5.25. Mean thrust Versus rotor speed response of the LIM using Lookup Tables. .....	59
Figure 5.26. Conceptual diagram of the control system. ....	62
Figure 5.27. Simulink Model of the LIM Using Lookup Tables and PID Controller ...	64
Figure 5.28. From top to bottom: Vr (Zoomed), Disturbance, PI response, Freq. response, Error. ....	65
Figure 5.29. Rotor speed (Vr) Vs Time. ....	66
Figure 5.30. PI Controller response. ....	67
Figure 5.31. Error between the referenced Vr and the actual Vr. ....	67
Figure 5.32. From top to bottom: Acceleration, speed and position of the rotor.....	68
Figure 5.33. From top to bottom: Stator and rotor currents.....	69
Figure 5.34. From top to bottom: Vr, Disturbance, PI response, Frequency response, and Error .....	70
Figure 5.35. Rotor speed Vr (Zoomed).....	70
Figure 5.36. PI Controller response. ....	71
Figure 5.37. Error between the referenced Vr and the actual Vr. ....	72
Figure 5.38. From top to bottom: Acceleration, speed and position of the rotor.....	72
Figure 5.39. From top to bottom: Stator and rotor currents.....	73

Figure 6.1. Per phase equivalent circuit of an induction motor. ....	76
Figure 6.2. Equivalent circuit for No-Load Test.....	77
Figure 6.3. Equivalent circuit for Locked Rotor Test.....	78
Figure 6.4. Transient Inductance parameter stored in the motor's drive. ....	84
Figure 6.5. RIM's per phase equivalent circuit.....	85
Figure 6.6. No-Load Test simplify circuit. ....	89
Figure 6.7. Test Bench configuration. ....	91
Figure 6.8. CTSOft interface, Menu 4: Torque and Current control. ....	91
Figure 6.9. Per-phase Equivalent circuits for a LIM (up) and a RIM (down). ....	95
Figure 6.10. Variation of the magnetic inductance ( $L_m$ ) with the frequency for Table 6.11.....	97
Figure 6.11. CTSOft parameters interface. Information for Table 6.8, Load=18.3 lb-in.98	
Figure 6.12. RIM simulation model for the actual motor of the Test Bench in steady state. ....	100
Figure 6.13. Simulation model for the equivalent LIM motor in steady state.....	100
Figure 6.14. RMS stator and rotor currents responses for the actual RIM. ....	101
Figure 6.15. RMS stator and rotor currents responses for the equivalent LIM. ....	101
Figure 6.16. From top to bottom: Acceleration, speed and position of the rotor.....	103
Figure 6.17. From top to bottom: Acceleration, speed and distance responses of the previous model.....	104
Figure 6.18. Thrust Vs Rotor speed of the equivalent LIM (new model). ....	105
Figure 6.19. Thrust Vs Rotor speed of previous model.....	105
Figure 8.1. Unidrive Display. ....	116
Figure 8.2. Flow chart of Unidrive menus.....	117
Figure 8.3. CTSOft interface. ....	122

## 1 INTRODUCTION

The history of Linear Induction Motors (LIM) started since 19<sup>th</sup> century, just a few years later after the discovery of the Rotary Induction Motor (RIM) principle, which is going to serve as the platform to understand the general concepts and operation of LIM's discussed in the sequel.

In general terms, the operation of a RIM is defined by the interaction of two main parts: the stator (or primary) and the rotor (also called secondary). The stator consists on a cylindrical slotted structure formed by a stack of steel laminations. Within the slots of the stator the polyphase windings are laid uniformly to produce a rotating sinusoidally distributed magnetic field at a speed depending on the frequency of the network and the number of poles. The relative motion between the rotating magnetic field and the conductors of the rotor, induces a voltage in the rotor producing currents flowing through the conductors which also generates its own magnetic field. The interaction (chasing) of these two magnetic fields will produce an electromagnetic torque that drags the rotor in the same direction of the magnetic fields.

From the RIM principle, the operation of the LIM can be explained if one imagines the cylindrical slotted structure and the rotor to cut open and rolled flat causing the magnetic fields to travel in a rectilinear direction instead of rotating. The primary field now

interacts with the secondary (also called secondary sheet) conductor, like an aluminum sheet, and produces a rectilinear force or thrust.

In the conceptual description of the LIM operation one can notice the similarities with the RIM. However, contrary to the RIM, the LIM has a beginning (leading edge) and an end(trailing edge). This specific characteristic of the LIM produces the so called “end effects” that adversely influences in its performance and are basically a field distortion at the entry and exit of the mobile part which can be the stator or the secondary sheet instead.

In need of an equivalent circuit that describes easily and reliably the response of a LIM, just like the one used in the RIM, many authors have studied the implications of these end effects and have proposed some models in this regard, like the one from J. Duncan (Duncan, 1983) which is the one used in this paper to developed the analysis and response of the system.

From among all the applications regarding LIM can be highlight such areas as: machine tools, material handling and storage, accelerators and launchers, low and medium speed trains, sliding doors operation, etc, and in general all kinds of operations in need of a rectilinear displacement with any particular characteristics, point at which the controllability of the system becomes important in some level depending on the application.

One motivation for this thesis is to implement a feedback control system considering the applications and conditions analogue to aircraft launcher systems. The transition to

Electromagnetic Aircraft Launch System (EMALS) will overcome certain deficiencies of actual steam catapult systems such as the large size, difficulty to maintain and limited control capabilities. These shortcomings are translated in non-uniform accelerations that induce overstresses upon the structure of the aircraft. Furthermore, faster aircraft requirement exceeds the capability of steam catapults.

This thesis focuses on three main points:

- Equivalences of the electrical parameters between RIM and LIM with their corresponding analysis and validation.
- Analysis, modeling and simulation of the dynamic response of the LIM as an electromechanical system.
- And finally, a PI control implementation that regulates the power source of the system in terms of the frequency and voltage amplitude, allowing the LIM to overcome to certain disturbing forces or changes in the desired speed reference.

## 2 PROBLEM STATEMENT

Regarding the general similarities between RIMs and LIMs, one of the objectives of this thesis is to establish an equivalence of the electrical parameters between them in order to predict the dynamics of the electrical response on both systems. At this point the question about what criterion is needed and under what specific conditions this can be done arises.

When it comes to describe a Linear Induction Motor in terms of the general dynamic response, one have to picture the system as an interaction between an electrical and a mechanical subsystem, thus conceiving it as a whole electromechanical system, where governing differential equations for each phenomena must be taken into account. An attempt to develop a reliable simulation model that represents the LIM dynamics will take place in this thesis.

Once the dynamics of the LIM are represented through a simulation model, a first stage approach on the control of the electromechanical system will be developed by implementing a PI controller, in which all the particularities of this highly nonlinear system will show up by the presence of disturbing forces or changes in the speed reference, but they will be overcome.

## 3 LITERATURE REVIEW

### 3.1 Overview

To get a better understanding of the equivalent circuit of a Linear Induction Motor (LIM), a review of some important aspects about transformers and rotary induction motors will take place in order to identify important differences and similarities among each particular case.

The operation of a rotary induction motor is very similar to as a real transformer, in which the stator (primary) induces voltages and currents into the rotor (secondary). The differences are, first, that the terminals of the rotor are short circuited and the output of the motor is a mechanical power due to an interaction between the stator magnetic field ( $B_s$ ) and the rotor magnetic field ( $B_R$ ) that results from the induced current in it, while the terminals in the secondary of a transformer are connected to a load, and the output is indeed, the induced values of voltage and current, determined by the ratio ( $a$ ) of the number of turns of the primary ( $N_1$ ) to the secondary ( $N_2$ ). Similarly, in the case of an induction motor, these induced physical quantities also depend on an effective turns ratio ( $a_{eff}$ ) which for the case of a wound-rotor motor is the ratio of the conductors per phase on the stator to the conductors per phase on the rotor modified by any pitch and distribution factor differences; for a cage rotor is more complex to determine this ratio as there are no distinct windings, but still applies the concept. Another aspect to consider is

the high reluctance of the air gap in the induction motor that must be overcome with a high magnetizing current ( $I_M$ ) which is translated into a much smaller value of leakage reactance ( $X_M$ ) compared to a transformer. Finally, the primary difference is related to the effects of a varying rotor frequency on the rotor voltage of the motor ( $E_R$ ) and the rotor impedances  $R_R$  and  $jX_R$  which are going to have some implications in the equivalent per phase circuit of the rotary induction motor compared to the transformer equivalent circuit (Chapman, 1999).

### 3.2 The Equivalent Circuit of a Real Transformer

Figure 3.1, represents the equivalent circuit for a real transformer (Chapman, 1999). This model is basically an adaptation of certain physical phenomena taken into account, with the ideal transformer purpose.

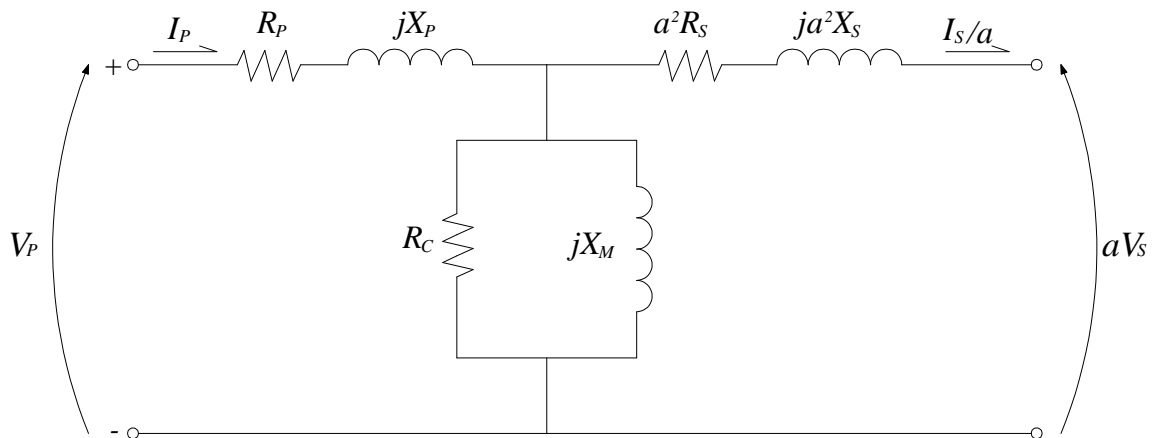


**Figure 3.1. Per-phase Equivalent Circuit of a Real Transformer.**

Where:

$V_P$ : is the phase voltage of the transformer.

$R_P$ : primary resistance.

$X_P$ : primary leakage reactance.

$R_C$  and  $X_M$ : represent the core losses of the system.

$a^2R_S$ : secondary resistance referred to the primary.

$a^2X_S$ : secondary leakage reactance referred to the primary.

### 3.2.1 Losses in a Real Transformer

- Copper losses ( $I^2R$ ). Represented by  $R_P$  and  $R_S$ , are the resistive heating losses in the primary and secondary windings of the transformer.
- Core excitation effects. Eddy current losses, caused when a time changing flux induces a voltage in the core the same way as it would in a wire wrapped around it, causing swirls of current flowing within the core known as eddy currents. As these currents are flowing in a resistive material (the iron core), energy is dissipated by heating the iron core. Hysteresis losses, associated with the rearrangement of the magnetic domains for each half cycle in the core. These core excitation effects are modeled by a magnetization current  $i_m$  proportional to the voltage applied to the core, lagging the applied voltage by  $90^\circ$ , so it can be modeled by a reactance  $X_M$  connected across the primary voltage source. Core-loss current  $i_{h+e}$  (h for hysteresis, e for eddy currents), represented by  $R_C$ , is a current proportional to the voltage applied to the core that is in phase with it. These losses are resistive heating losses in the core of the transformer and are proportional to the square of the voltage applied to the transformer.

- Leakage flux. The fluxes  $\Phi_{LP}$  and  $\Phi_{LS}$  escape the core and pass through only one of the transformer windings. These are leakage fluxes, that generate self inductance in both coils, and are represented by primary and secondary inductors ( $L_P$  and  $L_S$  or reactances  $X_P$  and  $X_S$ ).

### 3.3 The Equivalent Circuit of a Rotary Induction Motor

After taking into account the effects of varying speed over the impedance term in the rotor (represented by the slip  $s$ ), and referring the rotor circuit to the stator side, by means of the effective turns ratio  $a_{eff}$ , and also from a previous knowledge of transformers, it can be derive the equivalent circuit for rotary induction motors, as shown in Figure 3.2 (Chapman, 1999).

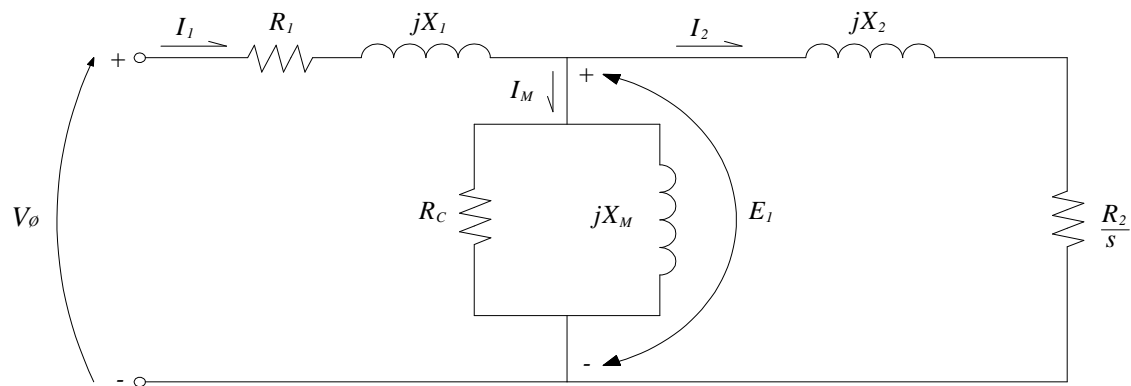


**Figure 3.2. Per-phase Equivalent Circuit of a Rotary Induction Motor.**

Where:

$V_\phi$ : is the phase voltage of the induction motor.

$R_1$ : stator resistance.

$X_1$ : Stator leakage reactance.

$R_c$  and  $X_M$ : representing once again the core losses of the system, accounting for the high reluctance of the air gap.

$R_2$ : rotor resistance referred to the stator.

$X_2$ : Rotor leakage reactance referred to the stator.

### 3.3.1 Losses in a Rotary Induction Motor

As in real transformers, the first losses are  $I^2R$  losses in the stator windings (stator copper loss  $P_{SCL}$ ). Then, some of the losses are due to hysteresis and eddy currents effects in the iron core of the stator ( $P_{core}$ ). The remaining power is transferred to the rotor across the air gap between the stator and the rotor, called the air gap power ( $P_{AG}$ ). Then there is some small amount of power loss  $I^2R$  in the windings of the rotor (rotor copper loss  $P_{RCL}$ ), and the rest is converted to mechanical power ( $P_{conv}$ ). At this stage, some mechanical losses like friction and windage losses ( $P_{F\&W}$ ) and stray losses ( $P_{misc}$ ) take place and must be subtracted to finally consider the remaining power as the output power ( $P_{out}$ ) of the motor (Chapman, 1999).

### 3.4 Linear Induction Motor (LIM)

The primary of a Linear Induction Motor (LIM), is basically the stator of a rotary induction motor cut open and rolled flat, so the currents in it generate a translational magnetic field (as opposed to the rotational trajectory of the stator magnetic field of a rotary induction motor). The secondary is a sheet conductor with a back iron return path for the magnetic flux (Duncan, 1983). This would be the configuration for a single-sided LIM or simply SLIM, as Figure 3.3 illustrates (Nowak, 2001). If instead, the back iron is

replaced by a gap and a second stator (primary), the configuration corresponds to a double-sided LIM or DSLIM.

Both of them are equivalent and the results describe next apply for either of them.

### 3.4.1 Performance Model Approach for the Establishment of the Equivalent Circuit

In need of an equivalent circuit that describes easily and reliably the response of a LIM, just like the one used in the per-phase circuit of a rotary induction motor (RIM), J. Duncan proposed a model in which the equivalent circuit of a RIM is modified to account for the “end effects” and is used to predict the output thrust as well as vertical forces and couples.

Before introducing the equivalent circuit for a LIM, a brief description about the “end effects” is going to take place for a better understanding of the system. At the end, as one shall see, the equivalent circuit for a LIM is going to be basically a modification of the equivalent circuit for a rotary induction motor accounting for these effects. Figure 3.4 illustrates the configuration and some important aspects related to the end effects of this machine.

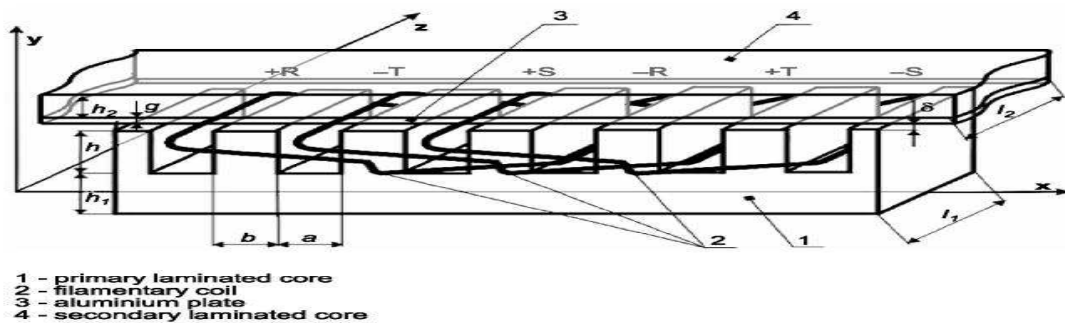
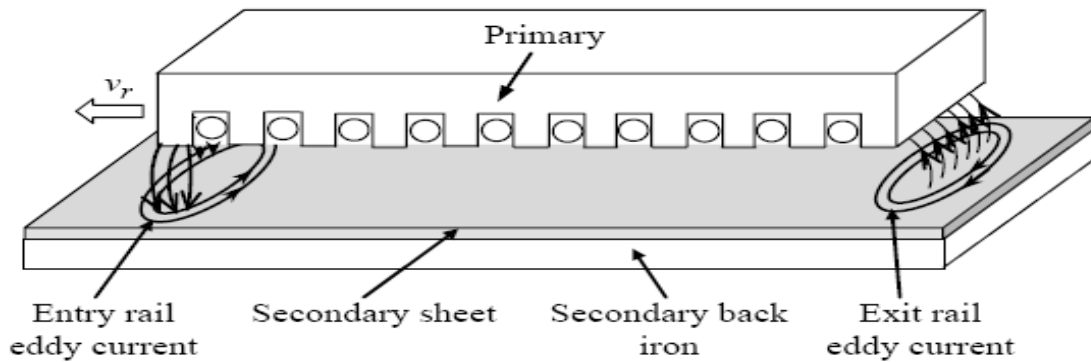


Figure 3.3. representation of a single-sided Linear Induction Motor (SLIM).

Figure 3.4, shows the end effects as the primary moves to the left, and is feed by 3-phase currents which produce a sinusoidal MMF per unit length and a sinusoidal flux density, which are implemented as RMS values, thus accounting as uniform values for the analysis (Boucheta, 2010). As the primary moves, new material (in the secondary) enters in the leading edge of the motor where eddy currents rise to their maximum value , and also reduce the flux density to zero, but start growing progressively with a time constant  $T_2$  as the eddy currents fade away.  $T_2$  is defined as follows:

$$T_2 = \frac{(L_m + L_{21})}{R_{21}} \quad (3.1)$$



**Figure 3.4. Side view of a Linear Induction Motor (LIM).**

$T_2$ , also called the total secondary time constant, is the time constant in which eddy currents will decay in the rail after it enters into the primary.

On the other hand, Figure 3.4 also illustrates some important facts related to the exit of material (secondary) from the primary. As no MMF from the primary is seen by the rail, eddy currents will emerge in it in order to maintain the airgap flux, but these will decay very rapidly with a time constant related to the leakage inductance of the rail.

J. Duncan represents these transient end effects of the motor in Figure 3.5 .

Where:

$$Q = \frac{DR_{21}}{(L_m + L_{21})v_r} \quad (3.2)$$

Q, represents the length of the motor on the normalized scale (by T<sub>2</sub>).

i<sub>me</sub>: effective magnetizing current per unit length, is the distribution of the MMF per unit length along the motor length. The average value is I<sub>mea</sub>.

i<sub>2e</sub>: eddy current per unit length. Appears like a negative MMF when referred to the primary. The average value is I<sub>2ea</sub>.

Now, the next step is to quantify and represent these end effects into the per phase equivalent circuit of a LIM. According to J. Duncan , these parameters are:

- At the entry section of the primary, the demagnetizing effect of eddy currents, represented as an inductor in parallel with L<sub>m</sub>, driving the current I<sub>2ea</sub> with an inductance value equivalent to the loss of excitation produced by I<sub>2ea</sub> over the motor length:

$$L_m \frac{I_{mea}}{I_{2ea}} = L_m \left\{ \frac{Q}{1 - e^{-Q}} - 1 \right\} \quad (3.3)$$

And solving the parallel with L<sub>m</sub>,

$$L_m \left\{ 1 - \frac{1 - e^{-Q}}{Q} \right\} \quad (3.4)$$

driving the current I<sub>m</sub> = I<sub>mea</sub> + I<sub>2ea</sub>.

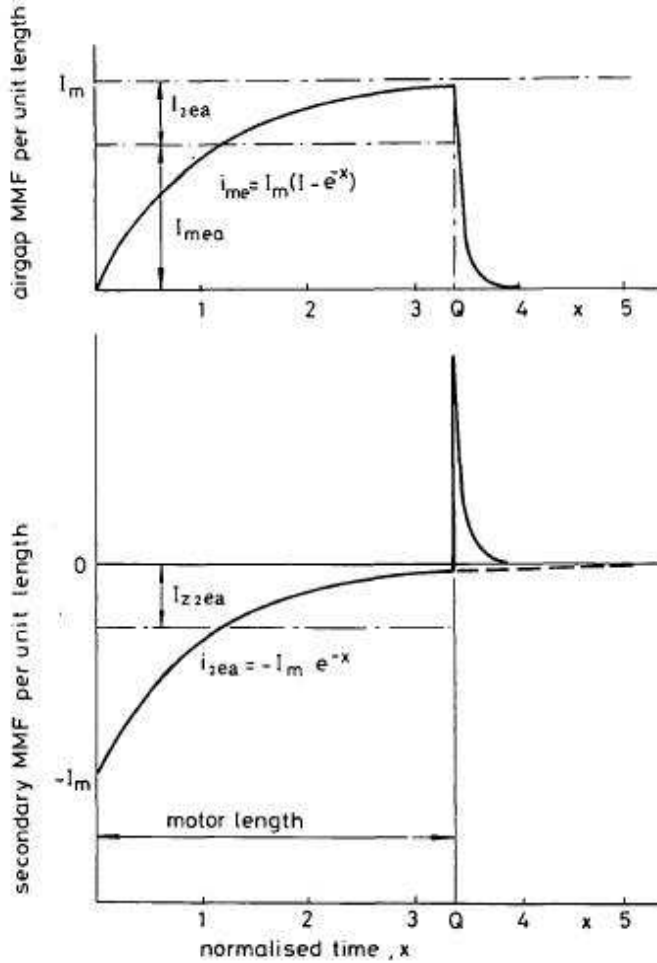


Figure 3.5. Distribution of effective MMF at velocity  $> 0$  (Duncan, 1983).

- Ohmic losses due to eddy currents for a resistance  $R_{21}$  of the circuit:

$$\text{Eddy current losses} = I_m^2 R_{21} \frac{1 - e^{-2Q}}{2Q} \quad (3.5)$$

applying for the section of rail under the primary.

As the motor passes the rail over, the MMF seen by the rail disappears and eddy currents will rise in order to maintain the gap flux, as depicted in Figure 3.4. The magnetic energy is

then dissipated in the ohmic resistance, and the power loss is defined by the following expression:

$$\text{Exit power loss} = I_m^2 R_{21} \frac{\{1 - e^{-\varrho}\}^2}{2Q} \quad (3.6)$$

And adding equations (3.5) and (3.6) the ohmic loss due to eddy currents is defined by:

$$\text{Total ohmic losses due to eddy currents in rail} = I_m^2 R_{21} \frac{\{1 - e^{-\varrho}\}}{Q} \quad (3.7)$$

These losses are represented in the equivalent circuit as a resistance in the magnetizing branch dependent on the value of Q :

$$R_{21} \frac{\{1 - e^{-\varrho}\}}{Q} \quad (3.8)$$

Thus, accounting for expressions (3.4) and (3.8) , and according to J. Duncan , Figure 3.6 represents the equivalent circuit of a linear induction motor (LIM):

Where:

**V<sub>1</sub>**: is the phase voltage of the Linear Induction Motor.

**R<sub>1</sub>**: primary resistance, indicates heating losses in the primary coils.

**L<sub>1</sub>**: Indicates leakage flux from the primary, which does not link with secondary.

**L<sub>M</sub>**: Represents the flux linking the primary and secondary

**R<sub>21</sub>**: secondary resistance referred to the primary, indicates heating losses in the secondary.

$L_{21}$ : Indicates leakage flux in the secondary, referred to the primary. For double sided LIM (DSLIM) there is no back iron, it is just the secondary sheet, thus  $L_2$  is negligible. In DSLIM, the back iron is replaced with another primary, however all the relations mentioned previously apply.

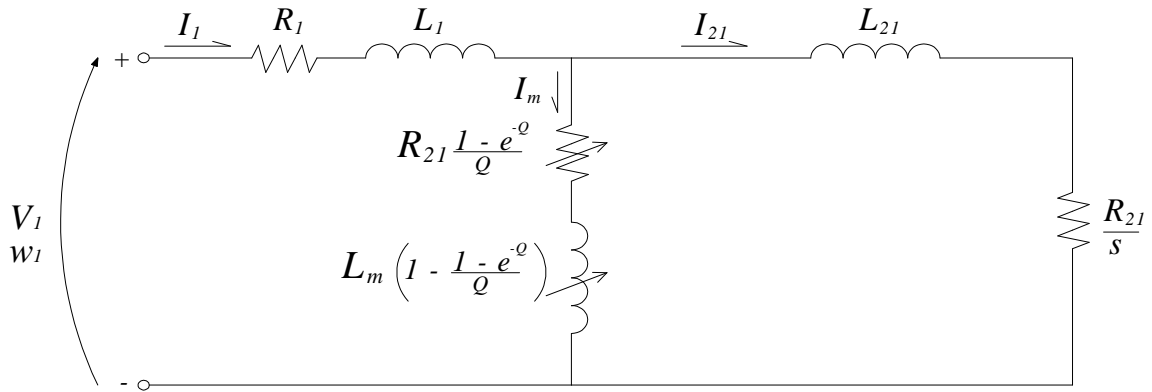


**Figure 3.6. Per-phase Equivalent circuit of a Linear Induction Motor (LIM).**

$$L_m \left\{ 1 - \frac{1 - e^{-q}}{Q} \right\} : \text{non-linear function that represents the resultant magnetizing flux in}$$

the air gap.

$$R_{21} \frac{\{1 - e^{-q}\}}{Q} : \text{non-linear function that represents the ohmic loss in the secondary due to}$$

eddy currents.

The J. Duncan model (recalling Figure 3.6) accounts for the forces and couples generated within a single sided linear induction motor (SLIM), that must be considered in the design of the structure of the motor. The vertical forces can be separated into two components and a turning couple. The first component is due to the attraction between

the back iron of the primary and the secondary, due to the main flux crossing the air gap and is defined as:

$$F_{va} = K_a L_m I_M^2 \left\{ 1 - \frac{(1 - \exp(-Q))(3 - \exp(-Q))}{2Q} \right\} \quad (3.9)$$

Where  $K_a$  is obtained from static tests and includes the factor 3 to convert from single to three phase.

The second component accounts for the repulsive force between the secondary slip current  $I_{21}$  and its reflected current in the primary winding and is defined as:

$$F_{vr} = K_r \frac{I_{21}^2}{d} \quad (3.10)$$

Where  $K_r$  is obtained from static tests and includes the factor 3 to convert from single to three phase, and  $d$  is the distance between the midpoints of the primary and secondary current layers.

However, in a Double Sided Linear Induction Motor (DSLIM), the effects of the vertical forces canceled each other.

The turning moment is the one generated by the attractive forces and is the one that produces the “bow wave” effect lowering the trailing edge of the motor with respect to the leading edge as the speed increases. This turning couple  $C$  is defined as:

$$C = (M / Q - 0.5) D F_{va} \quad (3.11)$$

Where  $M$  is the effective distance of the centroid of the area from the origin, and is defined as:

$$M = \frac{0.5Q^2 + 2(Q+1)\exp(-Q) - (0.5Q + 0.25)\exp(-2Q) - 1.75}{Q + 2\exp(-Q) - 0.5\exp(-2Q) - 1.5} \quad (3.12)$$

On the other hand, J. Duncan defines the total thrust of the motor as the one generated by the slip currents minus the one due to eddy currents, show as follows:

Motor thrust due to slip currents:

$$3I_{21}^2 R_{21} \frac{\pi}{\omega_2 \tau} N \quad (3.13)$$

Motor thrust due to eddy currents:

$$3I_M^2 R_{21} \frac{1 - \exp(-Q)}{vQ} N \quad (3.14)$$

Where:

$\tau$ : motor pole pitch.

$\omega_2$ : slip frequency.

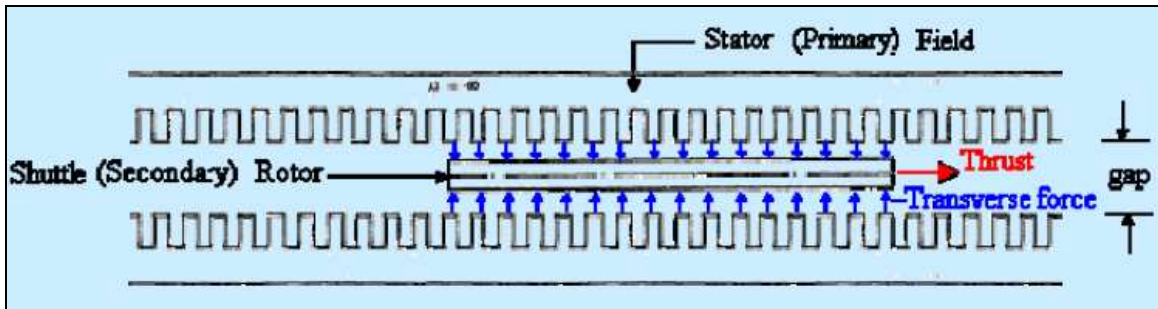


Figure 3.7. Vertical (transverse) forces and thrust on a LIM.

## 4 LIM EQUIVALENT CIRCUIT ANALYSIS

### 4.1 Overview

Next, a dynamic analysis is going to take place for the equivalent circuit model of the LIM, establishing the state-space equation for a better implementation in further control analysis.

### 4.2 Dynamic Analysis and State-Space Equation

Before applying the Kirchhoff's voltages and currents laws for the circuit it will be summarized some important relations for convenience:

From equation (3.2) we recall the parameter  $Q$  which represents the length of the motor on the normalized scale:

$$Q = \frac{DR_{21}}{(L_m + L_{21})v_r} \quad (3.2)$$

It will also be defined the function  $f(Q)$  as follows:

$$f(Q) = \frac{1 - e^{-Q}}{Q} \quad (4.1)$$

Doing so, and applying Kirchhoff's laws on the equivalent circuit shown in Figure 3.6 led into the following expressions:

$$V_1 = I_1 R_1 + L_1 \frac{dI_1}{dt} + (I_1 - I_{21}) R_{21} f(Q) + \frac{d}{dt} [L_m (1 - f(Q))(I_1 - I_{21})] \quad (4.2)$$

$$0 = L_2 \frac{dI_{21}}{dt} + I_{21} \frac{R_{21}}{s} + (I_{21} - I_1) R_{21} f(Q) + \frac{d}{dt} [L_m (1 - f(Q))(I_{21} - I_1)] \quad (4.3)$$

$$I_1 = I_{21} + I_m \quad (4.4)$$

Considering the derivatives of Q and f(Q):

$$\frac{dQ}{dt} = -\frac{Q}{v_r} \frac{dv_r}{dt} \quad (4.5)$$

$$\frac{df(Q)}{dt} = \frac{1}{v_r} \frac{dv_r}{dt} (f(Q) - e^{-Q}) \quad (4.6)$$

Solving the system of equations conduces to the next expressions:

$$\begin{aligned} [L_1 + L_m (1 - f(Q))] \frac{dI_1}{dt} - L_m [1 - f(Q)] \frac{dI_{21}}{dt} = V_1 - I_1 \left[ R_1 + R_{21} f(Q) - L_m \frac{df(Q)}{dt} \right] + \\ + I_{21} \left[ R_{21} f(Q) - L_m \frac{df(Q)}{dt} \right] \end{aligned} \quad (4.7)$$

$$-L_m [1 - f(Q)] \frac{dI_1}{dt} + [L_{21} + L_m (1 - f(Q))] \frac{dI_{21}}{dt} = I_1 R_{21} f(Q) - I_{21} \left[ R_{21} f(Q) + \frac{R_{21}}{s} \right] \quad (4.8)$$

Where  $s$  accounts for the slip and is defined as:

$$s = \frac{v_s - v_r}{v_s} \quad (4.9)$$

$v_s$  : synchronous speed.

$$v_s = \frac{2\omega R}{p} = 2f\tau \quad (4.10)$$

$R$ : radius of the rotary induction machine (RIM). As  $v_s$  cannot depend on a non-existing radius, expression at the right of equation (4.10) come up, where:

$\tau$  : Distance between two adjacent poles in the LIM.

$v_r$ : velocity of the rotor.

Equations (4.7) and (4.8) are considered in its state space form as follows:

$$\frac{d}{dt} [I_1, I_{21}]^T = A(t) \cdot \vec{u}(t) \quad (4.11)$$

Where:

$$A(t) = \frac{1}{L_1 L_{21} + L_m (L_1 + L_2) [1 - f(Q)]} \begin{bmatrix} L_m [1 - f(Q)] + L_2 & L_m [1 - f(Q)] \\ L_m [1 - f(Q)] & L_m [1 - f(Q)] + L_1 \end{bmatrix} \quad (4.12)$$

$$\vec{u}(t) = \begin{bmatrix} V_1 - I_1 \left[ R_1 + R_{21} f(Q) - L_m \frac{df(Q)}{dt} \right] + I_{21} \left[ R_2 f(Q) - L_m \frac{df(Q)}{dt} \right] \\ I_1 R_{21} f(Q) - I_{21} \left[ R_2 f(Q) + \frac{R_2}{s} \right] \end{bmatrix} \quad (4.13)$$

The same approach is used to developed the dynamics for the per phase equivalent circuit of a RIM (Figure 4.1), which is going to be used in simulation models in order to verify the equivalence between LIM and a RIM in terms of its parameters.

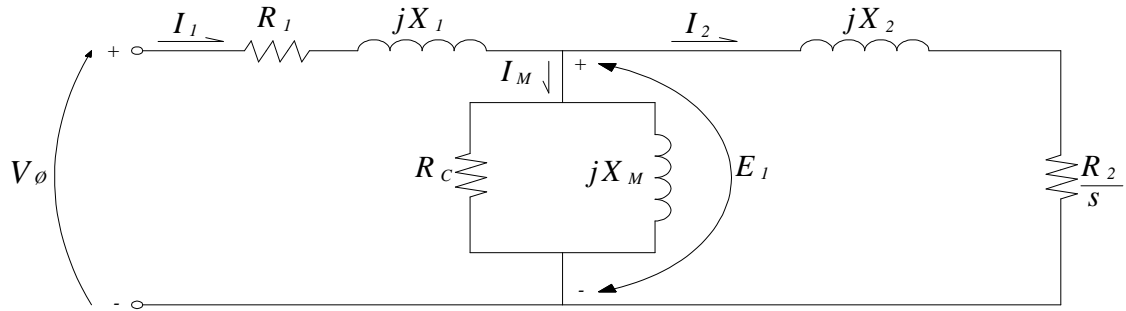


**Figure 4.1. Per-phase Equivalent Circuit of a Rotary Induction Motor.**

Applying Kirchhoff's laws let into the following expressions:

$$V_{\phi} = L_1 \frac{dI_1}{dt} + I_1 R_1 + \frac{d}{dt} (I_1 - I_2) L_M \quad (4.14)$$

$$0 = \frac{d}{dt} (I_2 - I_1) L_M + \frac{dI_2}{dt} L_2 + I_2 \frac{R_2}{s} \quad (4.15)$$

#### 4.3 Equivalence Analysis of the Corresponding Parameters Between LIM and RIM.

In this section an attempt to determine an equivalence between the corresponding parameters of LIM and RIM motors is going to be made for simulation purposes from an actual RIM in steady-state. Basically, for a special configuration of LIM an equivalent RIM set of parameters is going to be established.

Recalling the equivalent per-phase circuits for a RIM and a LIM, Figure 4.2 shows once again their configuration.

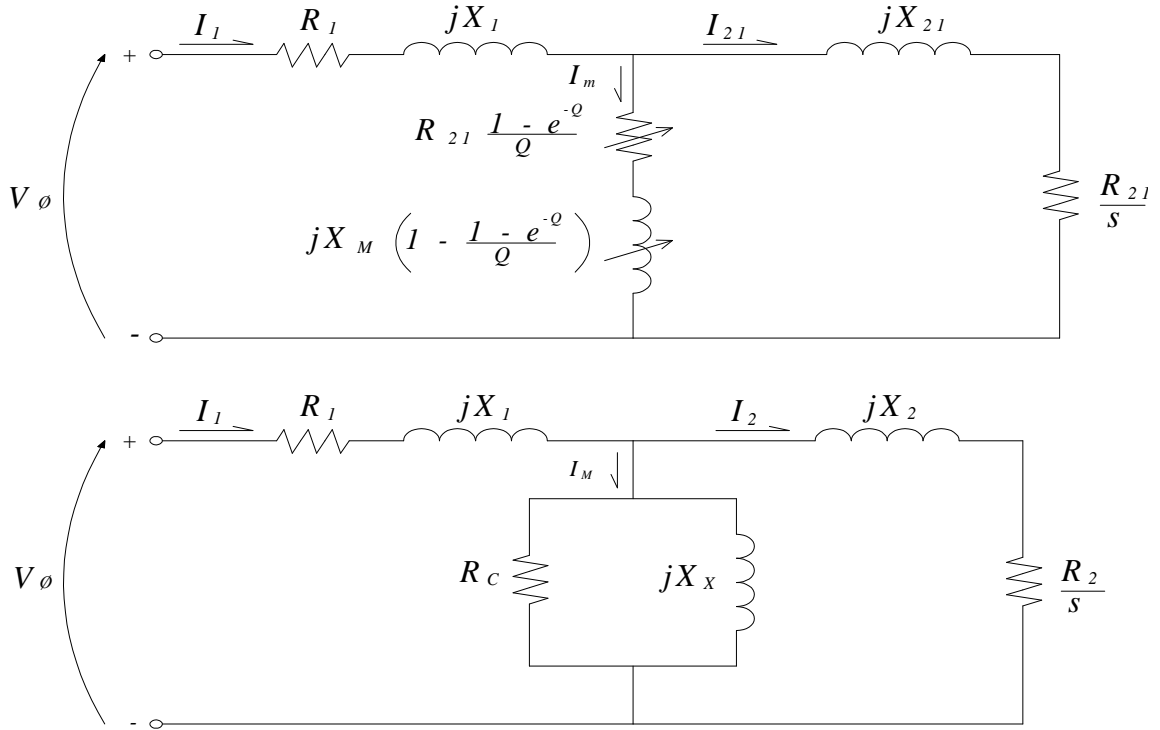


**Figure 4.2. Per-phase Equivalent circuits for a LIM (up) and a RIM (down) in steady-state.**

#### 4.3.1 First Case Analysis

Table 4.1 and Table 4.2, describe an equivalent set of parameters for a RIM from a particular configuration of LIM. The analysis will begin with the first case, in which all the parameters outside the magnetizing branch (the middle branch) are set equal in both machines, thus, allowing to equal the impedances of their magnetizing branches, to be able to find out the value of function  $f(Q)$  and the value of  $Q$  as well.

$$R_{21}f(Q) + jX_M(1 - f(Q)) = \frac{jX_x R_c}{jX_x + R_c} \quad (4.16)$$

Solving equation (4.16) one can separate the real part from the imaginary part and solve:

Real part:

$$R_{21}R_C f(Q) - X_M X_X (1 - f(Q)) = 0 \quad (4.17)$$

Imaginary part:

$$R_{21}f(Q)X_X + X_M R_C (1 - f(Q)) = X_X R_C \quad (4.18)$$

From equation (4.17) and replacing the parameters from Table 4.1 and Table 4.2, ones get:

$$f(Q) = \frac{X_M X_X}{R_2 R_C + X_M X_X} = \frac{26.3 X_M}{332 + 26.3 X_M} \quad (4.19)$$

From equation (4.19) and replacing the parameters from Table 4.1 and Table 4.2, and also setting  $R_C = 1000$  ohms, ones get:

$$f(Q) = \frac{X_X R_C - X_M R_C}{X_X R_{21} - X_M R_C} = \frac{26300 - 1000 X_M}{8.7316 - 1000 X_M} \quad (4.20)$$

By equating equations (4.19) and (4.20) ones get  $X_M = -24.29$  ohms and  $f(Q) = 2.082$ , thus getting the value of Q by recalling equation (4.1):

$$f(Q) = \frac{1 - e^{-Q}}{Q} = 2.082$$

This equation can be solved iterating values of Q for which  $f(Q)$  equals 2.082. This iteration is made using the Excel software solver application from which  $Q = -1.324$  and is already register in Table 4.1.

Finally, by recalling equation (3.2), the value of the velocity of the rotor can be found:

$$v = \frac{D.R_{21}}{Q(L_M + L_2)} = \frac{0.574m(0.332\Omega)}{(-1.324)\frac{1}{120\pi}(-24.29 + 0.464)H} = 2.278m/s$$

Also register in Table 4.1.

#### 4.3.2 General Analysis

In the general analysis, a Thevenin equivalent expression for the voltage and the impedance is calculated looking from the right side of the magnetizing branch for both machines. Then, it will be replaced the values from Table 4.1 on the equation for the LIM configuration with the corresponding modification, for example by changing the velocity of the rotor or some other parameter. The parameters for the RIM will be initially set the same as the ones from Table 4.1, but then the most dominant will be modified to get the same numeric values of the Thevenin quantities find out with the LIM configuration.

##### 4.3.2.1 LIM Thevenin Equivalent Quantities

Recalling Figure 4.2, the thevenin voltage for a LIM will be find out from the right side of the magnetizing branch making an open-circuit at this point and finding the open-circuit voltage present there.

$$V_{TH} = V_\phi \frac{Z_M}{Z_1 + Z_M} \quad (4.21)$$

$$V_{TH} = V_\phi \frac{(R_2 \cdot f(Q) + jX_M(1 - f(Q)))}{R_1 + j(X_1 + X_M(1 - f(Q)))} \quad (4.22)$$

And so the magnitude would be:

$$|V_{TH}| = |V_\phi| \frac{\left( (R_{21} \cdot f(Q))^2 + (X_M (1 - f(Q)))^2 \right)^{1/2}}{\left( R_1^2 + (X_1 + X_M (1 - f(Q)))^2 \right)^{1/2}} \quad (4.23)$$

The Thevenin impedance is found by making a short circuit in the phase voltage and getting the equivalent impedance seen from the right hand side of the magnetizing branch.

$$Z_{TH} = Z_1 // Z_M$$

$$Z_{TH} = \frac{(R_1 + jX_1)(R_{21} \cdot f(Q) + jX_M (1 - f(Q)))}{(R_1 + R_{21} \cdot f(Q)) + j(X_1 + X_M (1 - f(Q)))} \quad (4.24)$$

#### 4.3.2.2 RIM Thevenin Equivalent Quantities

Recalling Figure 4.2, the Thevenin voltage for a RIM will be find out from the right side of the magnetizing branch making an open-circuit at this point and finding the open-circuit voltage present there.

$$V_{TH} = V_\phi \frac{jX_M}{R_1 + j(X_1 + X_M)} \quad (4.25)$$

$$V_{TH} = V_\phi \frac{jX_M}{R_1 + j(X_1 + X_M)} \quad (4.26)$$

And so the magnitude would be:

$$|V_{TH}| = |V_\phi| \frac{X_M}{\left( R_1^2 + (X_1 + X_M)^2 \right)^{1/2}} \quad (4.27)$$

The Thevenin impedance is find out by making a short circuit in the phase voltage and getting the equivalent impedance seen from the right hand side of the magnetizing branch.

$$Z_{TH} = (R_1 + jX_1) // jX_M$$

$$Z_{TH} = \frac{(R_1 + jX_1)(jX_M)}{R_1 + j(X_1 + X_M)} \quad (4.28)$$

### 4.3.3 Analysis of each case

#### Case 1, 2 and 3

Case 1 was described in section 3.2.1 and it was the only case developed analytically. As mentioned before, the parameters of the circuit elements outside the magnetizing branch where considered the same for both machines, as one can see in Table 4.1 and Table 4.2. The analysis led to find the value of  $f(Q)$ ,  $Q$ , and finally the velocity of the rotor ( $v_r = 2.278$  m/s) corresponding to the configuration of the LIM. It can be seen from Table 4.1 and Table 4.2 that the Thevenin quantities are the same for both of them, therefore they are considered equivalent.

For cases 2 and 3, the parameters from case 1 were considered the same for the LIM except for the velocity of the rotor. As a consequence of it, the values of  $Q$  and  $f(Q)$  also change and thus the Thevenin quantities. It was analyzed for a mid and a high velocity of the rotor (10 m/s and 20 m/s respectively). In an attempt to equalize the Thevenin quantities for both machines the most predominant parameter was change ( $X_X$  as can be seen in Table 4.2) for the RIM configuration leaving all the rest as in case 1. A comparison of the Thevenin quantities for both motors gives a sense of an approximate

equivalence between both machines. Is imperative to mention the correlation between the velocity of the rotor and the Thevenin quantities (for the LIM), in which ones can see that an increment in this value produce an important decrement of the Thevenin voltage and a small decrement in the Thevenin impedance (see Table 4.1).

Case 4 and 5

Were developed for the same purpose. They are basically a modification of case 1 (for the LIM) in which the parameter  $X_M$  is changed (and so the values of  $Q$  and  $f(Q)$ ) but not the velocity of the rotor. An important decrement of the Thevenin quantities is observed, specially the voltage. Changing once again the value of  $X_X$  as the predominant parameter, an approximate equivalent is find out for the RIM configuration as can be seen in Table 4.2.

LINEAR (LIM)												
Xm	Xm(1-FQ)	X2	X1	R1	R2	v (m/s)	D	Q	FQ	Vth	Rth	Xth
-24.290	26.305	0.464	1.106	0.641	0.332	2.278	0.574	-1.324	2.083	255.286	0.591	1.074
-24.290	4.060	0.464	1.106	0.641	0.332	10.000	0.574	-0.302	1.167	208.399	0.407	0.902
-24.290	1.927	0.464	1.106	0.641	0.332	20.000	0.574	-0.151	1.079	168.172	0.299	0.725
0.069	0.068	0.464	1.106	0.641	0.332	2.278	0.574	59.137	0.017	13.593	0.007	0.065
1.000	0.954	0.464	1.106	0.641	0.332	2.278	0.574	21.542	0.046	117.609	0.130	0.549
1.000	0.627	0.464	1.106	0.641	0.332	20.000	0.574	2.454	0.373	92.047	0.129	0.412

**Table 4.1. Cases of analysis corresponding to different configurations of LIM.**

ROTARY (RIM)										DESCRIPTION
R1	R2	Xx	X2	X1	Vph	Vth	Rth	Xth	CASE	
0.641	0.332	26.300	0.464	1.106	266	255.2	0.590	1.075	1	The same parameters
0.641	0.332	4.107	0.464	1.106	266	208.0	0.392	0.920	2	v=10 m/s, same initial conditions
0.641	0.332	2.013	0.464	1.106	266	168.2	0.256	0.766	3	v=20m/s, same initial conditions
0.641	0.332	0.068	0.464	1.106	266	13.6	0.002	0.065	4	Xm=0.0693 H, and the same velocity as
0.641	0.332	0.954	0.464	1.106	266	117.6	0.125	0.551	5	Xm=1 H, and the same velocity as case
0.641	0.332	0.645	0.464	1.106	266	92.0	0.077	0.435	6	Xm=1 H, v=20m/s

**Table 4.2. Approximated equivalent set of parameters of a RIM.**

## 5 DYNAMIC ANALYSIS AND MATLAB SIMULATION FOR A LIM

### 5.1 Overview

Simulations of the overall LIM as an electromechanical system are going to be developed using the Simulink software. Recalling equations (3.13), (3.14), (4.7) and (4.8) and after some algebraic manipulation, and also taking into account the effects of disturbances and linear frictional load, the dynamics of the system are represented by the following equations:

Electrical dynamics:

$$\frac{dI_1}{dt} = \frac{V_1 - I_1 \left( R_1 + R_{21} * f(Q) - L_m \frac{df(Q)}{dt} \right) + I_{21} \left( R_{21} * f(Q) - L_m \frac{df(Q)}{dt} \right) + \frac{dI_{21}}{dt} L_m (1 - f(Q))}{L_1 + L_m (1 - f(Q))} \quad (5.1)$$

$$\frac{dI_2}{dt} = \frac{I_1 \left( R_{21} * f(Q) - L_m \frac{df(Q)}{dt} \right) - I_{21} \left( R_{21} * f(Q) + \frac{R_{21}}{s} - L_m \frac{df(Q)}{dt} \right) + \frac{dI_1}{dt} L_m (1 - f(Q))}{L_{21} + L_m (1 - f(Q))} \quad (5.2)$$

Mechanical dynamics:

The system will account for the mechanical part assumed as the conventional mass-spring-damper system represent by equation (3.1)

$$m\ddot{x} + b\dot{x} + kx = W_{em} - W_d(t) \quad (5.3)$$

:

In which  $m$  is the combined rotor and payload mass,  $b$  is the damping linear coefficient and  $k$  is some elastic coefficient.  $W_{em}$  is the electromagnetic thrust of the LIM and  $W_d$  is a disturbance force in time.

Thrust:

$$W_{em} = 3I_{21}^2 R_{21} \frac{\pi}{\omega_2 \tau} - 3I_m^2 R_{21} \frac{(1 - \exp(-Q))}{vQ} \quad (5.4)$$

Where:

$W_{em}$ : Total thrust

$\omega_2$ : slip frequency

$$slip = \frac{\omega_2}{\omega_1} = \frac{V_s - V_r}{V_s} = s$$

$$\omega_2 = s \omega_1$$

And,  $I_m = I_1 - I_{21}$  (5.5)

$\tau$ : motor pole pitch, assumed with a value of 0.0867 m.

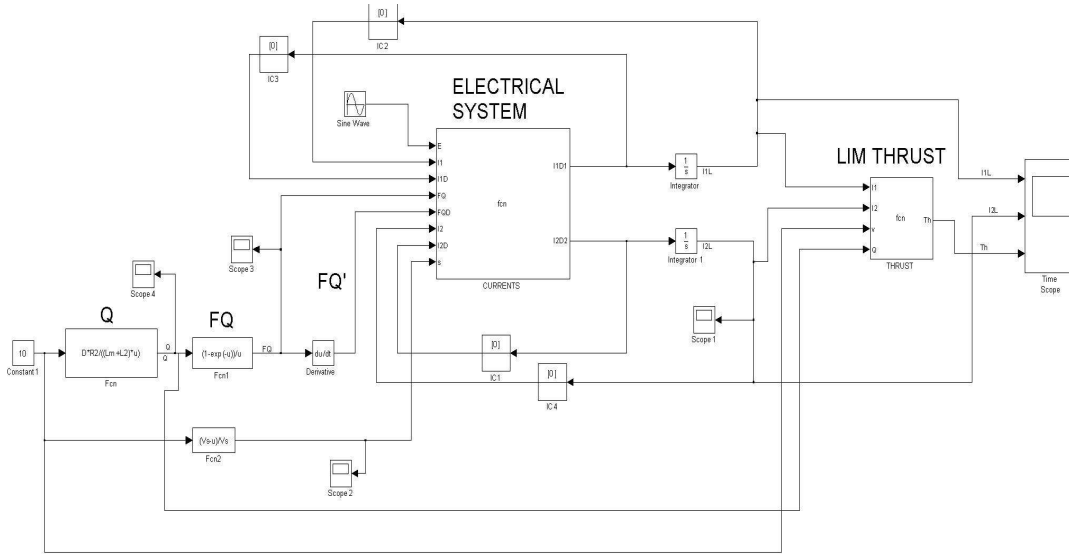
$b$ : linear frictional load coefficient.

## 5.2 Simulation of a LIM with a Constant Velocity of the Rotor.

Table 5.1, shows the parameters used for this simulation which are the same as the ones from case 2 of Table 4.1 and Figure 5.1 shows the Simulink simulation model.

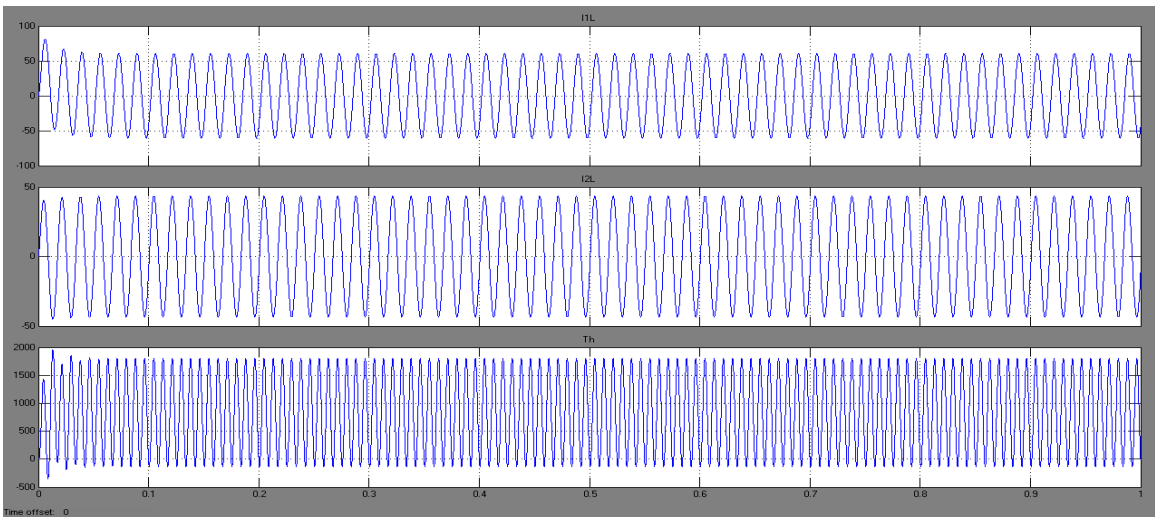
Parameters	R1 (ohms)	R2 (ohms)	L2 (H)	L1 (H)	Lm (H)	D (m)	$\tau$ (m)	Q	f(Q)	Vs (m/s)	Vr (m/s)	s	V (Volts)	F (Hz)
LIM	0.641	0.332	0.0012	0.0029	-0.064	0.574	0.0867	-0.3	1.167	10.4	9.36	0.1	220	60

**Table 5.1. Parameters for simulation case 2.**



**Figure 5.1. Simulink model for simulation case 1: constant velocity of the rotor**

Figure 5.2, shows the results for the response of the system accounting for the thrust:



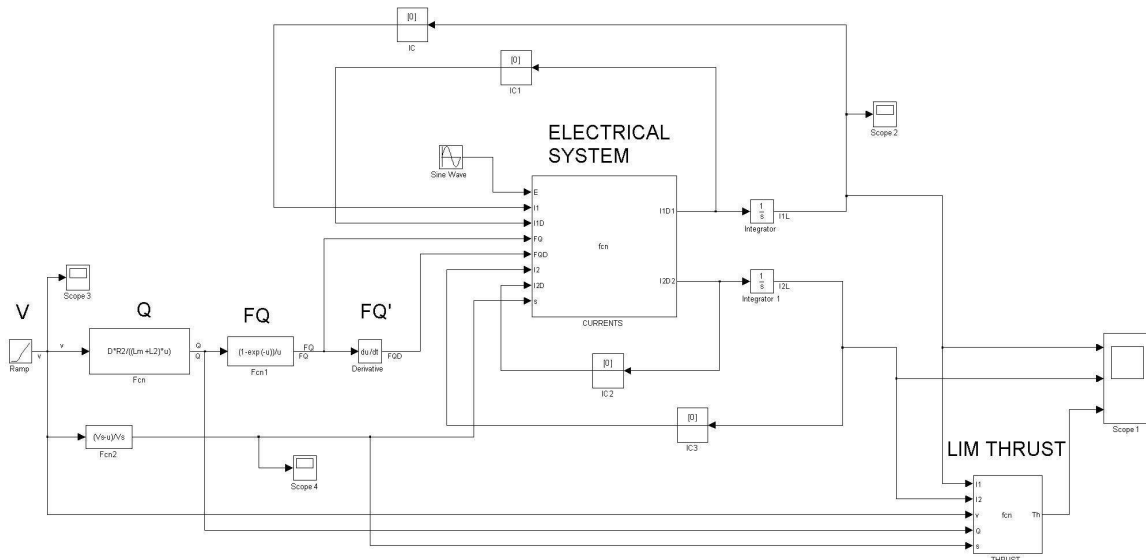
**Figure 5.2. From top to bottom: primary current (I1), secondary current (I2) and thrust (Th).**

Figure 5.1. Simulink model for simulation case 1: constant velocity of the rotor, reveals the response of the system to a constant velocity of the rotor which implies a constant

value of slip over time and thus an overall steady state response. The first plot (from top to bottom) corresponds to the response of the current of the stator ( $I_1$ ), with a peak value of 60 A. The second plot is the response of the current of the rotor ( $I_2$ ), with a peak value of 43 A, and the third plot refers to the response of the total thrust over the rotor with a steady state peak value of 1800 N.

### 5.3 Simulation of a LIM with a Linear Velocity of the Rotor.

The parameters are the same as the ones in Table 5.1, except for the linear velocity of the rotor ( $V_r$ ), and thus the slip,  $Q$  and  $f(Q)$  which depend on  $V_r$ . Figure 5.3, depicts the Simulink model for case 2.



**Figure 5.3. Simulink model for simulation case 2: linear velocity of the rotor.**

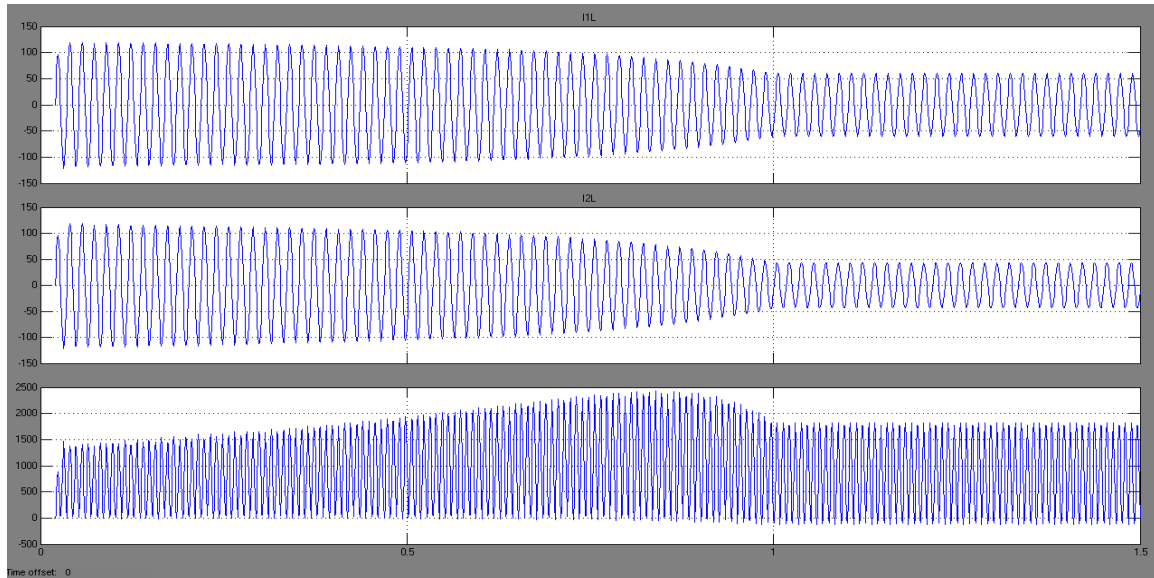


**Figure 5.4. From top to bottom: primary current ( $I_1$ ), secondary current ( $I_2$ ) and thrust ( $Th$ ).**

Figure 5.4 illustrates the response of the LIM for a varying linear speed of the rotor, starting at 0 s and then rising linearly until it reaches a rotor speed of 9.36 m/s at a time of 1 s remaining constant for 0.5 s more. The first plot (from top to bottom) corresponds to the response of the current of the stator ( $I_1$ ), with a maximum peak value of 118 A and a steady state value of 60 A after 1 s, the same as shown in Figure 5.2. The second plot is the response of the current of the rotor ( $I_2$ ), with the same maximum peak value as the stator current (118 A) and a steady state value of 43 A, also the same as shown in Figure 5.2. One can see how the current demand is high at the beginning where the speed of the rotor is very low and it starts to decay progressively until it reaches the steady state value of the speed of the rotor (9.36 m/s) at time 1 s. From this point forward the current response for both, rotor and stator stabilizes provided that they have reached their steady state. On the other hand, the response of the thrust in the third plot increases progressively from time 0 s with a peak value of 1090 N until it reaches its maximum

peak value of 2420 N at 0.8 s, just before it reaches its steady state at 1 s. At this time it decays very rapidly reaching the steady state with a peak value of 1800 N.

#### 5.4 Setting the Desired Thrust by Using Lookup Tables

The following analysis is going to be developed assuming a steady state of the system, where the frequency ( $f$ ), the rotor speed ( $V_r$ ) and the Thrust ( $T_h$ ) are going to be invariable through time. The mechanical system is not yet included at this instance.

The intention is to get a value of voltage amplitude ( $V_{ol}$ ) through a specific combination of the synchronous speed  $V_s$  (which is a function of  $f$ ),  $V_r$  and a set value of thrust, by using trilinear interpolation with a specific Simulink block called Lookup Table n-D (3-D in this case). Then this value is going to multiply the sinusoidal signal from which the frequency can be changed from an outer block in the model. The overall signal is going to be the input of the electrical system from which a close value of actual thrust compared to the reference thrust is expected.

Figure 5.5, shows the Simulink model configuration. One can identify almost the same blocks from previous models, except for the ones located in the upper-left corner. These blocks were implemented instead of the conventional sinusoidal source block, with the purpose of setting a frequency value from an outer block and calculating the voltage amplitude of the voltage signal prior to entering as an input of the electrical circuit block.



#### 5.4.1 Procedure for Lookup Table Implementation

As explained before, the objective of this model is to obtain an actual thrust of the system, close enough from the one set as reference, by use of a lookup table which outputs a voltage amplitude value for the voltage signal having as inputs  $V_s$ ,  $V_r$  and  $T_h$  (reference thrust). As the thrust is going to be one of the inputs of the lookup table one has to know the behavior of the actual thrust beforehand, however this is not the case. Instead, one can find the thrust response of the system by varying parameters such as frequency ( $f$ ), rotor speed ( $V_r$ ) and voltage amplitude ( $V_o$ ). Thus, this would be the first step before implementing the lookup table. A stepwise procedure is going to be developed as follows:

- 1) Define the intervals of  $V_s$ ,  $V_r$  and  $V_o$  for which the thrust needs to be defined as shown in the following table:

<b><math>V_s</math></b>	<b><math>V_r</math></b>	<b><math>V_o</math></b>
10.4	9.36	100
12.14	10.92	200
13.87	12.48	300
15.61	14.05	400
17.34	15.61	500

**Table 5.2. Values of  $V_s$ ,  $V_r$  and  $V_o$  for which the thrust needs to be defined.**

- 2) Get the values of Thrust for each combination  $V_s$ ,  $V_r$ ,  $V_o$ , in which

$V_s$ : synchronous speed

$V_r$ : Rotor velocity

$V_o$ : Amplitude of the voltage

$T_h$ : Thrust

Vs	Vr	Vol	Th	Slip	f
10.4	9.36	100	<b>221.15</b>	0.10	60
		200	<b>884.64</b>		
		300	<b>1990.53</b>		
		400	<b>3539.6</b>		
		500	<b>5529.19</b>		
10.4	10.92	X	<b>0</b>	X	
10.4	12.48	X	<b>0</b>	X	
10.4	14.05	X	<b>0</b>	X	
10.4	15.61	X	<b>0</b>	X	
12.14	9.36	100	<b>218</b>	0.23	70
		200	<b>872</b>		
		300	<b>1960</b>		
		400	<b>3490</b>		
		500	<b>5455</b>		
12.14	10.92	100	<b>174</b>	0.10	
		200	<b>697</b>		
		300	<b>1570</b>		
		400	<b>2790</b>		
		500	<b>4360</b>		
12.14	12.48	X	<b>0</b>	X	
12.14	14.05	X	<b>0</b>	X	
12.14	15.61	X	<b>0</b>	X	
13.87	9.36	100	<b>148.5</b>	0.33	80
		200	<b>594</b>		
		300	<b>1337</b>		
		400	<b>2375</b>		
		500	<b>3710</b>		
13.87	10.92	100	<b>169.3</b>	0.21	
		200	<b>676.5</b>		
		300	<b>1523</b>		
		400	<b>2707</b>		
		500	<b>4230</b>		
13.87	12.48	100	<b>138</b>	0.10	
		200	<b>552</b>		
		300	<b>1242</b>		
		400	<b>2207</b>		
		500	<b>3450</b>		
13.87	14.05	X	<b>0</b>	X	
13.87	15.61	X	<b>0</b>	X	

Table 5.3. Thrust for each combination Vs, Vr, Vol.

Vs	Vr	Vol	Th	Slip	f
15.61	9.36	100	<b>103.2</b>	0.40	90
		200	<b>414</b>		
		300	<b>932.65</b>		
		400	<b>1657.9</b>		
		500	<b>2575</b>		
15.61	10.92	100	<b>114.8</b>	0.30	
		200	<b>460.5</b>		
		300	<b>1031.5</b>		
		400	<b>1845</b>		
		500	<b>2871</b>		
15.61	12.48	100	<b>129.6</b>	0.20	
		200	<b>519.5</b>		
		300	<b>1169</b>		
		400	<b>2072</b>		
		500	<b>3237</b>		
15.61	14.05	100	<b>110.8</b>	0.10	
		200	<b>442.5</b>		
		300	<b>995.5</b>		
		400	<b>1770</b>		
		500	<b>2766</b>		
15.61	15.61	X	<b>0</b>		
17.34	9.36	100	<b>72</b>	0.46	100
		200	<b>288</b>		
		300	<b>648</b>		
		400	<b>1152</b>		
		500	<b>1800</b>		
17.34	10.92	100	<b>81</b>	0.37	
		200	<b>322</b>		
		300	<b>729</b>		
		400	<b>1285</b>		
		500	<b>2015</b>		
17.34	12.48	100	<b>92.4</b>	0.28	
		200	<b>369.5</b>		
		300	<b>832</b>		
		400	<b>1478.5</b>		
		500	<b>2310</b>		
17.34	14.05	100	<b>101.4</b>	0.19	
		200	<b>405.5</b>		
		300	<b>914.5</b>		
		400	<b>1620</b>		
		500	<b>2536</b>		
17.34	15.61	100	<b>89.9</b>	0.10	
		200	<b>360.7</b>		
		300	<b>811.5</b>		
		400	<b>1439</b>		
		500	<b>2254</b>		

The previous table gives some values that defined the response of the trust for different combinations of Vs, Vr and Vol.

- 3) After this table has been complete, a trilinear interpolation is used in order to define the thrust response for different values of the voltage amplitude in a range from 100 to 500 as defined in step 1) (See Section 8.1 for the Matlab script). The trilinear interpolation is made by implementing the interp3 function in matlab and is defined as follows:

$Th2 = \text{interp3}(Vs1, Vr1, Vol1, Th1, Vs2, Vr2, Vol2)$

Where:

$Vs1 = [10.40 \ 12.14 \ 13.87 \ 15.61 \ 17.34]$

$Vr1 = [9.36 \ 10.92 \ 12.48 \ 14.05 \ 15.61]$

$Vol1 = [100 \ 200 \ 300 \ 400 \ 500]$

Th1, is defined by a 3D matrix of 5x5x5 based on the information on Table 5.3, defined as follows:

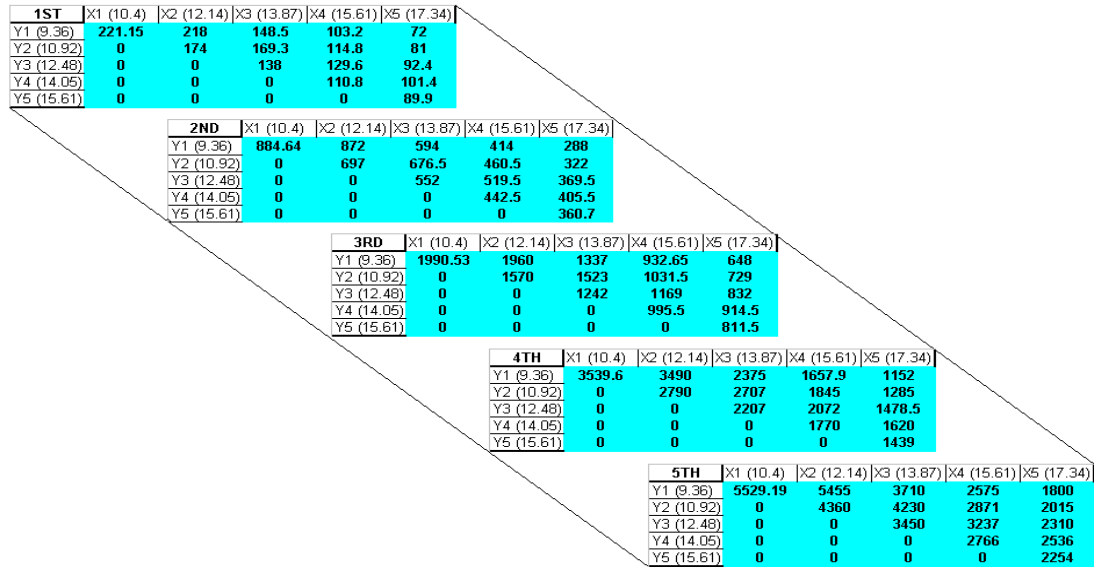


Figure 5.6. Thrust matrix with dimensions 5x5x5.

Vs2 and Vr2 is defined by each possible combination between each other.

Vol2=values of voltage amplitudes from 100 to 500 with a step of 10.

This procedure generates a list of Th2 for each possible combination between Vs2 and Vr2.

- Define a range of thrust for the system. The range was defined by the last set of values of thrust from Table 5.3, thus a new table needs to be created where the inputs are Vs, Vr and Thrust and the output is the voltage amplitude Vol, which is basically what is necessary to make the last 3D-interpolation using the 3-D Lookup Table block from Simulink for being able to set the desired value of thrust to the system. To build this table, one last interpolation is needed. This time is a 1-D interpolation between the values of Th2 and Vol2 for each set of thrust values chose. Once this is complete, a table like Table 5.4 is built.

5) The last trilinear interpolation is made by using the 3-D Lookup Table Simulink block, in which the data must be defined the same way as when using the interp3 matlab function explained in step 3) . The information is shown in the sequel:

Vs1=[10.40 12.14 13.87 15.61 17.34]

Vr1=[9.36 10.92 12.48 14.05 15.61]

Th1=[89.9 360.7 811.5 1439 2254]

Vol1, is defined by a 3D matrix of 5x5x5 based on the information on Table 5.4, and is shown in Figure 5.7.

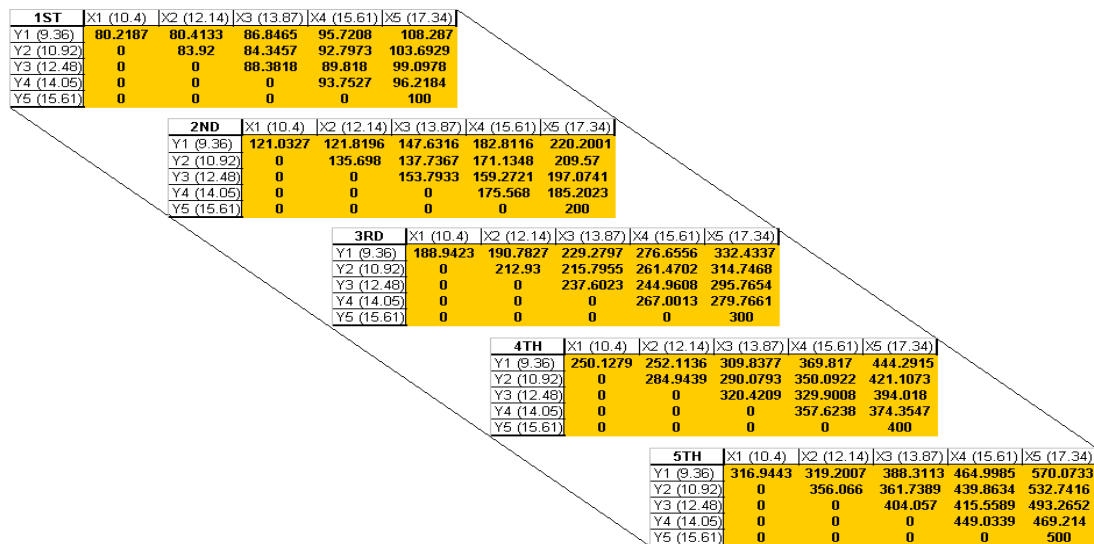


Figure 5.7. Voltage amplitude matrix with dimensions 5x5x5.

Vs	Vr	Th	Vol	f
10.4	9.36	89.9	80.2187	60
		360.7	121.0327	
		811.5	188.9423	
		1439	250.1279	
		2254	316.9443	
10.4	10.92	X	0	
10.4	12.48	X	0	
10.4	14.05	X	0	
10.4	15.61	X	0	
12.14	9.36	89.9	80.4133	70
		360.7	121.8196	
		811.5	190.7827	
		1439	252.1136	
		2254	319.2007	
12.14	10.92	89.9	83.92	
		360.7	135.698	
		811.5	212.93	
		1439	284.9439	
		2254	356.066	
12.14	12.48	X	0	
12.14	14.05	X	0	
12.14	15.61	X	0	
13.87	9.36	89.9	86.8465	80
		360.7	147.6316	
		811.5	229.2797	
		1439	309.8377	
		2254	388.3113	
13.87	10.92	89.9	84.3457	
		360.7	137.7367	
		811.5	215.7955	
		1439	290.0793	
		2254	361.7389	
13.87	12.48	89.9	88.3818	
		360.7	153.7933	
		811.5	237.6023	
		1439	320.4209	
		2254	404.057	
13.87	14.05	X	0	
13.87	15.61	X	0	

**Table 5.4. Voltage amplitude for each combination Vs, Vr and Th.**

Vs	Vr	Th	Vol	f
15.61	9.36	89.9	95.7208	90
		360.7	182.8116	
		811.5	276.6556	
		1439	369.817	
		2254	464.9985	
15.61	10.92	89.9	92.7973	
		360.7	171.1348	
		811.5	261.4702	
		1439	350.0922	
		2254	439.8634	
15.61	12.48	89.9	89.818	
		360.7	159.2721	
		811.5	244.9608	
		1439	329.9008	
		2254	415.5589	
15.61	14.05	89.9	93.7527	
		360.7	175.568	
		811.5	267.0013	
		1439	357.6238	
		2254	449.0339	
15.61	15.61	X	0	
17.34	9.36	89.9	108.287	100
		360.7	220.2001	
		811.5	332.4337	
		1439	444.2915	
		2254	570.0733	
17.34	10.92	89.9	103.6929	
		360.7	209.57	
		811.5	314.7468	
		1439	421.1073	
		2254	532.7416	
17.34	12.48	89.9	99.0978	
		360.7	197.0741	
		811.5	295.7654	
		1439	394.018	
		2254	493.2652	
17.34	14.05	89.9	96.2184	
		360.7	185.2023	
		811.5	279.7661	
		1439	374.3547	
		2254	469.214	
17.34	15.61	89.9	100	
		360.7	200	
		811.5	300	
		1439	400	
		2254	500	

- 6) After the previous information is defined, one can proceed to enter it on the Lookup Table Simulink block, from which the inputs are  $V_s$ ,  $V_r$  and a reference value of thrust  $T_h$ , and the output will be a voltage amplitude  $V_{ol}$ , as shown in

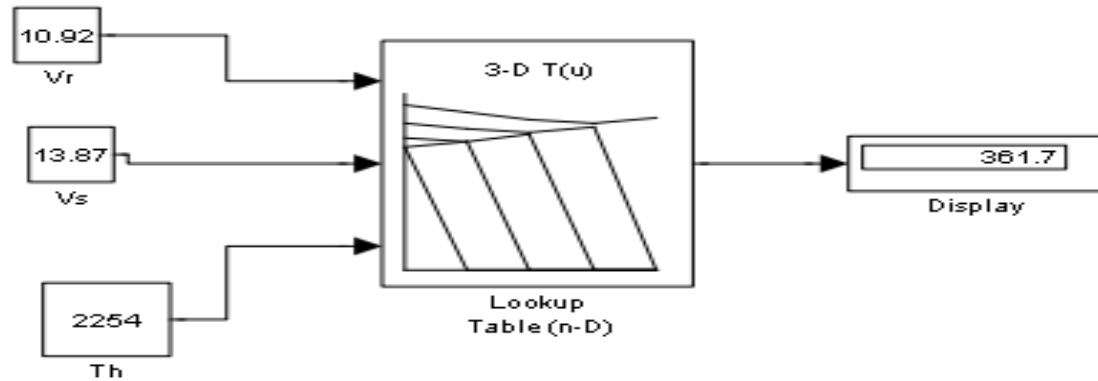


**Figure 5.8.** 3-D Lookup Table Simulink block with.

- 7) A verification of the procedure is going to be developed in the sequel for a set of arbitrary inputs. The results are summarized in Table 5.5.

f	$V_s$	$V_r$	Ref_Th	$V_{ol}$	Actual Th	Th Error	Figure
60	10.4	9.36	360.7	121	327.2	9.3%	Figure 5.9
70	12.14	10.92	550	167.9	490.8	10.7%	Figure 5.10
80	13.87	12.48	1200	288.9	1154	3.8%	Figure 5.11
90	15.61	14.05	1800	397.2	1754.2	2.5%	Figure 5.12
100	17.34	15.61	2254	500	2270.8	0.7%	Figure 5.13

**Table 5.5.** System response verification by using 3D-Lookup table.

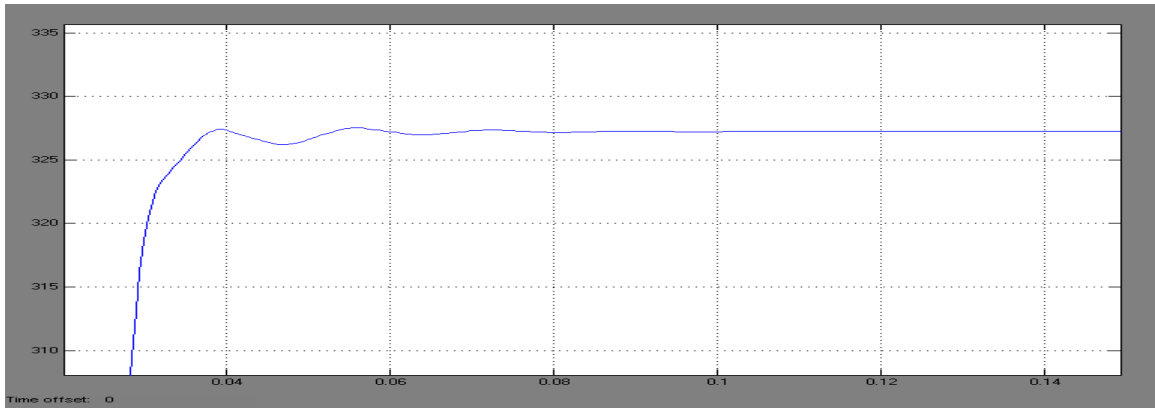


**Figure 5.9. Actual RMS value of Thrust for a reference thrust of 360.7 N.**

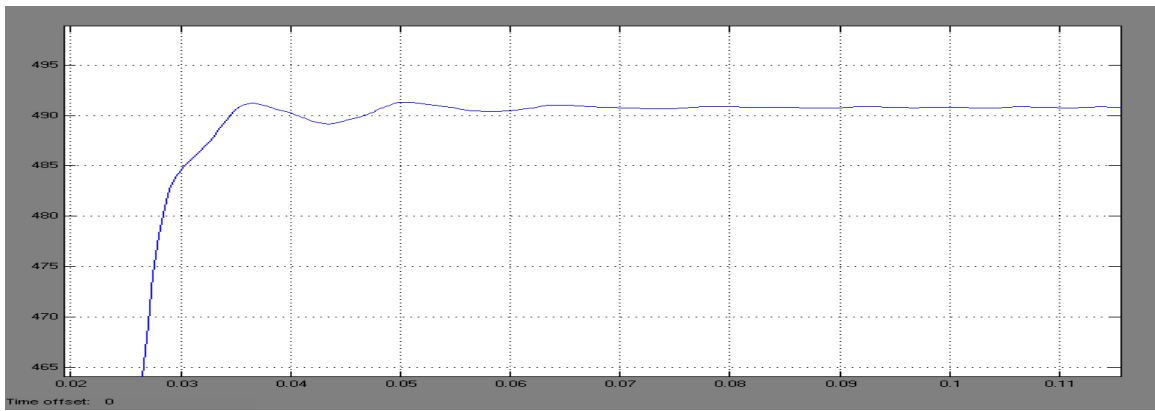


**Figure 5.10. Actual RMS value of Thrust for a reference thrust of 550 N.**

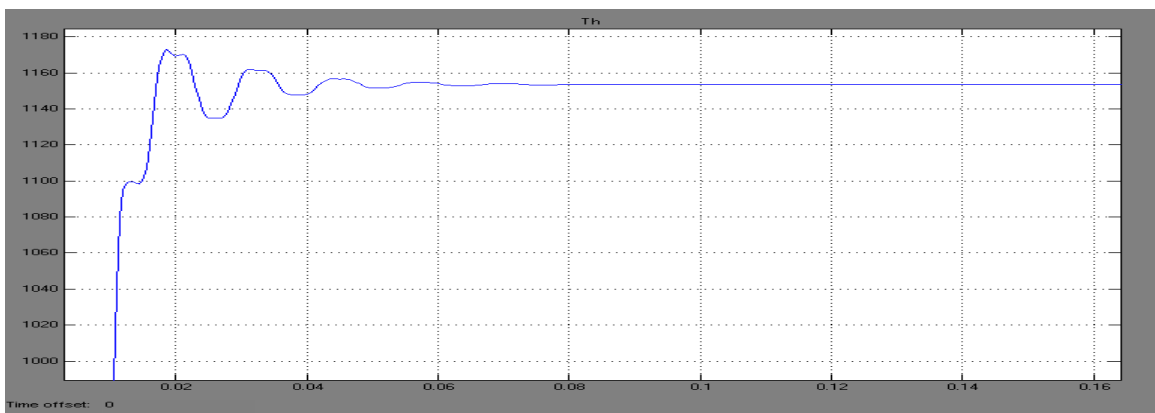


**Figure 5.11. Actual RMS value of Thrust for a reference thrust of 1200 N.**

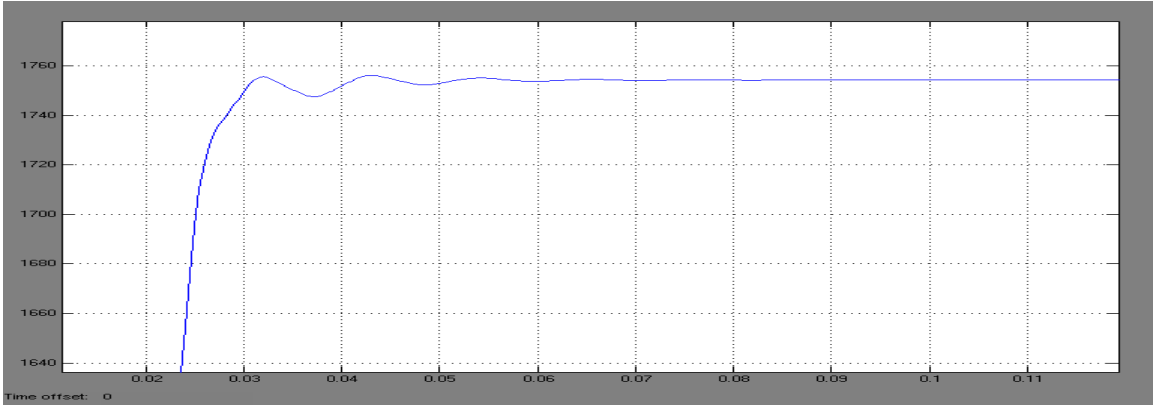


**Figure 5.12. Actual RMS value of Thrust for a reference thrust of 1800 N.**

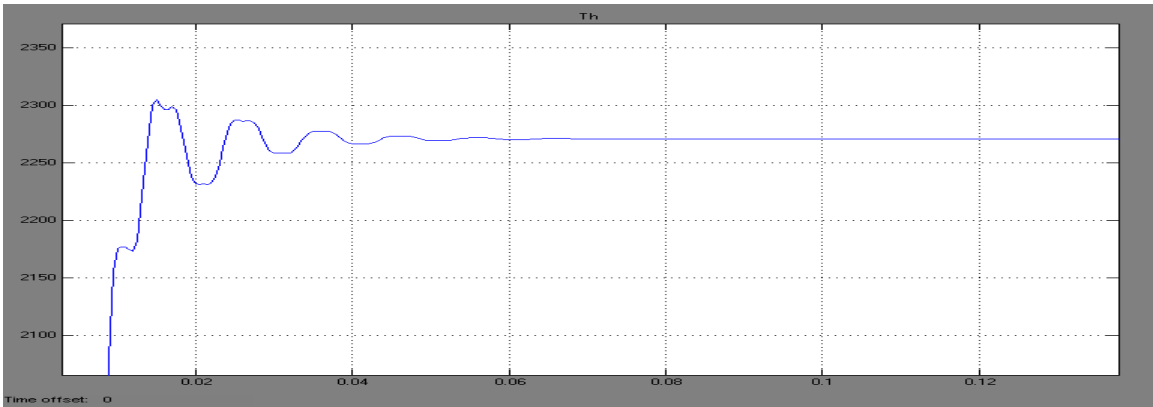


**Figure 5.13. Actual RMS value of Thrust for a reference thrust of 2254 N.**

Table 5.5, show the inputs  $V_s$ ,  $V_r$ , and  $Ref\_Th$  (reference value of thrust) and compares this last one with the actual thrust response of the system. One can see how the error tends to diminish while increasing the speed values which can be expected provided that the range of thrust was chose based on the thrust values for a synchronous speed of 17.34 m/s as explained in step 4). This however, would be a first approach on controlling the thrust in a LIM for these particular conditions. For details about the Matlab script go to Appendix, Section 8.1.

## 5.5 Analysis and Simulation of the LIM as an Electromechanical System

At this point, the value of the rotor speed  $V_r$  is no longer going to be assumed. Instead, the mechanical response is going to account for the overall response of the system and will be assumed as the conventional mass-spring-damper system represent by equation (5.3) :

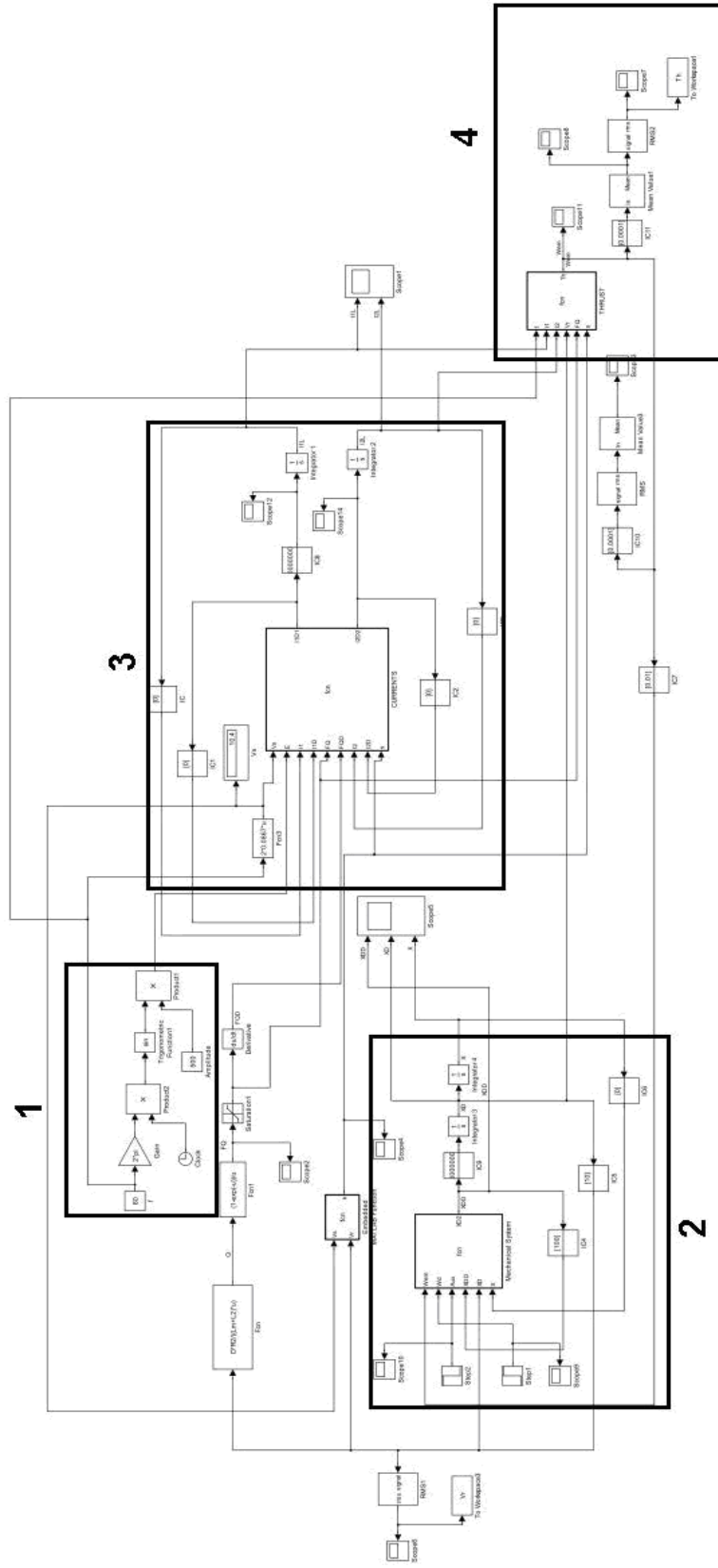
$$m\ddot{x} + b\dot{x} + kx = W_{em} - W_d(t) \quad (5.3)$$

In which  $m$  is the combined rotor and payload mass,  $b$  is the damping linear coefficient and  $k$  is some elastic coefficient.  $W_{em}$  is the electromagnetic thrust of the LIM and  $W_d$  is a disturbance force in time. Table 5.6, shows the electrical and physical characteristics of the motor.

A brief explanation of each block set displayed in Figure 5.14 is going to take place in the sequel.

Figure 5.14.

Simulink Model for the Electromechanical System



Parameters	NAME	LIM
R1 (ohms)	Stator Resistance	0.641
R2 (ohms)	Rotor Resistance	0.332
L2 (H)	Rotor Inductance	0.0012
L1 (H)	Stator Inductance	0.0029
Lm (H)	Magnetizing Inductance	-0.0644
F (Hz)	Frequency	60
D (m)	Effective Length of motor	0.574
$\tau$ (m)	motor pole pitch	0.0867
Vs (m/s)	Synchronous Velocity	10.4
M (Kg)	Mass	300
V (Volts)	Phase Voltage Amplitude	300

**Table 5.6. Parameters and quantities for the LIM.**

### 5.5.1 Block Set Explanation

**Block set 1:** This set of blocks correspond to the voltage signal (sinusoidal), where the values of frequency (f) and voltage amplitude (Vol) are set in order to feed the electrical system.

**Block Set 2:** This set of blocks correspond to the mechanical system which is represented by equation (3.1):

For simulation purposes these were the values:

The inputs are:  $W_{em}$ ,  $W_d$ ,  $A_r$ ,  $V_r$ ,  $X_r$  (acceleration, speed and distance of the rotor).

The output is:  $A_r$ .

$m=300$ ,  $b=0$ ,  $k=0$ ,  $W_d=0$  (No disturbance of any kind)

No disturbance is considered in this model as to reach a value close to the synchronous speed is needed.

**Block Set 3:** This set represents the electrical subsystem of the model or more precisely the per phase equivalent circuit of the LIM.

The inputs are:  $V_s$ ,  $E$ ,  $I_1$ ,  $I_{1D}$ ,  $FQ$ ,  $FQD$ ,  $I_2$ ,  $I_{2D}$ ,  $s$ , where:

$V_s$ : synchronous speed.

$E$ : instantaneous voltage signal.

$I_1$ : stator current.

$I_2$ : rotor current.

$FQ$ : function of  $Q$ , see equation (4.1)

The outputs are:  $I_{1D}$  and  $I_{2D}$ , where:

$I_{1D}$ : derivative with respect to time of the stator current.

$I_{2D}$ : derivative with respect to time of the rotor current.

$S$ : slip value, which is going to be variable as  $V_r$  is varying.

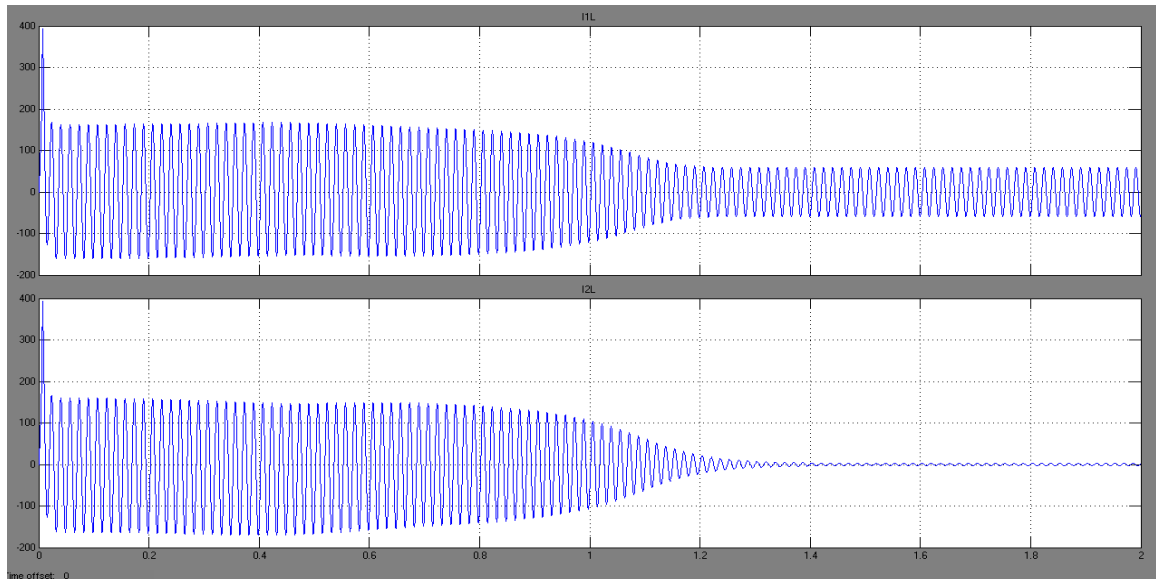
From this set, the primary and secondary current response is acquired and become the two main inputs of Block Set 4.

**Block Set 4:** The response (output) of this set is the thrust ( $W_{em}$ ) over time.

The inputs are:  $f$ ,  $I_1$ ,  $I_2$ ,  $V_r$ ,  $FQ$ ,  $S$ . This thrust response will feed the mechanical system as one can see in the mechanical system equation.

### 5.5.2 Results

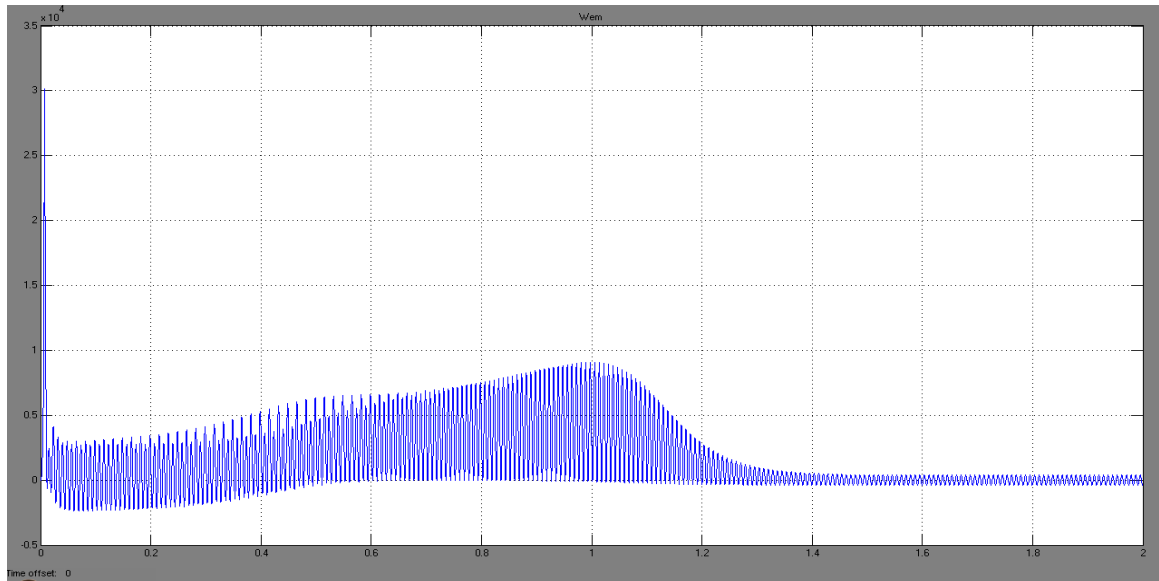
Figure 5.15, shows the response in time of the stator and the rotor currents. One can see an initial maximum peak value of almost 400 A for both currents at the start, when the rotor speed is zero. After the rotor starts moving the current decays to less than half the value of the maximum peak and maintain this value until they start to decay once again in a progressive way until they reach the steady state value. One can notice that in the case of the rotor speed, the steady state value is very close to zero provided that the synchronous speed of the LIM has been reached so there is no longer current demand.



**Figure 5.15. Stator and rotor currents response in time of the LIM.**

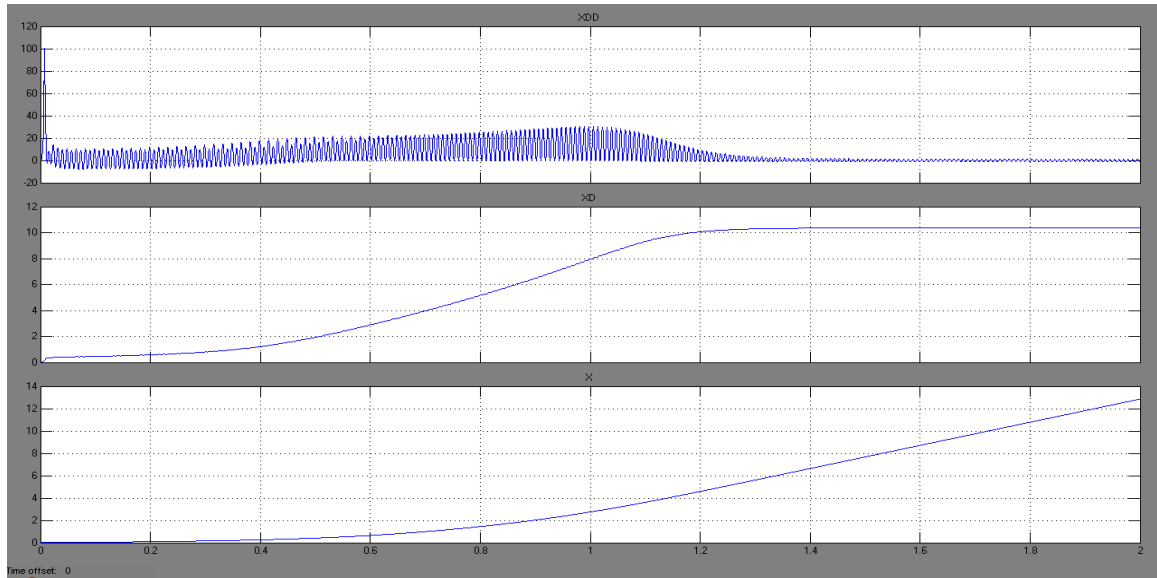
Figure 5.16, shows the response of the thrust over time in which a maximum peak value of 30000 N stand out at the starting stage, the same way as the stator and rotor currents do. Soon afterwards the thrust response decays rapidly until it reaches its lowest value and from this point on it begins to increase gradually until it reaches a maximum value at

time 1 s, time at which it begins to decay once again until it reaches the steady state value around 0 N, provided that the rotor speed has been reached, and so no thrust is needed.



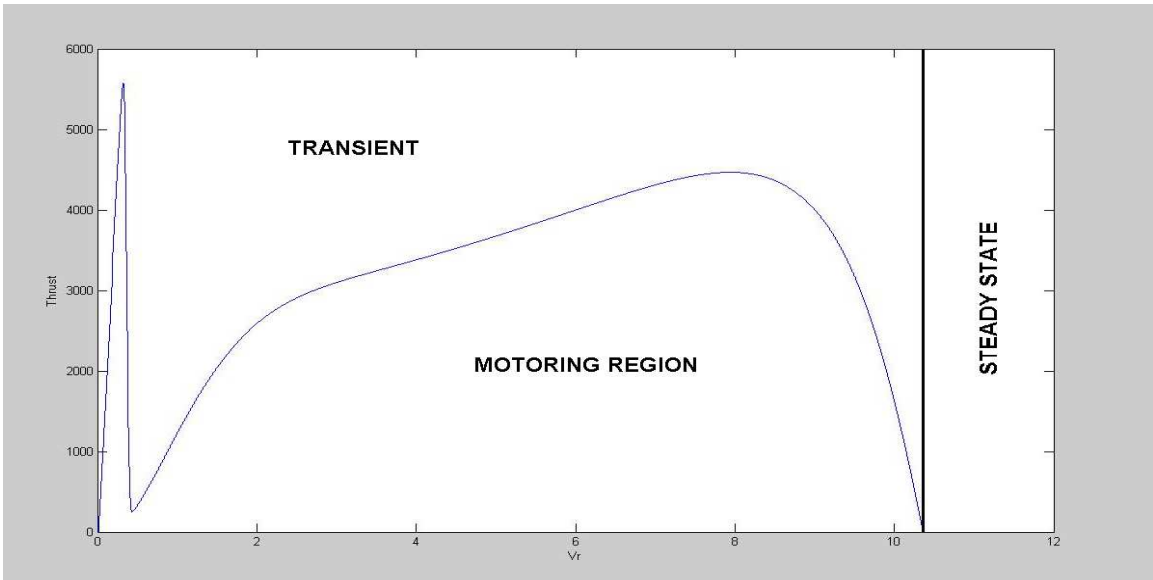
**Figure 5.16. Thrust response in time of the LIM.**

Figure 5.17, shows the response of the acceleration, speed and position of the rotor. The acceleration behaves the same way as the thrust does, with a maximum peak value of  $100 \text{ m/s}^2$  at the initial stage. The speed starts at zero and makes an abrupt jump corresponding to the acceleration peak and then it traces a smooth path which increases gradually until it stabilizes at the steady state value around  $10.36 \text{ m/s}$ . The position is traced by a smooth and progressive path which starts at  $0 \text{ m}$ , reach  $7 \text{ m}$  when the motor reaches the steady state, and after  $2 \text{ s}$  the rotor has traveled around  $13 \text{ m}$ .



**Figure 5.17. Acceleration, speed and position response in time, of the rotor.**

Figure 5.18, shows the response of the thrust by varying the speed of the rotor. It can be noticed once again a maximum peak value at the initial stage with a value 5570 N which drops rapidly to 250 N and then starts to increase faster until it reaches some value around 3000 N, time at which it continues increasing slower until it reaches a maximum value around 4470 N and then begins to decay quickly until it reaches 0 N, time at which the rotor speed has reached the synchronous speed and remains in steady state, so thrust is no longer needed. Two main zones can be identified from the figure, the transient and the steady state zone. The transient is due to the intrinsic nonlinearities of the system as well as the startup characteristics of the LIM. One also can notice that the LIM is being operated in the motoring region, so no electric power generation is present.



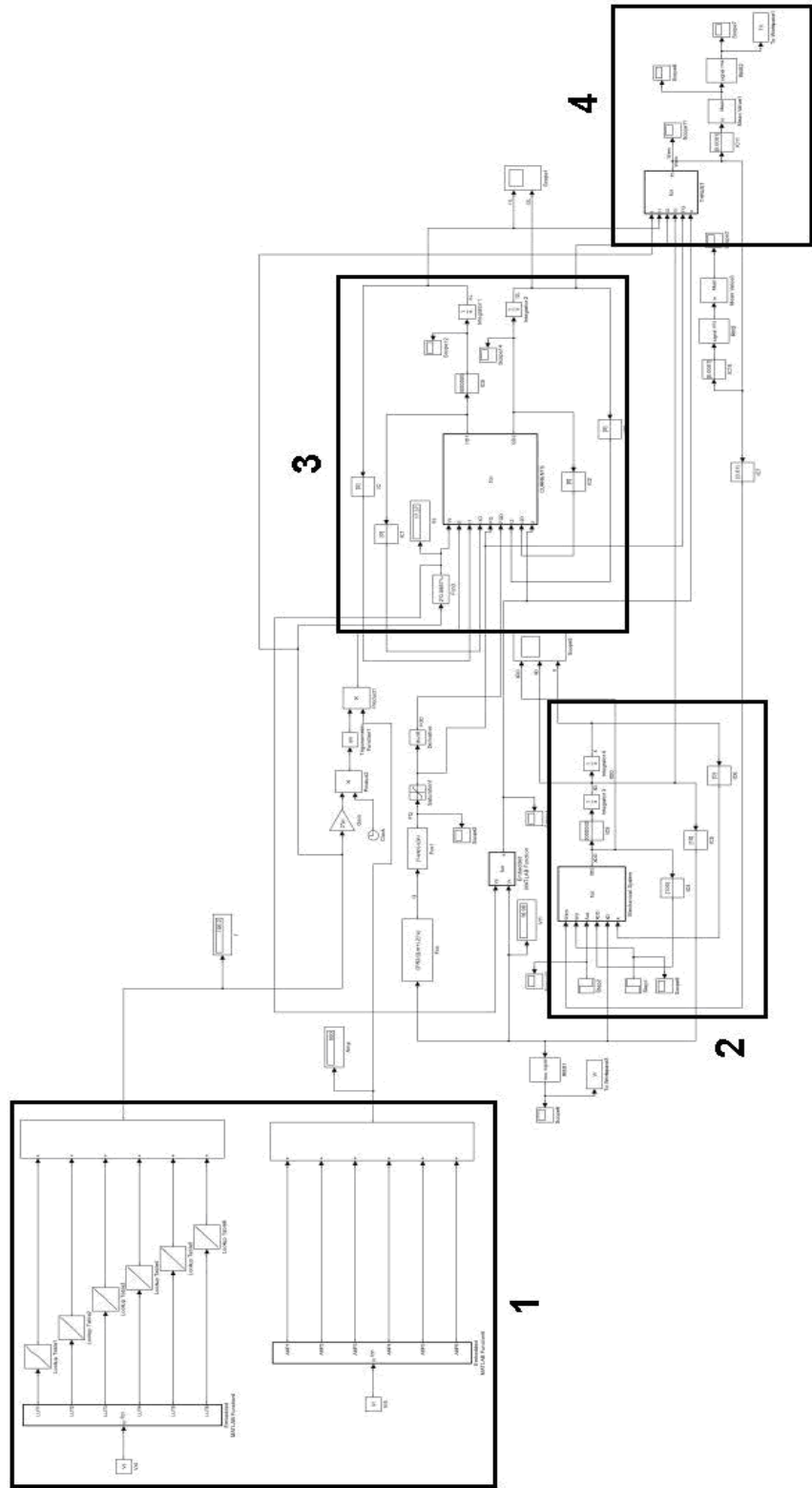
**Figure 5.18. Mean thrust Versus rotor speed response of the LIM.**

### 5.6 Setting the Desired Speed by Using Lookup Tables

The objective of the following simulation is to set a reference value of rotor speed as an input to the system, while the system generates a response close enough from the one set as reference. The parameters of the motor are going to be the same as the ones in Table 5.6 except for the frequency and voltage amplitude values which are going to vary to allow the system to reach the desired conditions. A disturbing force is also added to the mechanical system all the time with a constant value of  $Wd = 1000$  N.

Figure 5.19, illustrates the Simulink model for the LIM accounting for the new block set 1. Block sets 2, 3 and 4 are basically the same from the ones explained on Section 5.5.1. However, in block set 1 of Section 5.5.1, values of frequency ( $f$ ) and voltage amplitude (Vol) were set arbitrary. This model was developed in order to set a desired specific value

Figure 5.19.  
 Simulink Model of the LIM Using Lookup Tables to Set a Desired Rotor Speed



of rotor speed and transforming this value in to a specific value of frequency and voltage amplitude calculated by use of lookup tables, all this executed in block set 1.

### 5.6.1 Procedure for Lookup Table Implementation

- 1) Values of frequency were taken for different voltage amplitudes (50, 100, 200, 300, 400, 500 Volts) under the criterion that the steady state had to be reached before 2 seconds. These values are shown as follows:

AMPLITUDE = 50 V			
f	Vr	Vs	s
0	0	0	00
3	0.4831	0.5202	0.071319
5	0.805	0.867	0.071511
8	1.1156	1.3872	0.19579
10	1.513	1.734	0.127451
AMPLITUDE = 100 V			
f	Vr	Vs	s
10	1.675	1.734	0.034025
13.5	2.25	2.3409	0.038831
17	2.807	2.9478	0.047764
20	3.265	3.468	0.058535
23	3.706	3.9882	0.070759
26	4.1252	4.5084	0.084997
AMPLITUDE = 200 V			
f	Vr	Vs	s
26	4.414	4.5084	0.020939
29	4.911	5.0286	0.023386
33	5.568	5.7222	0.026948
36	6.056	6.2424	0.02986
39	6.54	6.7626	0.032916
42	7.02	7.2828	0.036085
AMPLITUDE = 300 V			
f	Vr	Vs	s
42	7.1532	7.2828	0.017795
45	7.653	7.803	0.019223
49	8.32	8.4966	0.020785
52	8.81	9.0168	0.022935
55	9.3	9.537	0.024851
58	9.795	10.0572	0.026071
60	10.12	10.404	0.027297
AMPLITUDE = 400 V			
f	Vr	Vs	s
60	10.23	10.404	0.016724
63	10.73	10.9242	0.017777
66	11.229	11.4444	0.018821
69	11.727	11.9646	0.019859
72	12.223	12.4848	0.020969
AMPLITUDE = 500 V			
f	Vr	Vs	s
72	12.3	12.4848	0.014802
74	12.64	12.8316	0.014932
77	13.138	13.3518	0.016013
80	13.64	13.872	0.016724
83	14.14	14.3922	0.017523
85	14.473	14.739	0.018047

**Table 5.7. Rotor speed values for each f, Vol combination.**

Table 5.7, shows all the range of rotor speeds covered from 0 m/s to 14.7 m/s, for a frequency range from 0 Hz to 85 Hz and a voltage magnitude from 50 V to 500 V. Each of these values were obtain under the criterion mentioned before, in which the steady state was reached before 2 s.

- 2) Create a 1-D Lookup Table for each of the 6 previous tables. By making this, a range of frequency from 0 to 85 Hz is covered which implies a range from 0 to 14.473 m/s covered for the desired speed of the rotor. However, values larger than 14.473 m/s can also be set provided that the Lookup Tables allow extrapolation, in which case the Lookup Table corresponding to voltage amplitude of 500 V would be used although the steady state would not be reached before 2 seconds, that is, it would not obey to the efficiency criterion.

This means that if the desired speed is  $V_r = 5.7$  m/s, the Lookup Table corresponding to a voltage amplitude of 200 V will be used and the frequency will be somewhere between 33 and 36 Hz. Thus, one can see the need to demultiplex the input  $V_r$  for one of the 6 lookup tables depending on its value.

- 3) Demultiplex  $V_r$  to select the corresponding Lookup Table and get the optimum frequency value:

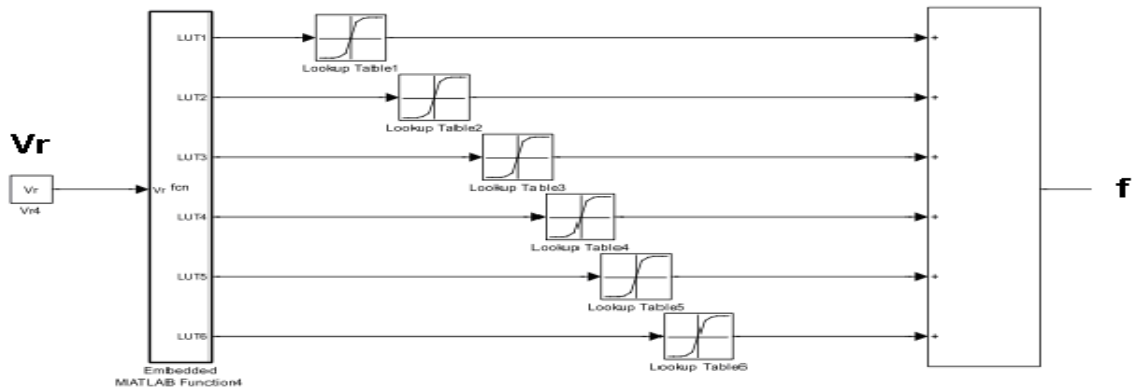
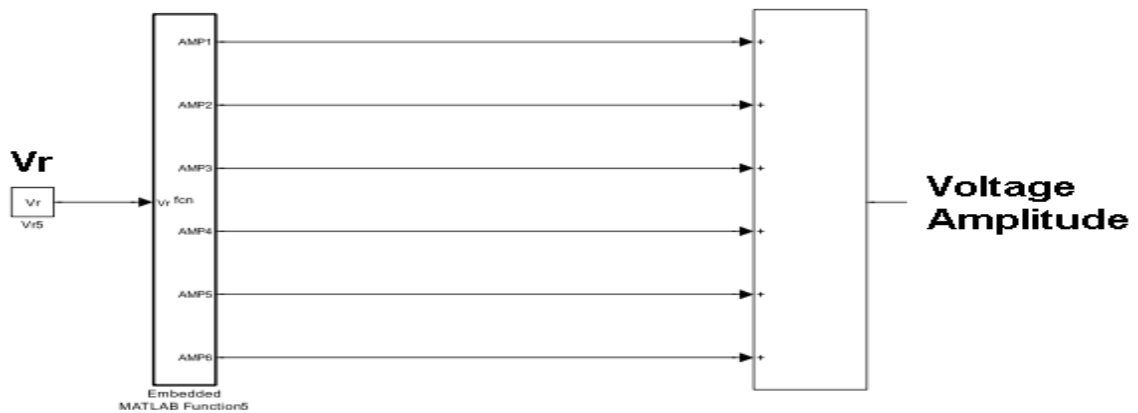


Figure 5.20. Frequency demultiplexer block.

Figure 5.20, shows the blocks corresponding to the demultiplex action in which an arbitrary value of rotor speed ( $V_r$ ) is set and a specific Lookup Table is implemented depending on the range of voltage amplitude and frequency  $V_r$  is located. After the optimum lookup table is chosen, they output the value of frequency to be part of the sinusoidal voltage source that enters in the electrical block, that is block 3. In Figure 5.21 one can see another demultiplex implementation for which an optimum value of amplitude voltage is set upon the range under the reference value of  $V_r$  is covered. At this point, the voltage source of the system is completely defined, and the actual rotor speed value of the system is expected to be really close from the reference value,  $V_r$ , after the system reaches the steady state, which of course must be before 2 s, as established in step 1).



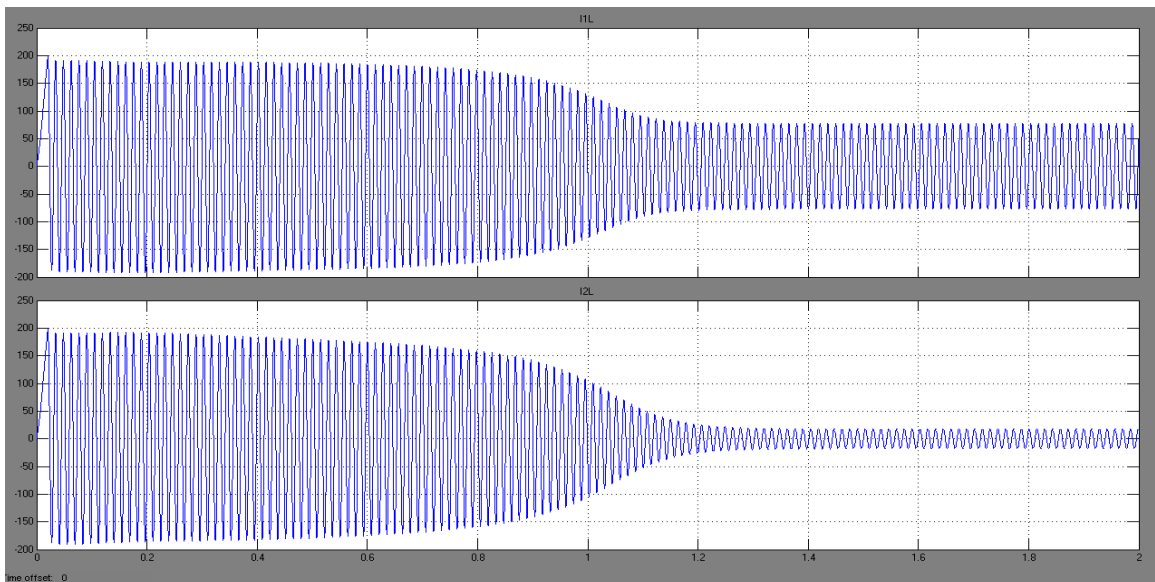
**Figure 5.21. Voltage amplitude, demultiplexer block.**

4) Validation of the simulation. Recalling the parameters of the model we have:

Desired  $V_r = 12$  m/s

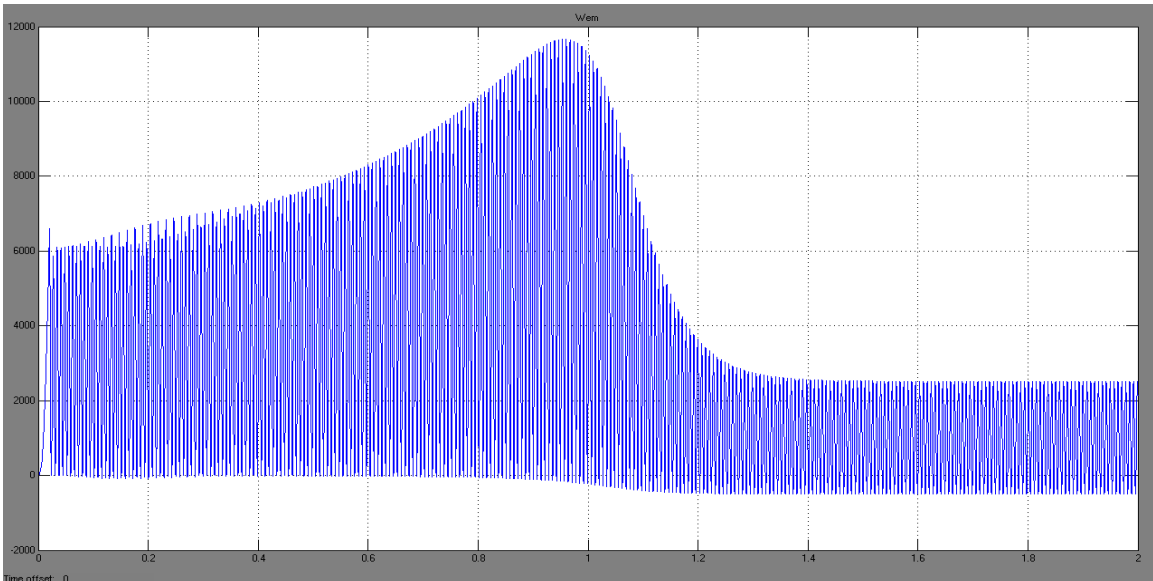
$m=300$  Kg,  $W_d=1000$  N,  $b=0$ ,  $c=0$ ,

Figure 5.22, shows the response in time of the stator and the rotor currents. One can see an initial maximum peak value of almost 200 A, for both currents at the start, when the speed rotor is zero. After the rotor starts moving the current has a small decay and maintain this value until they start to decay once again in a progressive way until they reach the steady state value. One can notice that in the case of the rotor speed, the steady state value is very close to zero provided that the synchronous speed of the LIM has been reached so there is no longer current demand.



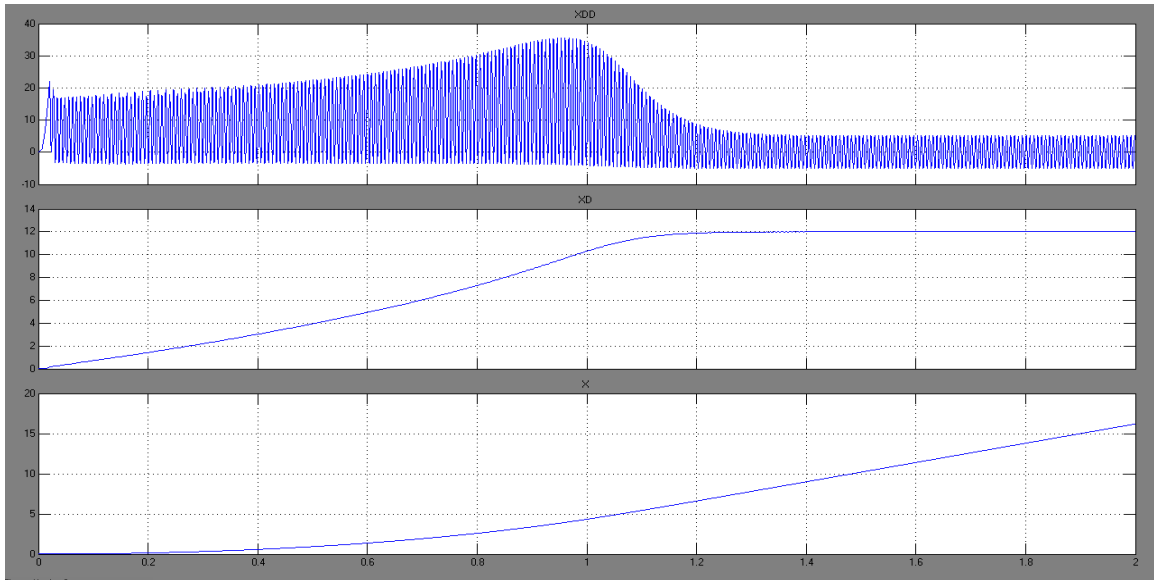
**Figure 5.22. Stator and rotor currents response using Lookup Tables.**

Figure 5.23, shows the response of the thrust over time (instantaneous thrust) in which a maximum peak value of 6600 N stands out at the starting stage, the same way as the stator and rotor currents do. Soon afterwards the thrust response has a small decay rapidly until it reaches its lowest value and from this point on it begins to increase gradually until it reaches a maximum value of 11666 at time 0.96 s, time at which it begins to decay until it reaches the steady state response.



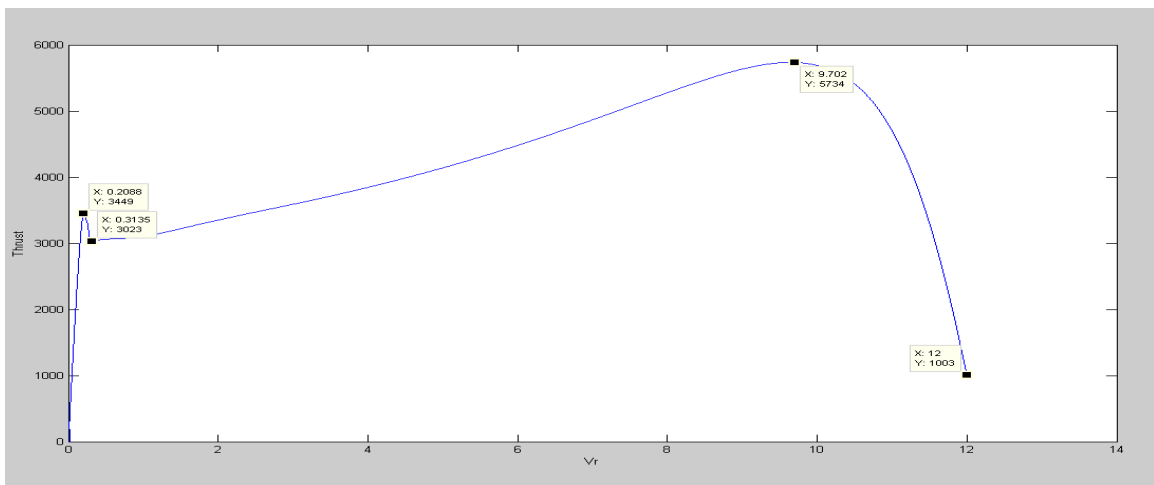
**Figure 5.23. Thrust response in time of the LIM using Lookup Tables.**

Figure 5.24, shows the response of the acceleration, speed and position of the rotor. The acceleration behaves the same way as the thrust does, with a maximum peak value of  $22 \text{ m/s}^2$  at the initial stage. The speed starts at zero and then it traces a smooth path which increases gradually until it stabilizes at the steady state value around  $12 \text{ m/s}$ , which was the value set as reference from the beginning. The position is traced by a smooth and progressive path which starts at  $0 \text{ m}$ , reach  $9 \text{ m}$  when the motor reaches the steady state, and after  $2 \text{ s}$  the rotor has traveled around  $16.2 \text{ m}$ . One can notice that the objective of implementing the lookup tables was reached in which a rotor speed reference was enter as input to the system and the system returns the same value in the actual response.



**Figure 5.24. Acceleration, speed and position response of the rotor.**

Figure 5.25, shows the response of the mean thrust by varying the speed of the rotor. It can be notice once again a maximum peak value at the initial stage with a value 3449 N which drops rapidly to 3023 N and then starts to increase gradually until it reaches a maximum value around 5734 N and then begin to decay quickly until it reaches and settle at 1003 N, time at which the rotor speed has reached the steady state speed of 12 m/s<sup>2</sup>.



**Figure 5.25. Mean thrust Versus rotor speed response of the LIM using Lookup Tables.**

## 5.7 Calibration of a PID Controller

### 5.7.1 The PID Controller

PID stands for Proportional-Integrative-Derivative which corresponds to the terms operating over the error signal in the controller. The PID controller is the most widely used feedback controller in the industry. It calculates an error value as the difference between an actual (measured) signal and a reference value and then minimizes this error by adjusting the input of the system.

The PID controller is defined by the following equation:

$$u(t) = K_p e(t) + K_I \int e(t) dt + K_D \frac{d}{dt} e(t) \quad (5.6)$$

Where  $u(t)$  is the output of the PID Controller,  $K_p$ ,  $K_I$  and  $K_D$  are the proportional, integrative and derivative gains respectively and  $e(t)$  is the error signal define as:

$$e(t) = r(t) - y(t) \quad (5.7)$$

Where  $r(t)$  is the reference value and  $y(t)$  is the output of the system.

By adjusting (tuning) the three gains, the controller can provide a good control action for a specific requirement, even with no knowledge of the dynamics of the process (Ang, 2005).

The proportional term is the main gain. It makes a change to the value proportional to the current error value. A high proportional gain results in a large change in the output of the

system for a certain change in the error and if it's too high can drive the system to instability.

The integral of the integrative term is the sum of the instantaneous errors over time and it gives the accumulated offset that should have been corrected previously. The integral is then multiplied by the integrative gain and added to the controller output, decreasing the rise time and eliminating the steady state error which cannot be accomplished only with the proportional term. However, if the gain is too high it can cause undesired overshoots.

The derivative term is calculates the rate of change of the error in time and multiplies it by the derivative gain. It reduces the magnitude of the overshoot impart by the integrative term in exchange of slowing the transient response of the controller (Ang, 2005).

For this project, a PI controller was considered under the assumption that the inertia of the payload mass of the system will damp the response of the motor keeping simple the calibration of the controller. Thus, the response of the controller will be limited to only the first to terms of equation (5.6).

Figure 5.26, represents a conceptual diagram of the control system for this application, constituted mainly by the PI controller, the input voltage and the LIM. As can be seen, the PI Controller operates over the error signal, imparting the incremental of frequency necessary to lead the response of the motor to the reference value. The lookup tables block is the one that sets the nominal frequency corresponding to the value of the speed reference.

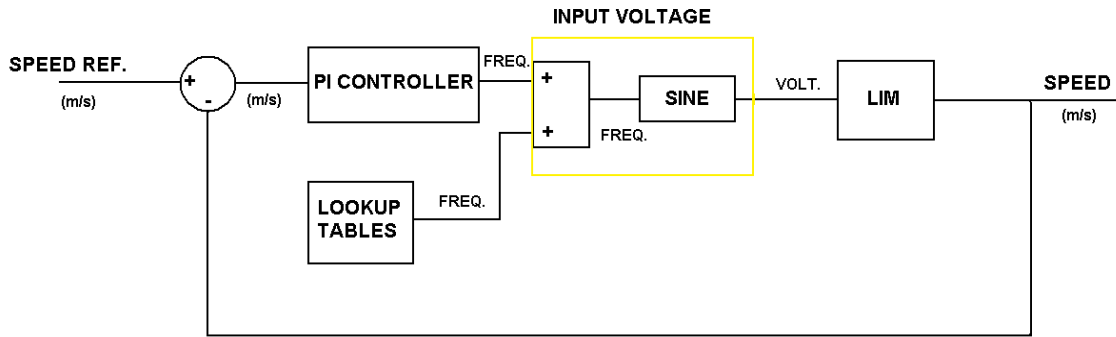


Figure 5.26. Conceptual diagram of the control system.

## 5.7.2 Methods of calibration

### Manual Tuning

Set  $K_I$  and  $K_D$  to zero, and start changing  $K_P$  until the response of the system begins to oscillate, then  $K_P$  should be set to half of that value for a "quarter amplitude decay" type response. Then increase  $K_I$  until any offset is correct in sufficient time for the process. However, too much  $K_I$  will cause instability. Finally, increase  $K_D$ , if required, until the loop is acceptably quick to reach its reference after a load disturbance. However, too much  $K_D$  will cause excessive response and overshoot.

### Ziegler–Nichols method

Another tuning method is formally known as the Ziegler–Nichols method. As in the method above, the  $K_I$  and  $K_D$  gains are first set to zero. The  $P$  gain is increased until it reaches the ultimate gain,  $K_u$ , at which the output of the loop starts to oscillate.  $K_u$  and the oscillation period  $P_u$  are used to set the gains as shown:

Control Type	$K_P$	$K_I$	$K_D$
P	$0.5 K_u$	--	--
PI	$0.45 K_u$	$1.2 K_P/P_u$	--
PID	$0.6 K_u$	$2 K_P/P_u$	$K_P P_u/8$

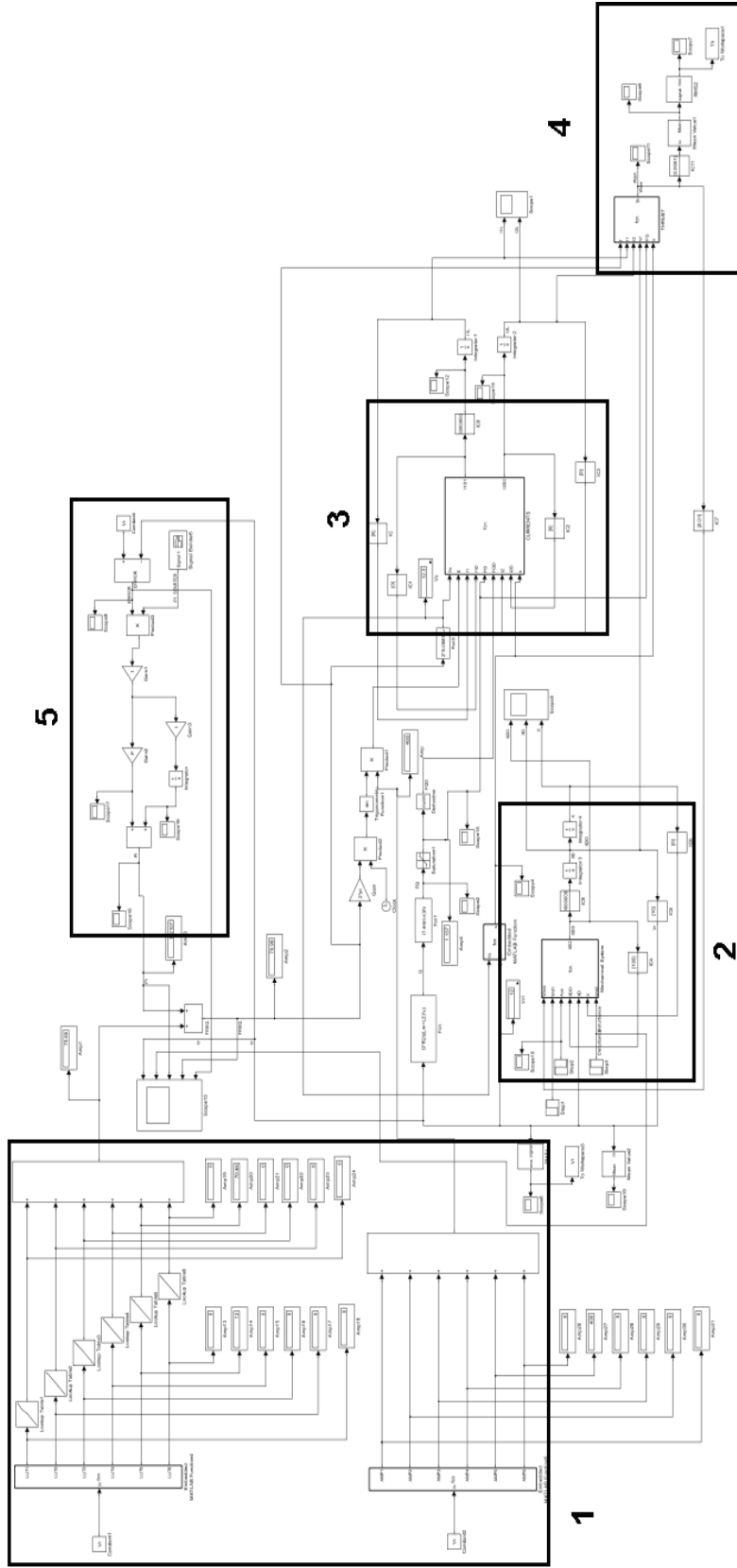
**Table 5.8. Ziegler-Nichols calibration parameters.**

(Ogata, 2002).

## 5.8 PI Controller

Figure 5.27.

Simulink Model of the LIM Using Lookup Tables and PID Controller



### 5.8.1 PI Controller response to a Disturbing Force

In the following analysis, a disturbing force of 100% of the nominal load with a value of 1000 N was added to the system at time 2 s as one can see in Figure 5.28 on the second plot from top to bottom. One also can see from this figure, that this adverse force led the system to diminish the rotor speed  $V_r$  from the reference value of 12 m/s to 11.8 m/s. The system remain this way until the PI controller is activated just before 3 s, thus leading the system to reach ones again the reference rotor speed  $V_r$  in an interval of 0.2 s (rise time) and settling after 0.4 s (settling time), allowing to identify in Figure 5.29 four main zones in the response of the system: the Transient Zone, the Steady State, the Disturbance zone and finally the PI Activated Zone where  $V_r$  stabilizes in the reference value even though the disturbance and the PI response coexist.

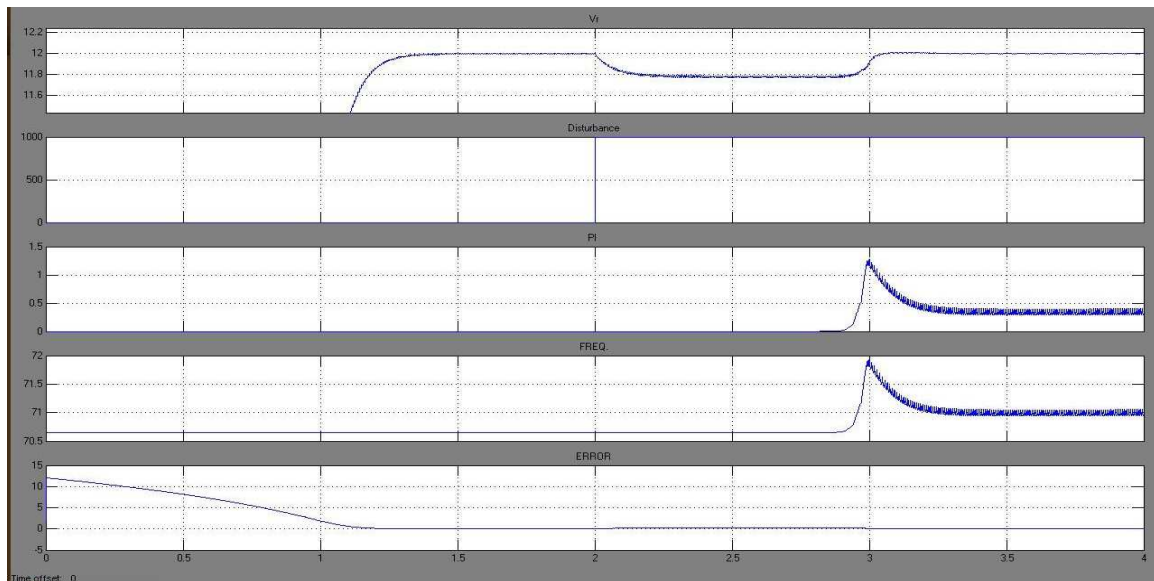


**Figure 5.28. From top to bottom:  $V_r$  (Zoomed), Disturbance, PI response, Freq. response, Error.**

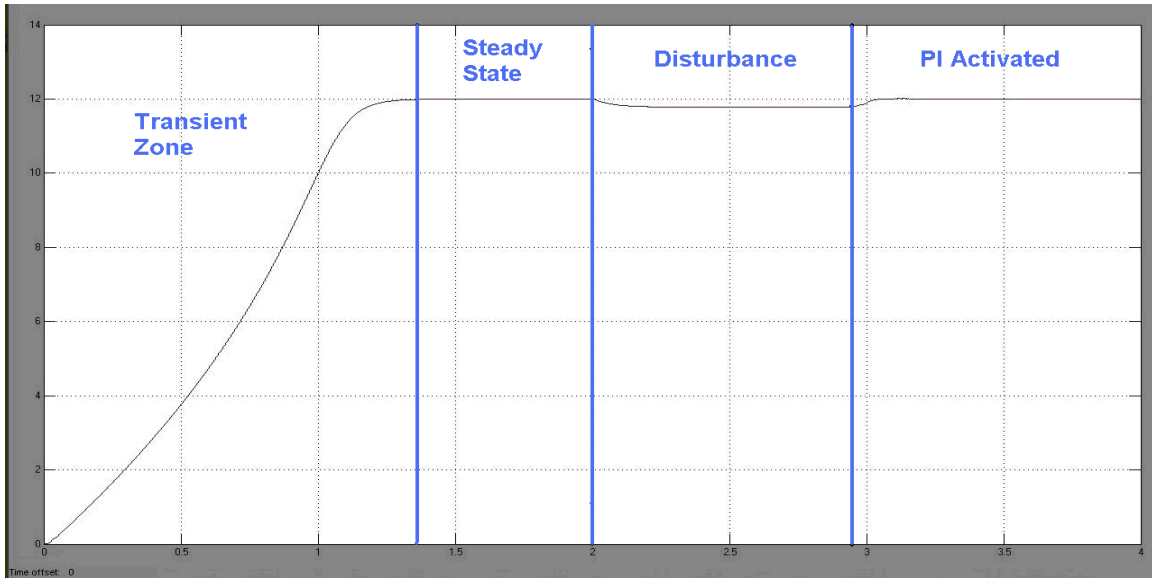


**Figure 5.29. Rotor speed ( $V_r$ ) Vs Time.**

Figure 5.28, also shows the simultaneously response of the PI controller and the Error, which are shown in detail on Figure 5.30 and Figure 5.31. One can see how the PI controller provide the system with an incremental of frequency with a maximum value of 1.3 Hz at 3 s and then drops rapidly until it stabilizes in a mean value of 0.35 Hz. The gains of the PI controller were  $P = 15$  and  $I = 300$  obtain by manual calibration, since the Ziegler-Nichols method didn't result in an optimum response attributed to the high nonlinearities of the system. In Figure 5.31, one can see how the error comes from high values corresponding to the transient response of the system, until it reaches the steady state and settles around zero. Then, the disturbing force at 2 s increase the error to a value of 0.23 m/s and remains this way until the PI controller is activated at a time close to 3 s settling the error signal again to zero after 0.4 s.

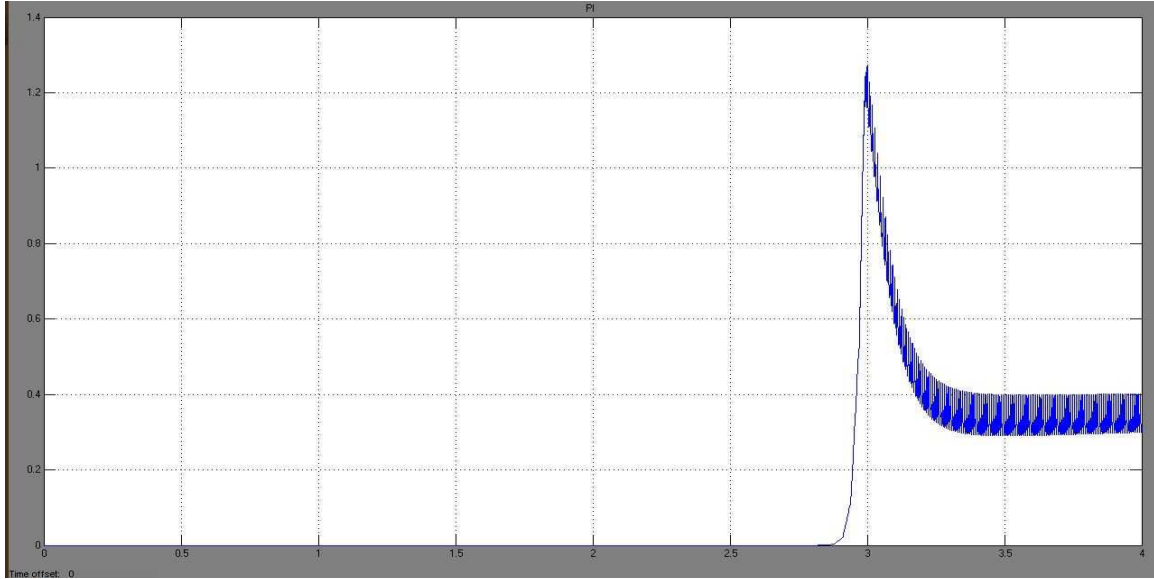


**Figure 5.30. PI Controller response.**

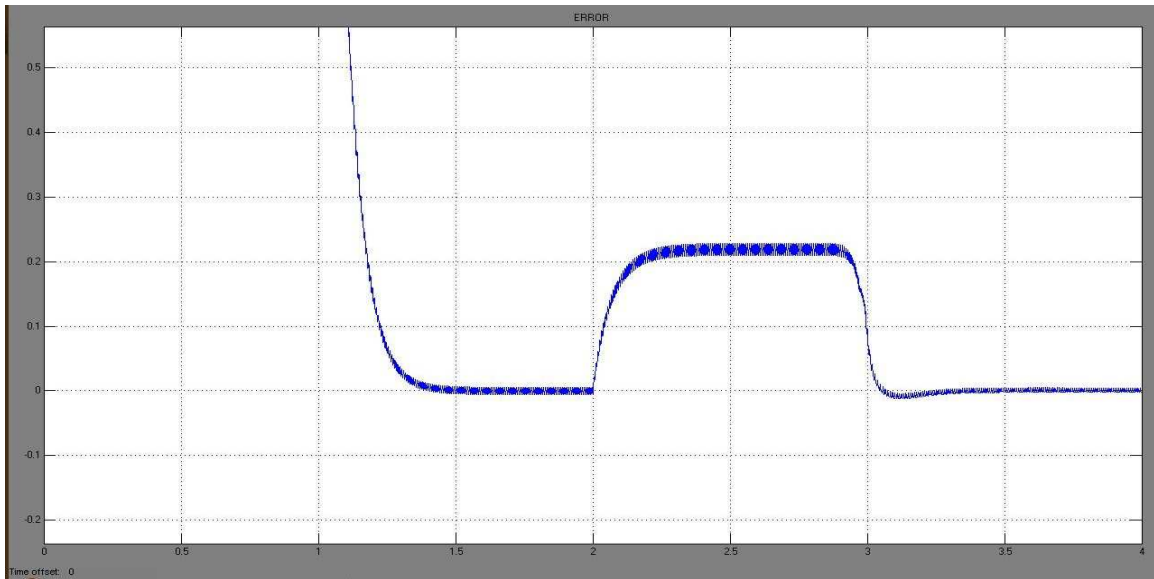


**Figure 5.31. Error between the referenced  $V_r$  and the actual  $V_r$ .**

Figure 5.32, shows the response of the rotor in terms of acceleration, speed and position. One can see how changes in the acceleration reflect the onset of the disturbing force and

the PI response. One also can notice how the rotor has traveled around 40 m after 4 s over a smooth response path.

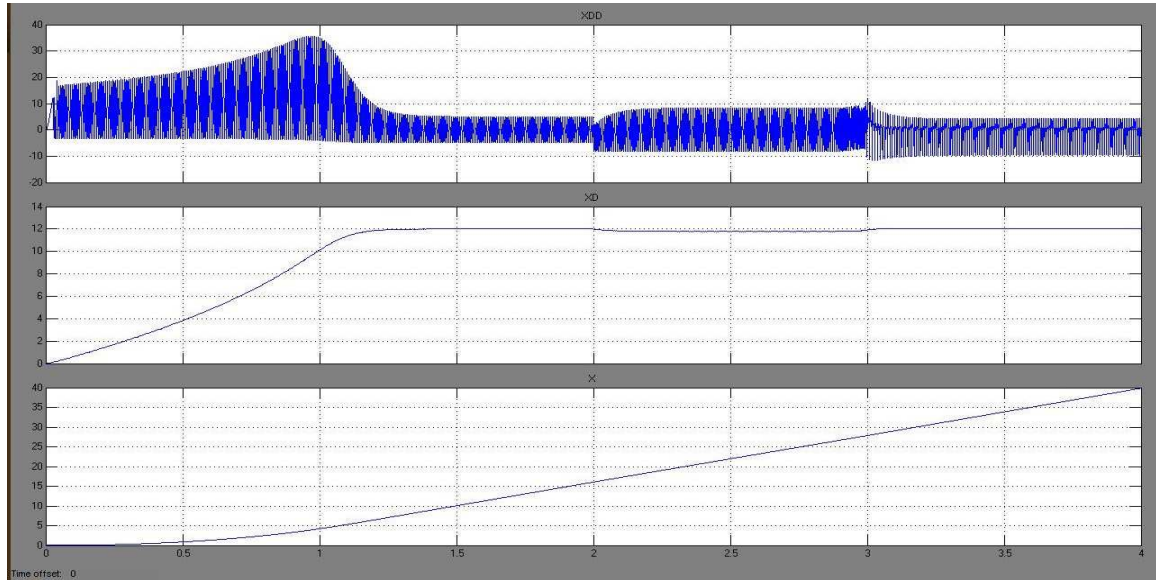


**Figure 5.32. From top to bottom: Acceleration, speed and position of the rotor.**

Figure 5.33, also shows how the onset of the disturbance and the PI response affect the electric response of the system by trying to overcome these effects. For example one can notice how the rotor current is increased when the disturbance appears but then it decreases by the action of the PI controller. The stator current trace the same tendency in its response, however it increases its amplitude after the PI, provided that by increasing  $V_r$ ,  $R_2/s$  will increase while  $R_2f(Q)$  and  $L_m(1-f(Q))$  will decrease in the per phase equivalent circuit, thus decreasing  $I_2$  but having a large increase in the magnetizing current ( $I_m$ ) and as a consequence an overall increase in the stator current  $I_1$ .

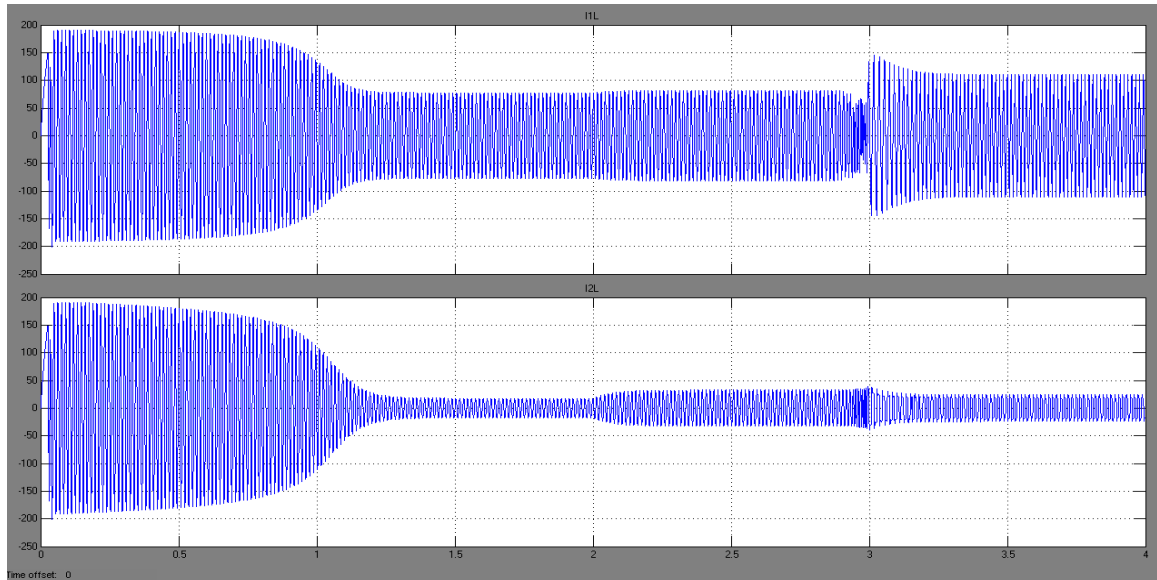


**Figure 5.33. From top to bottom: Stator and rotor currents.**

### 5.8.2 PI Controller response to a Disturbing Force and a change on the Referenced Rotor Speed ( $V_r$ ).

A disturbing force of 100% of the nominal load with a value of 1000 N was added to the system at time 2 s as one can see in Figure 5.34. However the PI controller was also activated at the same time trying to overcome the effect of the disturbance immediately, settling the rotor speed to the referenced value after 0.5 s, as can be seen in Figure 5.35.

Then, at a time close to 3s, a change in the reference value of the rotor speed  $V_r$  take place. In terms of the simulation model, this means that the reference value of  $V_r$  changes for the input of the lookup tables and also changes as the set value of the PI controller. Once the change on the set value is done, the lookup tables change immediately the response to the new value of frequency, and if is necessary the second demultiplexer also will change the value of the voltage amplitude. Simultaneously, the

PI controller is still activated and is absorbing all the possible instabilities this action causes. Finally, the system reaches the new speed reference after 0.4 s and settles 0.3 s later. The gains of the PI controller have changed to  $P=6$  and  $I=50$ , once again by manual calibration, since different conditions are affecting the stability of the system.

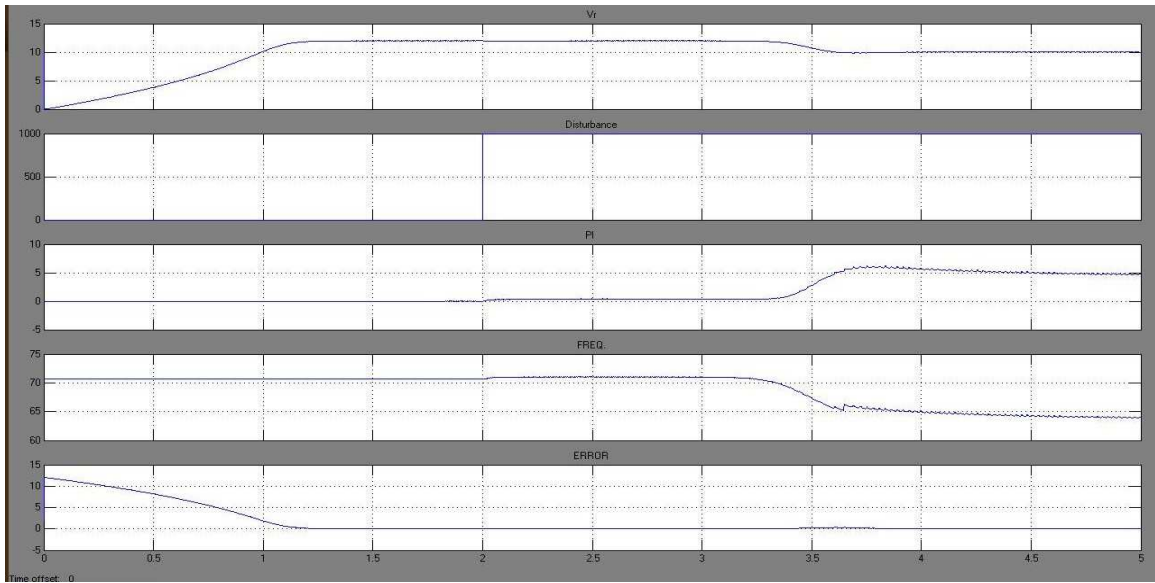


Figure 5.34. From top to bottom: Vr, Disturbance, PI response, Frequency response, and Error

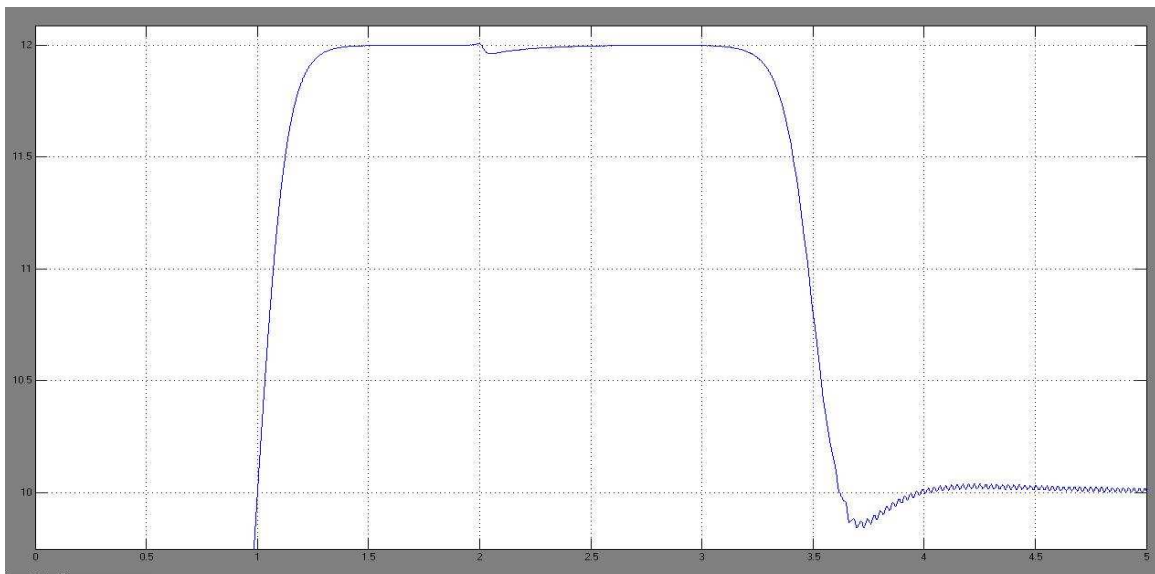
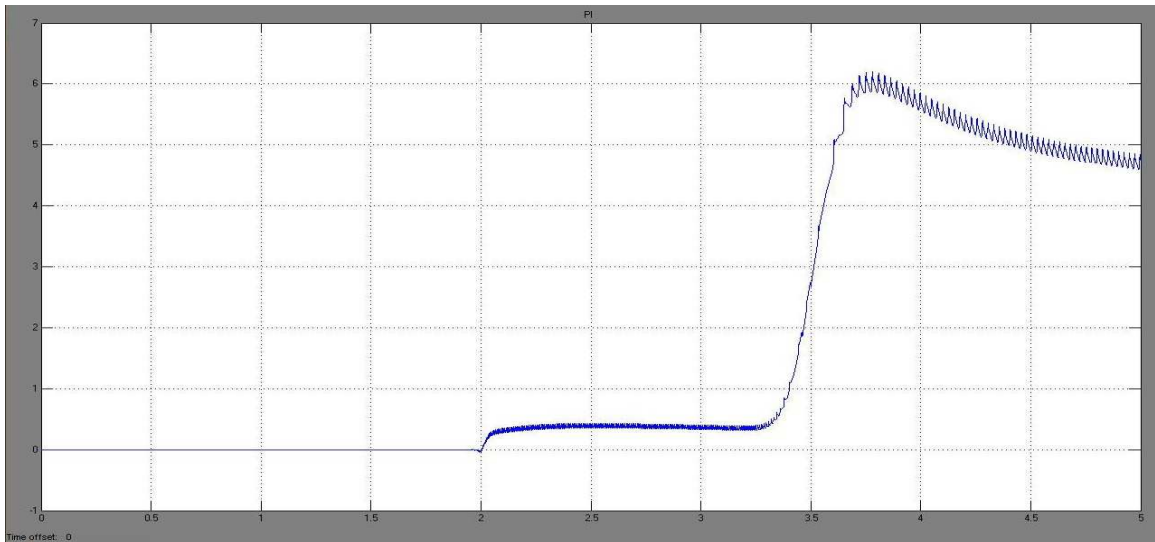
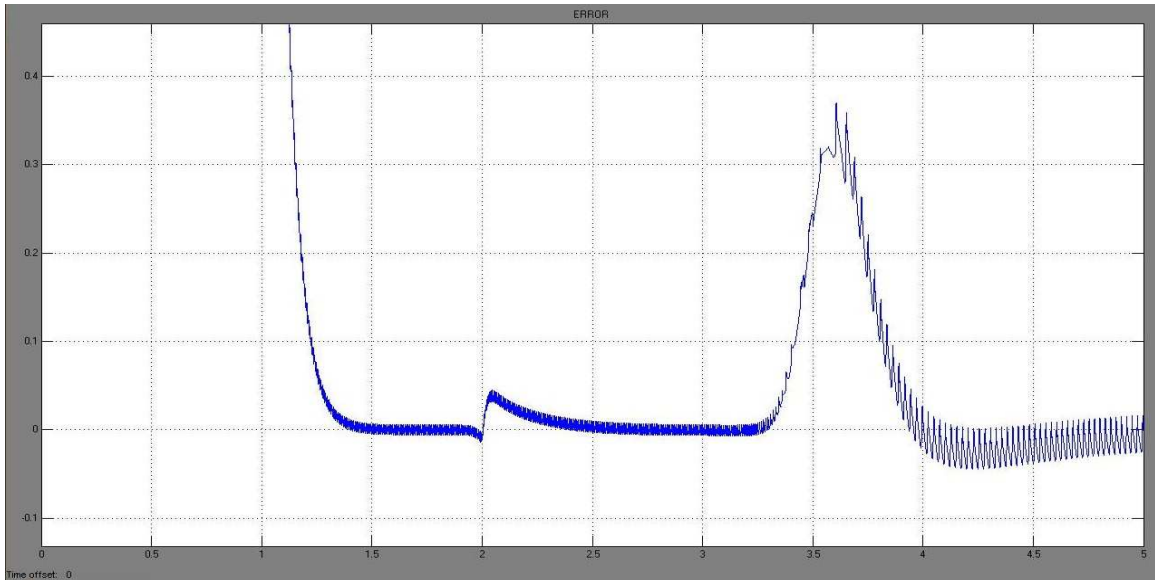


Figure 5.35. Rotor speed Vr (Zoomed).

Figure 5.34, also shows the simultaneously response of the PI controller and the Error, which are shown in detail on Figure 5.36 and Figure 5.37. One can see how the PI controller provide the system with the required frequency for each situation. At first it delivers a small value of frequency around 0.5 Hz that leads the system to overcome the disturbance effects and reach the reference speed. Then, 1.3 s later it increases rapidly to a higher value of frequency, about 6 Hz that overcomes the effects of changing the reference speed. Once it gets to the maximum value, it starts to decrease gradually until some value around 4.7 Hz. In Figure 5.37, one can see how the error comes from high values corresponding to the transient response of the system, until it reaches the steady state and settles around zero. Then, the disturbing force at 2 s increases the error to a maximum value of 0.05 m/s. As the PI controller has been already activated, this small error drops and settles after 0.5 s. Then, as the speed reference changed, the error increases rapidly to a maximum value of 0.35 m/s and starts decreasing by action of the PI controller settling the error signal again to zero after 0.7 s.

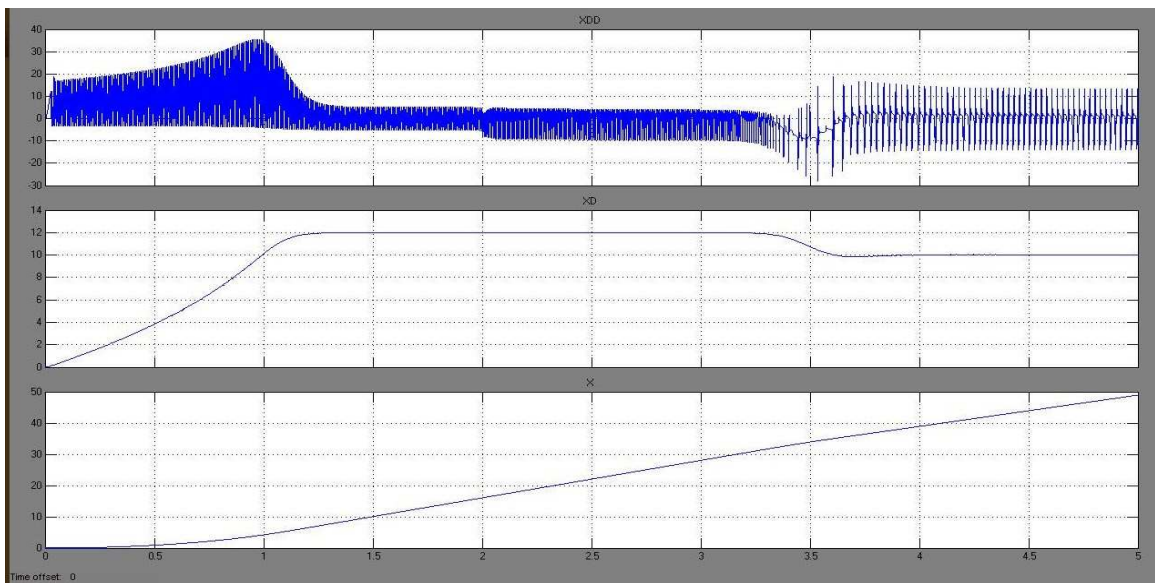


**Figure 5.36. PI Controller response.**



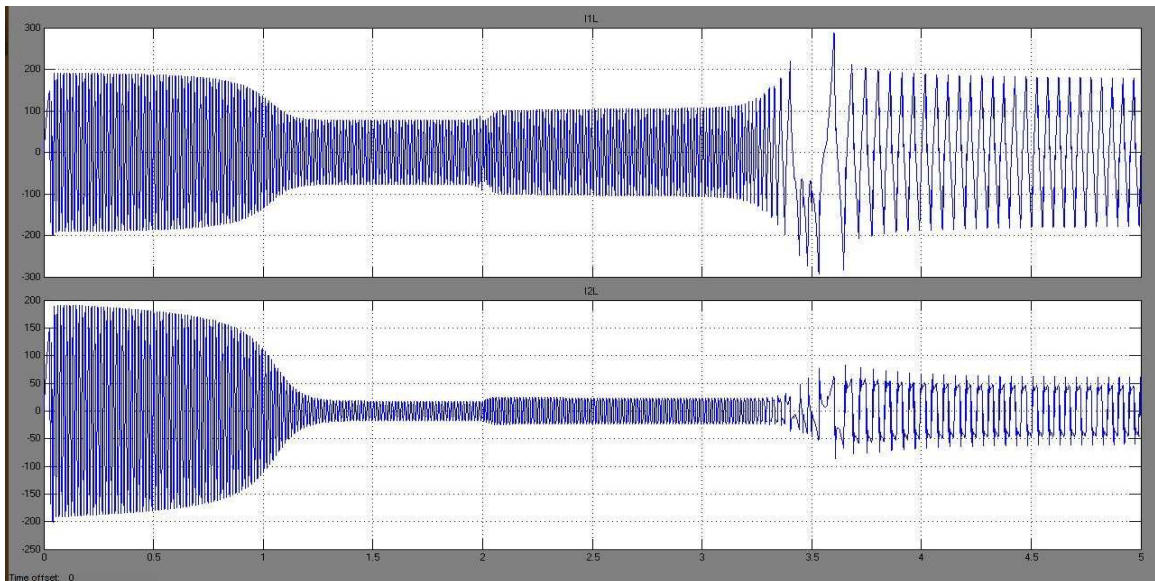
**Figure 5.37. Error between the referenced Vr and the actual Vr.**

Figure 5.38, shows the response of the rotor in terms of acceleration, speed and position. One can see how changes in the acceleration reflect the onset of the disturbing force, the change in the speed reference and the PI response. One also can notice how the rotor has traveled around 50 m after 5 s over a smooth response.



**Figure 5.38. From top to bottom: Acceleration, speed and position of the rotor.**

Figure 5.39, also shows how the onset of the disturbance, the change of speed reference and the PI response, affect the electric response of the system by trying to overcome these effects. For example one can notice how the rotor current has a small increase when the disturbance appears simultaneously with the PI response and how it has a major increase due to the change of speed reference. The stator current trace the same tendency in its response. The increase in both currents due to the change of speed reference, can be explained as a decrease in  $V_r$  causes the slip ( $s$ ) and  $R_2/s$  to decrease, while  $R_2f(Q)$  and  $L_m(1-f(Q))$  increase, thus increasing the value of  $I_2$  and decreasing the magnetizing current ( $I_m$ ), resulting in an overall increase of the stator current  $I_1$ . Refer to Figure 3.6 which illustrate the per phase equivalent circuit for a LIM.



**Figure 5.39. From top to bottom: Stator and rotor currents.**

## 6 METHODOLOGY AND PROCEDURES

### 6.1 Overview

Next, the Baldor Motors Platform (Motor Test-Bench), located in the Ocean Energy Lab at Seatech (Florida Atlantic University), is going to be used in order to validate previous analysis and simulations, in which was concluded that a Linear Induction Motor (LIM) response in terms of its stator and rotor currents is practically the same as the response of a Rotary Induction Motor (RIM) in steady state, establishing certain equivalences by changing the most predominant parameter ( $X_X$  as can be seen in Table 4.2 for the RIM) in order to equalize the Thevenin values for both machines.

### 6.2 Test Bench: General Specifications

Machine	HP	Volts	Amps	Hz	RPM	Ph	Poles	Design	Frame	Drive
Motor	2	208-230/460	6.8-6.3/3.15	60	1755	3	4	B	145T	SP1203
Generator	3	230/460	7.6/3.8	60	1750	3	4	B	182TC	SP1204

**Table 6.1. General specifications for the motors in the Test Bench.**

Unidrive	Input Volt	Output Volt	Input Freq	Ph	Peak current normal duty	Max. output curr. Heavy duty
SP1204	208-230 V	0-230 V	50-60 Hz	3	12.1 A	10.6 A
SP1203	208-230 V	0-230 V	50-60 Hz	3	10.5 A	7.5 A

**Table 6.2. General specifications for the controlling drives.**

### 6.3 Motor parameters identification

In Section 4.3 was shown that a RIM and a LIM can be equivalent in terms of the thevenin voltage and impedance. This results led to specific modifications of the magnetizing reactance ( $X_m$ ), which is the predominant parameter of the LIM in order to tune the system to get an approximated equivalent thevenin circuit with respect to the one from the RIM, for different values of the velocity of the rotor. Then, from the dynamics of a RIM and a LIM, and using the results from Table 4.1 and Table 4.2 for case 2, simulations for both machines were done in order to obtain the electrical response for both systems, which, as was expected, was practically the same, in terms of the stator and rotor currents, thus validating the previous analysis in steady-state.

In this section, a first step for the comparison between the theoretical electric response of a LIM and an actual RIM motor is going to take place by extracting the parameters of the RIM. This is done by implementing to different tests, the No-Load Test and the Locked-Rotor Test.

#### 6.3.1 Using the Motor Test Bench to run the tests.

All the parameters stored in the drives of the test bench can be read and/or change through the key pad located directly in the front face of each drive, or by using a special software called CTSoft, which is a better and easier way to access and manipulate parameters and information in general about the system. Table 6.3, shows some parameters obtained by using the CTSoft software which are going to be used for data analysis and to obtain the basic parameters of the motor.

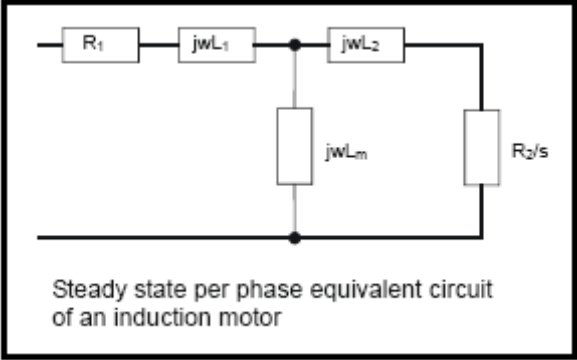
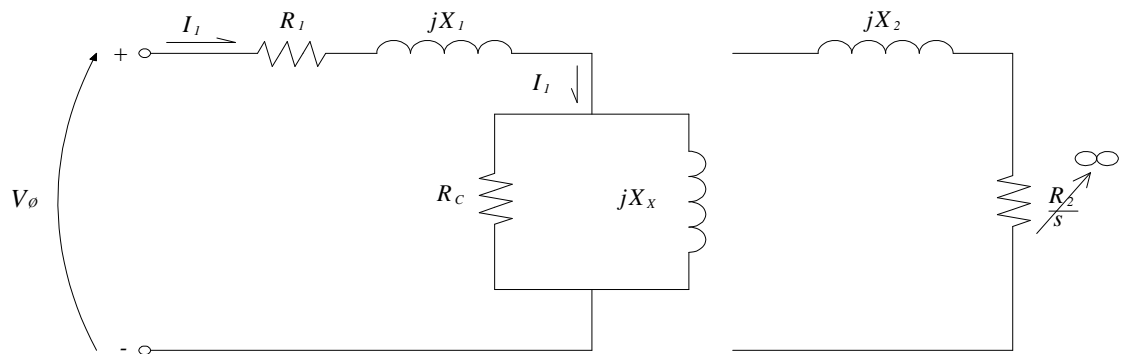
Deno.	CTSoft Param.	Description
$I_1$	Pr 4.01	Current Magnitude. Is the RMS current from each output phase of the drive. The phase current consist of an active and a reactive component.
$I_A$	Pr 4.02	Active Current. This is the torque producing current for a motor drive.
$I_R$	Pr 4.17	Reactive Current. Is the magnetizing or flux producing current for a motor drive.
V	Pr 5.02	Output Voltage. This is the modulus of the RMS line to line voltage at the inverter at the drive output frequency.
P	Pr 5.03	Output Power. Is the dot product of the output voltage and current vectors.
f	Pr 5.06	Rated frequency.
I	Pr 5.07	Motor Rated Current. Should be set at the motor nameplate value for rated current.
RPM	Pr 5.08	Motor Full Load RPM. Should be set at the motor nameplate value.
$V_{LL}$	Pr 5.09	Rated voltage (line to line)
PF	Pr 5.10	Rated power factor. Is the true power factor of the motor.
$R_s$	Pr 5.17	Stator Resistance
$\sigma L_S$	Pr 5.24	Transient Inductance. Is defined as $\sigma L_S = L_1 + (L_2 L_m / (L_2 + L_m))$  <p>Steady state per phase equivalent circuit of an induction motor</p>
$L_S$	Pr 5.25	Stator Inductance. It holds the stator inductance of the motor with rated flux. Is defined as $L_S = L_1 + L_m$ from the steady state equivalent circuit ( <b>Fig. 5.1</b> ). If this parameter is changed from a non-zero value to zero, the power factor (Pr 5.10) is automatically set to 0.85.

Table 6.3. Parameters obtained from CTSoft software.

### 6.3.2 No-Load Test

Is equivalent to the open circuit test made on transformers. It gives information related to exciting current and rotational losses. It consists on applying the rated voltage at the rated frequency to the motor. The small power provided to the motor is due to core losses, winding losses and mechanical friction. As the rotor will rotate as almost the synchronous speed, the slip value of the motor can be considered as zero and the per-phase equivalent circuit is considered as shown in Figure 6.2:



**Figure 6.2. Equivalent circuit for No-Load Test.**

Currents passing through  $R_C$  and  $L_X$  are defined by the following equations:

$$I_m = I_1 \sin \theta \quad (6.1)$$

$$I_C = I_1 \cos \theta \quad (6.2)$$

Where  $\theta$  is the impedance angle of the circuit, and  $PF = \cos \theta$ .

Once the two components of the current are known, the first two basic parameters can be obtain from this test, namely the magnetizing inductance ( $L_m$ ) and the resistance in the magnetizing branch ( $R_C$ ) defined by the following equations:

$$L_m = \frac{V_{PH}}{2\pi f I_m} \quad (6.3)$$

$$R_C = \frac{V_{PH}}{I_C} \quad (6.4)$$

### 6.3.3 Locked Rotor Test

Its equivalent to the short circuit test on transformers which provides information about leakage impedances and the rotor resistance. While the rotor is stand still low voltage is applied to the stator at the rated current. Slip = 1, as no rotation of the rotor is present, thus , the equivalent per-phase circuit is represented as follows:

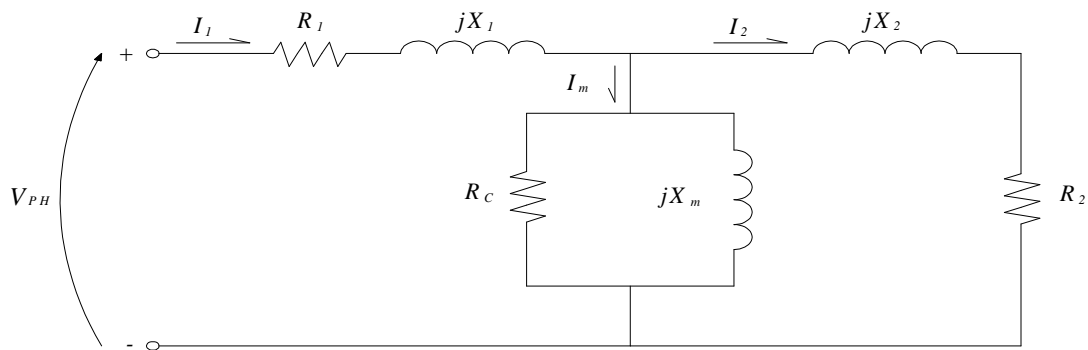


**Figure 6.3. Equivalent circuit for Locked Rotor Test.**

Since  $R_2$  is much less than  $R_C$ , the magnetizing branch is not taken into account for the next analysis:

$$Z_{sc} = \frac{V_{PH}}{I_1} \quad (6.5)$$

$$R_2 = Z_{sc} \cos \theta - R_1 \quad (6.6)$$

$$X_{eq} = Z_{sc} \sin \theta = X_1 + X_2 \quad (6.7)$$

The contribution for each reactance is determined by the following empiric table [1]:

TYPE	X <sub>1</sub> and X <sub>2</sub> as functions of X <sub>eq</sub>	
	X <sub>1</sub>	X <sub>2</sub>
Wound Rotor	0.5 X <sub>eq</sub>	0.5 X <sub>eq</sub>
Design A	0.5 X <sub>eq</sub>	0.5 X <sub>eq</sub>
Design B	0.4 X <sub>eq</sub>	0.6 X <sub>eq</sub>
Design C	0.3 X <sub>eq</sub>	0.7 X <sub>eq</sub>
Design D	0.5 X <sub>eq</sub>	0.5 X <sub>eq</sub>

**Table 6.4. Reactances proportions for the Locked Rotor Test.**

Since the motor in question is a Design B type the inductance values are determined by the following expression:

$$L_1 = \frac{2}{3} L_2 \quad (6.8)$$

#### 6.4 Actual Tests

At first instance it was clear how to proceed in the extraction of the physical parameters of the motor of the Test Bench, first by performing a No-Load Test, and then by performing the Locked-Rotor Test as was explained previously. However, it came up the question on how to block the rotor in order to keep it stand still as applying a low voltage at the rated current in the case of the Locked-Rotor Test. The main restriction was that the rotor cannot be blocked by any mechanical means, like clamps or something alike.

Then, as the Test Bench consists of a generator and the motor coupled each other, the shaft of the motor was tried to immobilize with the generator by setting a speed reference on the generator (acting as a motor) at 0 RPM and then increasing the speed reference of the motor in a progressive way using the CTSOft software. Although the generator was able to hold the motor's shaft, the test was meaningless using the drive as it will go into a current limit and/or it will trip offline long before reaching the Locked Rotor Current of the motor. An alternative way was thought by using some of the parameters stored in the drive of the motor displayed by CTSOft. This will be discussed in detail in the sequel.

#### 6.4.1 First Approach

This first approach consists on doing a No-Load Test combined with certain parameters stored in the drives and some circuit analysis as well, that finally lead into the extraction of the physical parameters of the motor

##### 6.4.1.1 No Load Test

Recalling some of the parameters in Table 6.3, a set of 5 No-Load Tests were performed in order to acquired a better approximation for the values of the physical parameters of the motor  $L_m$  and  $R_c$  by averaging the measures.

Even though the power factor is given by CTSOft, this value is not the actual one, instead it is the rated PF calculated from the autotune run in first place, which is going to be explained in detail in the Test Bench procedures section in Section 8.3.3.1 of the Appendix. Remember the PF is the cosine of the impedance angle, the angle by which

the current lags the voltage, and since the impedance is going to be a function of the slip, PF will also be a function of the slip, thus is going to be variable.

By using equations (6.1) to (6.4) and parameters from Table 6.3, the values of Rc and Lm can be found as follows:

- Calculation of the impedance angle.

$$\cos \theta = \frac{P_{PH}}{V_{PH} I_1} = \frac{(\text{Pr 5.03})/3}{\frac{(\text{Pr 5.02})}{\sqrt{3}} * (\text{Pr 4.01})}$$

$$\theta = a \cos \left( \frac{(\text{Pr 5.03})/3}{\frac{(\text{Pr 5.02})}{\sqrt{3}} * (\text{Pr 4.01})} \right) \quad (6.9)$$

- Calculation of the currents passing through Rc (Ic) and Lm (Im):

$$I_m = I_1 \sin \theta = (\text{Pr 4.01}) \sin \theta$$

$$I_c = I_1 \cos \theta = (\text{Pr 4.01}) \cos \theta \quad (6.10)$$

- Calculation of the parameters Lm and Rc:

$$L_m = \frac{V_{PH}}{2\pi f I_m} = \frac{(\text{Pr 5.02})}{2\pi (\text{Pr 5.01}) I_m}$$

$$R_c = \frac{V_{PH}}{I_c} = \frac{(\text{Pr 5.02})}{I_c} \quad (6.11)$$

Table 6.5 shows the parameters measured in the 5 No-Load Tests as well as the corresponding values of  $L_m$  and  $R_c$  by use of equations (6.9) to (6.11).

<b>NO LOAD TEST MOTOR</b>							
<b>Parameters</b>	<b>NAME</b>	<b>TEST 1</b>	<b>TEST 2</b>	<b>TEST 3</b>	<b>TEST 4</b>	<b>TEST 5</b>	<b>MEAN</b>
Pr 5.02	Output Voltage (V)	204	204	204	204	204	204
Pr 4.01	Current Magnitude (A)	3.01	3.01	3.01	3.01	3.01	3.01
Pr 5.10	Rated Power Factor	0.824	0.824	0.824	0.824	0.824	0.824
Pr 5.17	Stator Resistance (ohms)	1.14	1.14	1.14	1.14	1.14	1.14
Pr 5.03	Output Power (W)	90	90	90	90	90	90
Pr 5.01	Output Freq.	60.1	60.1	60.1	60.1	60.1	60.1
$\cos\theta$	Actual PF	0.085	0.085	0.085	0.085	0.085	0.085
$\theta$	Impedance Angle (rad)	1.486	1.486	1.486	1.486	1.486	1.486
$\theta$	Impedance Angle (deg)	85.146	85.146	85.146	85.146	85.146	85.146
$I_m$	Magnetizing Current	2.999	2.999	2.999	2.999	2.999	2.999
$I_c$	Current through $R_c$	0.255	0.255	0.255	0.255	0.255	0.255
$L_m$	Magnetizing Inductance	0.104	0.104	0.104	0.104	0.104	0.104
$R_c$	Core Loss Resistance	462.400	462.400	462.400	462.400	462.400	462.400

**Table 6.5. No-Load Tests measurements and results for the motor.**

By applying the same procedure the set of 5 No-Load Tests are done also for the generator. Table 6.6 show these results.

NO LOAD TEST DYNO							
Parameters	NAME	TEST 1	TEST 2	TEST 3	TEST 4	TEST 5	MEAN
Pr 5.02	Output Voltage (V)	203	204	204	204	203	203.6
Pr 4.01	Current Magnitude (A)	3.03	3.04	3.05	3.04	3.04	3.04
Pr 5.10	Rated Power Factor	0.823	0.823	0.823	0.823	0.823	0.823
Pr 5.17	Stator Resistance (ohms)	0.566	0.566	0.566	0.566	0.566	0.566
Pr 5.03	Output Power (W)	90	90	90	90	90	90
Pr 5.01	Output Freq.	60	60	60	60	60	60
Cos $\Theta$	Actual PF	0.084	0.084	0.084	0.084	0.084	0.084
$\Theta$	Impedance Angle (rad)	1.486	1.487	1.487	1.487	1.486	1.487
$\Theta$	Impedance Angle (deg)	85.154	85.194	85.210	85.194	85.170	85.184
Im	Magnetizing Current	3.019	3.029	3.039	3.029	3.029	3.029
Ic	Current through Rc	0.256	0.255	0.255	0.255	0.256	0.255
Lm	Magnetizing Inductance	0.103	0.103	0.103	0.103	0.103	0.103
Rc	Core Loss Resistance	457.878	462.400	462.400	462.400	457.878	460.591

**Table 6.6. No-Load Tests measurements and results for the generator.**

#### 6.4.1.2 Using parameters stored on the Drives of the Test Bench

Now, the calculations of  $L_1$  and  $L_2$  are going to take place based on the definition of the Transient Inductance parameter (Pr 5.24) taken from the Control Techniques Manual: (Control Techniques, 2007)

5.24		Transient inductance ( $\sigma L_s$ )														
Drive modes	Open-loop, Closed-loop vector, Servo															
Coding	Bit	SP	FI	DE	Txt	VM	DP	ND	RA	NC	NV	PT	US	RW	BU	PS
							3		1				1	1	1	
Range	Open-loop, Closed-loop vector, Servo							0.000 to 500.000 mH								
Default	Open-loop, Closed-loop vector, Servo							0.000								
Second motor parameter	Open-loop, Closed-loop vector, Servo							Pr 21.14								
Update rate	Background read															

Open-loop, Closed-loop vector

With reference to the diagram below, the transient inductance is defined as

$$\sigma L_s = L_1 + (L_2 \cdot L_m / (L_2 + L_m))$$

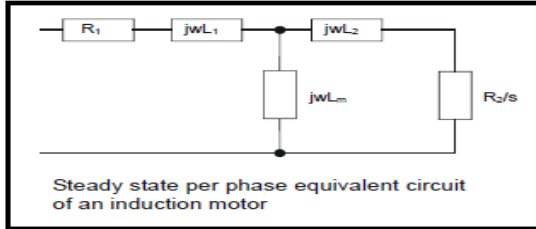


Figure 6.4. Transient Inductance parameter stored in the motor's drive.

Taken into account the fact that  $L_2=1.5L_1$  for a rotor design B and the value for the transient inductance from **Table 5.4** and its corresponding equation one can solve algebraically:

$$\sigma L_s = L_1 + \left( \frac{L_2 L_m}{L_2 + L_m} \right) \quad (6.12)$$

$$\sigma L_s = \frac{2}{3} L_2 + \left( \frac{L_2 L_m}{L_2 + L_m} \right) \quad (6.13)$$

$$\frac{2}{3} L_2^2 + L_2 \left( \frac{2}{3} L_m + L_m - \sigma L_s \right) - L_m \sigma L_s = 0 \quad (6.14)$$

By solving this equation ones find the following values for the motor and the generator:

Parameters	NAME	MOTOR	DYNO
Lm	Magnetizing Inductance (H)	0.104	0.103
Pr 5.24	Transient Inductance (mH)	10.361	8.282
L2	Rotor's Inductance (H)	0.006442	0.005114
L1	Stator's Inductance (H)	0.004295	0.003410

**Table 6.7. Values of inductance for the motor and the generator.**

At this point the values of  $R_1$ ,  $R_C$ ,  $L_1$ ,  $L_2$ , and  $L_m$  are known. The only parameter left to calculate is  $R_2$ , which can be calculated by circuit analysis for a lower frequency, for example 15 Hz, and for different loads by taking advantage of the fact that the motor and the generator are coupled and one can be programmed to be the load of the other, provided that all other parameters are known and the current magnitude (Pr 4.01) can be taken from CTSOft and represents the RMS value of the current of the stator ( $I_1$ ) in the per phase equivalent circuit shown in Figure 6.5.

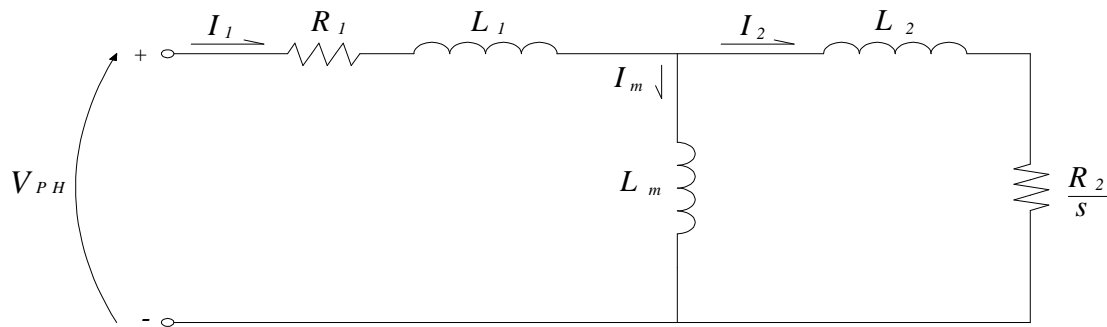


**Figure 6.5. RIM's per phase equivalent circuit.**

Where:

$$V_{PH} = \frac{(\text{Pr 5.02})}{\sqrt{3}} \quad (\text{RMS Value with } \theta = 0) \quad (6.15)$$

$$s = \frac{n_s - n_M}{n_s} \quad (6.16)$$

$$n_s = \frac{120f}{P} \quad (6.17)$$

$$I_1 = \sqrt{2}I_1 \cdot \cos(\omega_1 t - \theta)$$

$I_1 = (\text{Pr 4.01})$ , Current Magnitude. Is the RMS current from each output phase of the drive. (6.18)

$$\cos \theta = \frac{P_{PH}}{V_{PH} I_1} = \frac{(\text{Pr 5.03})/3}{\frac{(\text{Pr 5.02}) * (\text{Pr 4.01})}{\sqrt{3}}} \quad (6.19)$$

$$\theta = \cos^{-1} \left( \frac{(\text{Pr 5.03})/3}{\frac{(\text{Pr 5.02}) * (\text{Pr 4.01})}{\sqrt{3}}} \right)$$

Thus,  $I_1$  is completely defined and the only unknowns would be  $I_2$  and  $R_2$  which, as stated before, can be calculated by circuit analysis as shown in the sequel.

LOOP 1)

$$I_1(R_1 + j\omega(L_1 + L_m)) - I_2(j\omega L_m) = V_{PH}$$

$$I_2 = \frac{I_1(R_1 + j\omega(L_1 + L_m)) - V_{PH}}{j\omega L_m} \quad (6.20)$$

LOOP 2)

$$\begin{aligned}
& -I_1(j\omega L_m) + I_2\left(\frac{R_2}{s} + j\omega(L_2 + L_m)\right) = 0 \\
& -(\text{Re}\{I_1\} + j\text{Im}\{I_1\})(j\omega L_m) + (\text{Re}\{I_2\} + j\text{Im}\{I_2\})\left(\frac{R_2}{s} + j\omega(L_2 + L_m)\right) = 0
\end{aligned} \tag{6.21}$$

From the real part ones get:

$$\begin{aligned}
& \text{Im}\{I_1\}\omega L_m + \text{Re}\{I_2\}\left(\frac{R_2}{s}\right) - \text{Im}\{I_2\}\omega(L_2 + L_m) = 0 \\
& R_2 = \frac{\text{Im}\{I_2\}\omega(L_2 + L_m) - \text{Im}\{I_1\}\omega L_m}{\frac{\text{Re}\{I_2\}}{s}}
\end{aligned} \tag{6.22}$$

Three tests were made for three different loads at a frequency of 15 Hz, corresponding for a synchronous speed of 450 RPM. Table 6.8, reviews the measures and results for each test. A final average result for the current (I2) and the resistance of the rotor (R2) is shown in the last column.

The same tests were performed for the generator in order to find the same values. Table 6.9, reviews all the measurements and results.

MOTOR 15 HZ TO GET R2 AND I2					
Parameters	NAME	Load=18.3 lb-in	Load=31.1 lb-in	Load=41.9 lb-in	AVERAGE
Pr 5.02	Output Voltage (V)	56	58	60	58
Pr 4.01	Current Magnitude (A)	3.36	3.85	4.34	3.85
Pr 5.10	Rated Power Factor	0.824	0.824	0.824	0.824
Pr 5.17	Stator Resistance (ohms)	1.14	1.14	1.14	1.14
Pr 5.03	Output Power (W)	150	210	300	220
Pr 5.01	Output Freq. (Hz)	15.3	15.6	15.8	15.567
Ns	Synchronous speed	459	468	474	467
Cosθ	Actual PF	0.460	0.543	0.665	0.556
θ	Impedance Angle	1.093	0.997	0.843	0.977

	(rad)				
$\Theta$	Impedance Angle (deg)	62.596	57.114	48.306	56.006
Nr feedback	Rotor velocity	449.2	447.4	445.8	447.467
I2	Secondary current magnitude	1.270	1.842	2.670	1.927
$\Theta 2$	Secondary current angle (deg)	-2.223	-9.870	-7.269	-6.454
R2	Secondary Resistance	0.493	0.717	0.668	0.626

**Table 6.8. Measurements and results for the 15 Hz tests for three different loads on the motor.**

<b>DYNO 15 HZ TO GET R2 AND I2</b>							
<b>Parameters</b>	<b>NAME</b>	<b>Load=0 lb-in</b>	<b>Load=8 .4 lb-in</b>	<b>Load=1 3.1 lb-in</b>	<b>Load=1 7.9 lb-in</b>	<b>Load=4 2.8 lb-in</b>	<b>AVERAG E</b>
Pr 5.02	Output Voltage (V)	58	58	58	59	60	58
Pr 4.01	Current Magnitude (A)	3.51	3.59	3.69	3.79	4.61	3.597
Pr 5.10	Rated Power Factor	0.823	0.823	0.823	0.823	0.823	0.823
Pr 5.17	Stator Resistance (ohms)	0.566	0.566	0.566	0.566	0.566	0.566
Pr 5.03	Output Power (W)	30	60	90	120	270	60
Pr 5.01	Output Freq. (Hz)	15	15	15	15	15	15
Ns	Synchronous speed	450	450	450	450	450	450
Cos $\Theta$	Actual PF	0.085	0.166	0.243	0.310	0.564	0.165
$\Theta$	Impedance Angle (rad)	1.486	1.404	1.326	1.256	0.972	1.405
$\Theta$	Impedance Angle (deg)	85.119	80.423	75.949	71.951	55.697	80.497
Nr feedback	Rotor velocity	449.4	446.8	445.2	443.6	434.8	447.133
I2	Secondary current magnitude	0.208	0.476	0.776	1.041	2.516	0.487
$\Theta 2$	Secondary current angle	-60.307	-30.654	-22.834	-15.741	-11.858	-37.932
R2	Secondary Resistance	0.415	0.554	0.473	0.456	0.435	0.481

**Table 6.9. Measurements and results for the 15 Hz tests for five different loads on the generator.**

Finally, all the parameters are shown in Table 6.10:

Parameters	NAME	MOTOR	DYNO
R1	Primary Resistance (ohms)	1.14	0.566
R2	Secondary Resistance (ohms)	0.626	0.4805
Rc	Core Loss Resistance (ohms)	462.4	460.5911
L2	Rotor's Inductance (H)	0.006442	0.005114
L1	Stator's Inductance (H)	0.004295	0.003410
Lm	Magnetizing Inductance (H)	0.104	0.103

**Table 6.10. Physical parameters for the motor and the generator from the Test Bench.**

#### 6.4.2 Second Approach

This second approach consists on the combination of the same No-Load Test developed in the previous section and circuit analysis, thus, not accounting with any sort of parameter stored in the motor's drive. This procedure is going to be developed without numerical values, just as an illustrative manner.

After being developed the No-Load Test, the values of  $L_m$  and  $R_c$  are known but one can still work on the simplify circuit corresponding to this test, shown on **Figure 5.7**.

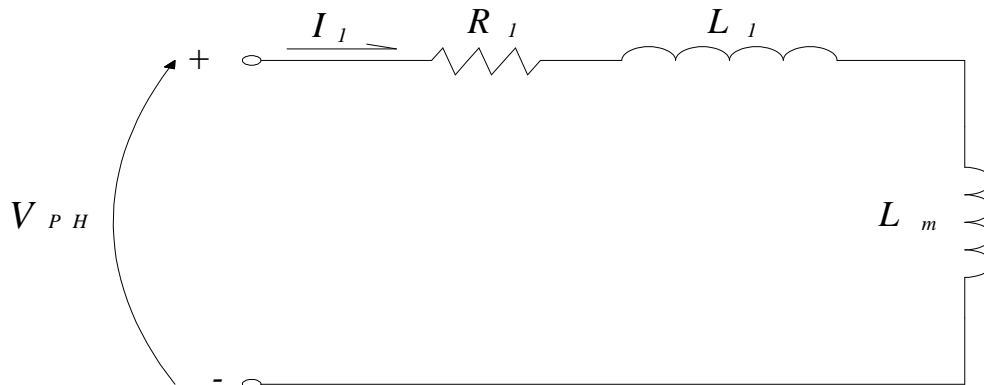


**Figure 6.6. No-Load Test simplify circuit.**

Using complex and phasorial notation:

$$\begin{aligned}
 (I_1 \angle -\theta)(R_1 + j\omega(L_1 + L_m)) &= V_{PH} \angle 0 \\
 R_1 + j\omega(L_1 + L_m) &= \frac{V \angle 0}{I_1 \angle -\theta} = Z \angle \theta
 \end{aligned}
 \tag{6.23}$$

Where  $Z \angle \theta$  is the total impedance of the circuit (is a complex number).

Then, accounting for the real part of equation (6.23) ones get the inductance of the stator

$L_1$ :

$$\begin{aligned}
 \omega L_1 + \omega L_m &= \text{Im}\{Z\} \\
 L_1 &= \frac{\text{Im}\{Z\}}{\omega} - L_m
 \end{aligned}
 \tag{6.24}$$

Now accounting for the fact that  $L_2 = 1.5L_1$  from Table 6.4 for a rotor design B,  $L_2$  is also known.

At this point the parameters  $L_m$ ,  $R_c$ ,  $L_1$  and  $L_2$  are known, thus the only parameter left is  $R_2$  which can be found by proceeding exactly the same way as developed in equations (6.15) to (6.22) .

### 6.4.3 Third Approach

The third approach consists on using the Test Bench in a way that ones could set different loads on the generator (remember that the motor and the generator are coupled), while the motor tries to overcome each load. A measure of torque, speed and slip will be taken by using the torque cell from which the signal is taken and shown through a special display device in the front door of the Test Bench. For better results, 5 sets of 5 different loads are recommended.

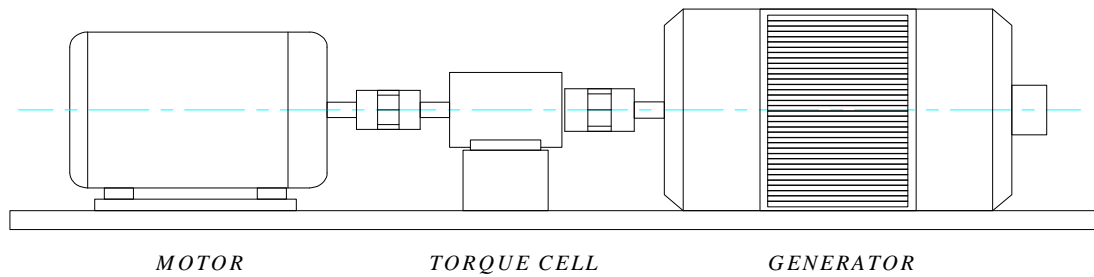


Figure 6.7. Test Bench configuration.

This is possible by using the keypad of the generator’s drive. However a better way is by using the CTSOft software, from which one can have access to all the parameters stored in the drive of the generator. These loads are set as percentages of the maximum torque (Parameter 4.08: Torque Reference). **Figure 5.9** illustrates how this is visualized on CTSOft.

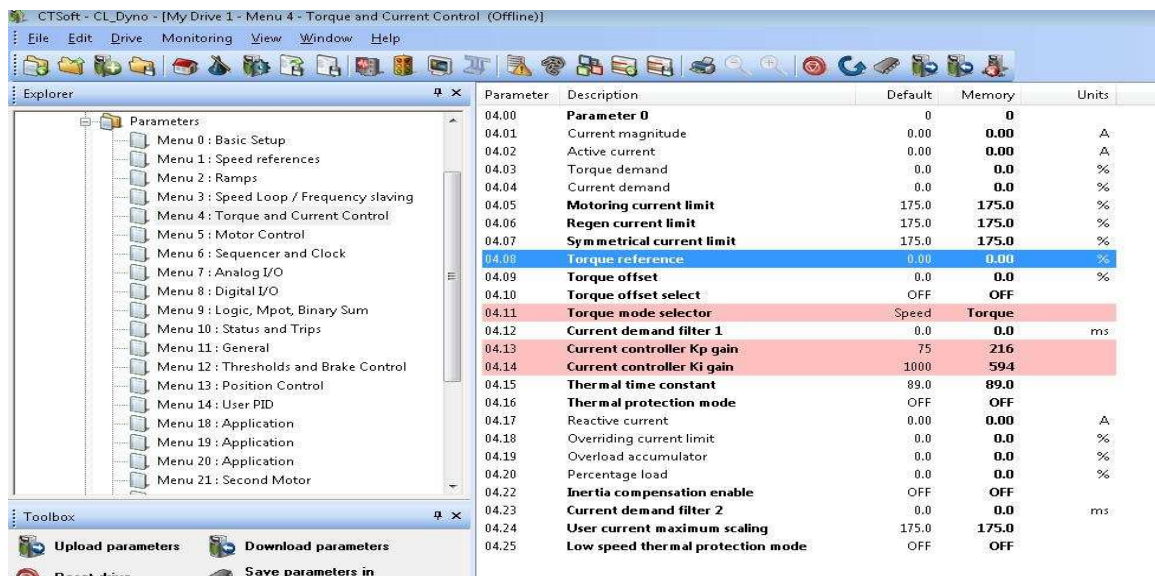


Figure 6.8. CTSOft interface, Menu 4: Torque and Current control.

### 6.4.3.1 Theoretical Calculations

The number of loads per set is explained by the implementation of the following induction motor torque equation:

$$T_e = \frac{3V_{TH}^2 \frac{R_2}{s}}{\omega_s \left[ \left( R_{TH} + \frac{R_2}{s} \right)^2 + (X_{TH} + X_2)^2 \right]} \quad (6.25)$$

As explained before, measures of torque and slip for each load are taken. Those values ( $T_e$  and  $s$ ) will be replaced on equation (6.25); then, a set of 5 unknowns still remain on the equation, namely  $V_{TH}$ ,  $R_{TH}$ ,  $X_{TH}$ ,  $R_2$  and  $X_2$ . This explains why for each set, 5 different loads have to be measured and thus 5 equations per set with a Torque-Slip pair measured for each equation is required. In other words, ones get 5 equations for 5 unknowns per each set. However, equation (6.25) is a nonlinear equation, thus a program in Matlab which solves nonlinear systems of equations is implemented and will be shown in Section 8.2 of the Appendix.

The values of  $R_s$ ,  $X_s$  and  $X_m$  can be solved by using the equations from the equivalent thevenin circuit:

$$X_m = \frac{V_{TH} X_s}{V_\phi - V_{TH}} \quad (6.26)$$

$$R_s = \frac{R_{TH} (X_s + X_m)^2}{X_m^2} \quad (6.27)$$

$$X_s = X_{TH} \quad (6.28)$$

#### 6.4.3.2 Definition of load sets

Four sets of different arbitrary loads can be set in order to average the results and have a better approximation to the actual values of the physical parameters of the motor. It's also important to account for the maximum torque of the motor which according to Horlick tests (Horlick, 2009) is 15 N.m, thus limiting the maximum load. A tentative set of loads is defined as follows:

1<sup>st</sup> set of loads: 2,5,8,11,14 N.m

2<sup>nd</sup> set of loads: 2,4,8,12,14 N.m

3<sup>rd</sup> set of loads: 3,6,9,12,14 N.m

4<sup>th</sup> set of loads: 3,5,8,11,13 N.m

Once the motor reaches its steady state for each load, measures of torque and slip must be taken and replaced in each equation until the system of 5 nonlinear equations and 5 unknowns is complete for each set.

#### 6.4.3.3 Matlab Program

Once the measures are taken, a Matlab program (MotorParam.m in conjunction with the function myfunk.m) will calculate the values of the parameters by solving the system of 5 nonlinear equations (See Section 8.2 for the script). The inputs of the program are the

number of sets, the frequency of operation, the number of poles of the motor, the torque (given by the torque cell of the test bench) and the mechanical speed (also shown in the torque cell display screen although is sensed by the encoder), thus a matrix of torque, mechanical speed and slip each with dimensions defined by (No. of sets) x 5 are built creating the system of equations.

#### 6.5 Equivalences of Parameters between the actual RIM motor and a corresponding LIM

Recalling Section 4.3, the analysis of the equivalences of the physical parameters between LIM and RIM was made by equating all the parameters outside the magnetizing branch (the middle branch) in both machines, thus allowing to equate the impedances of their magnetizing branches to finally find the value of function  $f(Q)$ ,  $Q$ , the magnetizing reactance  $X_M$  and the velocity of the rotor  $V_r$  of the LIM in terms of the physical parameters of the RIM and some other parameters of the LIM such as its geometric characteristics (stator length  $D$ ). Figure 6.9 shows once again the particularities of each per-phase equivalent circuit.

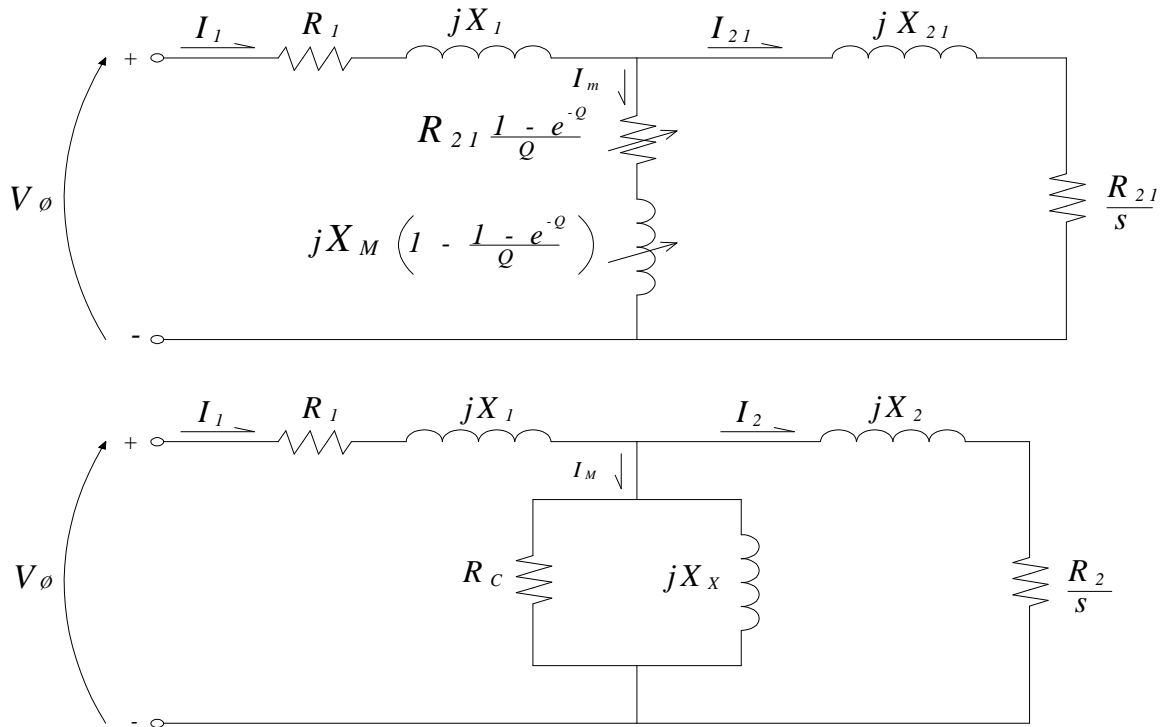


**Figure 6.9. Per-phase Equivalent circuits for a LIM (up) and a RIM (down).**

### 6.5.1 Equivalence Analysis

Although some parameters of the motor can be indirectly adjusted through the driver set of parameters, constant values of the physical parameters of the motor are going to be considered in order to validate the analysis.

Table 6.11, contains information about the physical parameters of the actual RIM motor from the Test Bench as well as data regarding how the Thevenin quantities such as the Thevenin Voltage and Thevenin Impedance vary by varying the frequency from 5 to 60 Hz.

Table 6.12, contains information regarding the physical parameters of an equivalent linear induction motor (LIM) in terms of the Thevenin values, for each specific frequency. One can see that for different frequencies, different velocities of the rotor ( $V_r$ ), as well as different magnetic inductances ( $L_m$ ) are described in the table in order to approach the Thevenin quantities from the RIM in Table 6.11.

Figure 6.10, illustrates the variation of the magnetizing inductance ( $L_m$ ) with the frequency according to Table 6.12. One can distinguished some important values by looking at the tendency of the graph. For example, in a frequency value near to 25 Hz a maximum value of  $L_m$  can be reached with a some value around 1.312 H according to Table 6.12. It is also important to notice that at a frequency near 30 Hz the parameter  $L_m$  decays to zero, and from that point on, negative values for  $L_m$  onset by incrementing the frequency. Although a negative value of  $L_m$  can arise from a certain point, this doesn't mean that the total magnetizing inductance is negative since the function  $f(Q)$  must account in the total magnetizing inductance.

It is also important to mention that Table 6.12 was built based on steady states of the LIM defined by each frequency and rotor velocity which led to a constant slip were the synchronous speed is defined as:

$$V_s = 2.\tau.f \quad (6.29)$$

Where  $\tau$  is the pole pitch of the LIM and was considered to be 0.65 m in a stator length (D) of 5.74 m. This last geometric parameter is also very important because is directly proportional to the parameter  $Q$  which is related to the velocity of the rotor as shown in

equation

(3.2).

ROTARY (RIM)													
f	w	Ns	R1	R2	Lx	L2	L1	Rc	Vph	Vth	Rth	Xth	
5	31.416	150	1.140	0.626	0.104	0.006	0.004	462.400	266.000	242.215	0.945	0.446	
10	62.832	300	1.140	0.626	0.104	0.006	0.004	462.400	266.000	251.940	1.023	0.430	
15	94.248	450	1.140	0.626	0.104	0.006	0.004	462.400	266.000	253.872	1.038	0.505	
20	125.664	600	1.140	0.626	0.104	0.006	0.004	462.400	266.000	254.559	1.044	0.606	
25	157.080	750	1.140	0.626	0.104	0.006	0.004	462.400	266.000	254.879	1.047	0.718	
30	188.496	900	1.140	0.626	0.104	0.006	0.004	462.400	266.000	255.054	1.048	0.836	
35	219.911	1050	1.140	0.626	0.104	0.006	0.004	462.400	266.000	255.159	1.049	0.957	
40	251.327	1200	1.140	0.626	0.104	0.006	0.004	462.400	266.000	255.227	1.050	1.081	
45	282.743	1350	1.140	0.626	0.104	0.006	0.004	462.400	266.000	255.274	1.050	1.205	
50	314.159	1500	1.140	0.626	0.104	0.006	0.004	462.400	266.000	255.308	1.050	1.331	
55	345.575	1650	1.140	0.626	0.104	0.006	0.004	462.400	266.000	255.333	1.050	1.457	
60	376.991	1800	1.140	0.626	0.104	0.006	0.004	462.400	266.000	255.352	1.051	1.584	

**Table 6.11. Variation of Thevenin quantities with the frequency for the actual RIM motor from the Test Bench.**

LINEAR (LIM)															
Lm	Lm(1-FQ)	L2	L1	R1	R2	Vs (m/s)	Vr (m/s)	s	D	Q	FQ	Vth	Rth	Xth	
0.108	0.104	0.006	0.004	1.14	0.626	6.5	1.160	0.822	5.740	27.073	0.037	242.217	0.944	0.444	
0.122	0.104	0.006	0.004	1.14	0.626	13	4.118	0.683	5.740	6.795	0.147	251.971	1.021	0.429	
0.156	0.104	0.006	0.004	1.14	0.626	19.5	7.823	0.599	5.740	2.835	0.332	253.919	1.037	0.502	
0.253	0.104	0.006	0.004	1.14	0.626	26	11.853	0.544	5.740	1.168	0.590	254.640	1.042	0.603	
1.312	0.104	0.006	0.004	1.14	0.626	32.5	16.331	0.497	5.740	0.167	0.921	254.999	1.045	0.715	
-0.319	0.104	0.006	0.004	1.14	0.626	39	21.328	0.453	5.740	-0.539	1.325	255.255	1.047	0.832	
-0.129	0.104	0.006	0.004	1.14	0.626	45.5	27.034	0.406	5.740	-1.082	1.803	255.449	1.049	0.953	
-0.077	0.104	0.006	0.004	1.14	0.626	52	33.634	0.353	5.740	-1.522	2.353	255.603	1.050	1.076	
-0.052	0.104	0.006	0.004	1.14	0.626	58.5	41.309	0.294	5.740	-1.891	2.975	255.747	1.051	1.200	
-0.039	0.104	0.006	0.004	1.14	0.626	65	50.324	0.226	5.740	-2.209	3.670	255.894	1.052	1.325	
-0.030	0.103	0.006	0.004	1.14	0.626	71.5	61.073	0.146	5.740	-2.488	4.436	256.041	1.053	1.451	
-0.024	0.103	0.006	0.004	1.14	0.626	78	74.088	0.050	5.740	-2.736	5.273	256.194	1.054	1.577	

**Table 6.12. Equivalent LIM in steady state.**

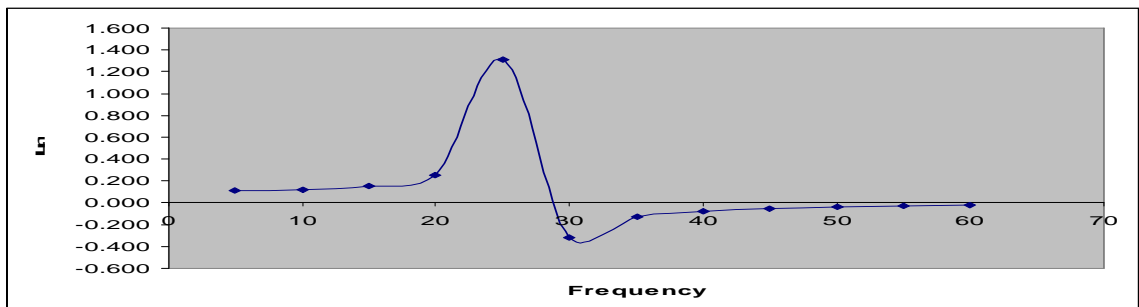


**Figure 6.10. Variation of the magnetic inductance (Lm) with the frequency for Table 6.11.**

6.5.2 Validation of equivalent RIM and LIM machines for the parameters of the actual motor of the Test Bench.

Recalling Table 6.8, the motor of the Test Bench was tested at a frequency of 15 Hz for a load of 18.3 lb-in for the first case, demanding a current magnitude (RMS value) of 3.36 A, according to the value stored in the drive that was visualized through the use of CTSoft software as shown in Figure 6.11.

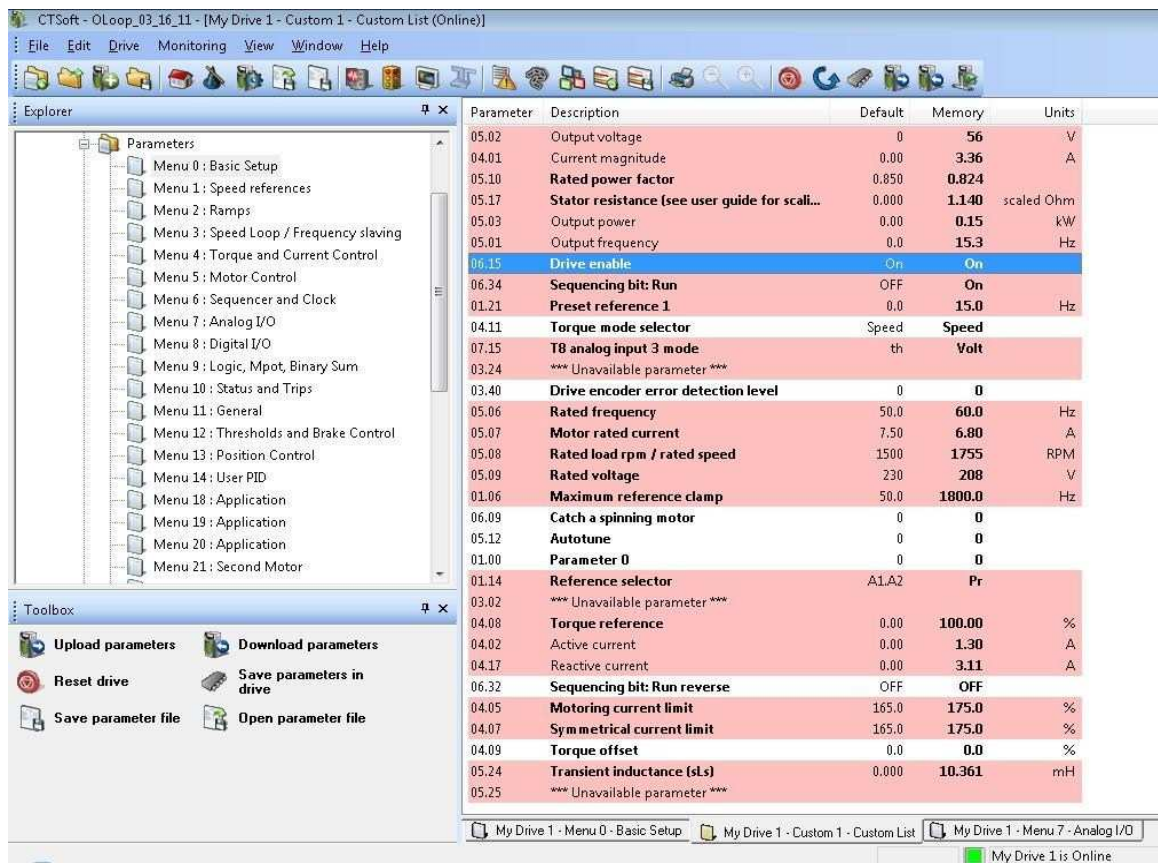


Figure 6.11. CTSoft parameters interface. Information for Table 6.8, Load=18.3 lb-in.

By using this specific load case on Table 6.8, simulations of the actual RIM and the equivalent LIM are going to take place in the sequel.

Figure 6.12 and Figure 6.13, are the Simulink models corresponding to the actual motor from the Test Bench and the equivalent LIM . Parameters for the RIM and the LIM models are reviewed in the following tables:

Parameters	NAME	LIM
R1 (ohms)	Stator Resistance	1.14
R2 (ohms)	Rotor Resistance	0.626
L2 (H)	Rotor Inductance	0.006442
L1 (H)	Stator Inductance	0.004295
Lm (H)	Magnetizing Inductance	0.156
Vs (m/s)	Synchronous Velocity	8
Vr (m/s)	Rotor Velocity	7.82
S	Slip	0.022
D (m)	Effective Length of motor	5.74
T (m)	motor pole pitch	0.26645
Q	Dimensionless parameter	2.835
f(Q)	A function of Q	0.332

**Table 6.13. . Equivalent LIM parameters.**

Parameters	NAME	RIM
R1	Primary Resistance (ohms)	1.14
R2	Secondary Resistance (ohms)	0.626
Rc	Core Loss Resistance (ohms)	462.4
L2	Rotor's Inductance (H)	0.006442
L1	Stator's Inductance (H)	0.004295
Lm	Magnetizing Inductance (H)	0.104
S	Slip	0.022

**Table 6.14. Actual RIM parameters.**

As one can see, the basic parameters are the same for both machines, except the one corresponding to the magnetizing inductance (Lm). Furthermore, the LIM motor also has other varying parameters like Q and f(Q) which induce nonlinearities to the whole system.

One can see from Figure 6.14 and Figure 6.15, that the responses for these machines is the same in terms of the RMS value of the stator current and the rotor current. One also should notice that the stator currents for both machines with a value of 3.23 A, are close from the one measured (3.36 A) shown in Table 6.8 and Figure 6.11, with an error of

3.9%, which leads to the fact that the calculated physical parameters from Table 6.14 are close to the real ones.

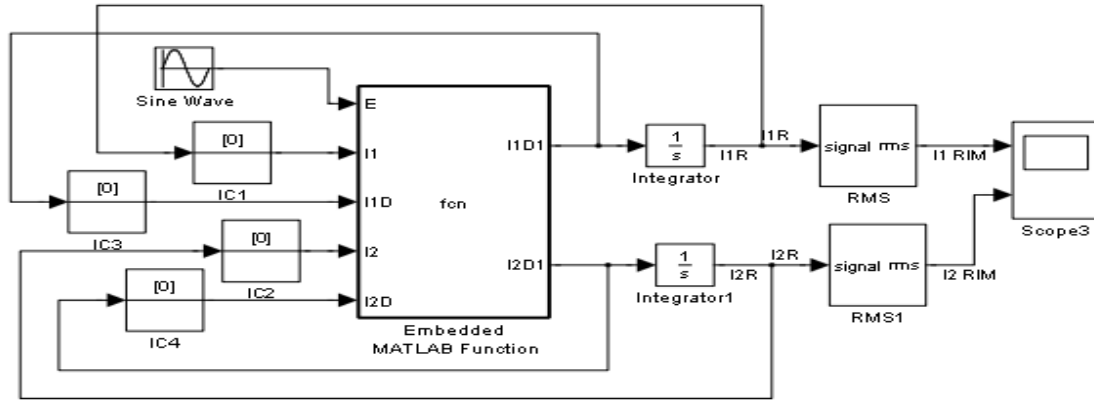


Figure 6.12. RIM simulation model for the actual motor of the Test Bench in steady state.

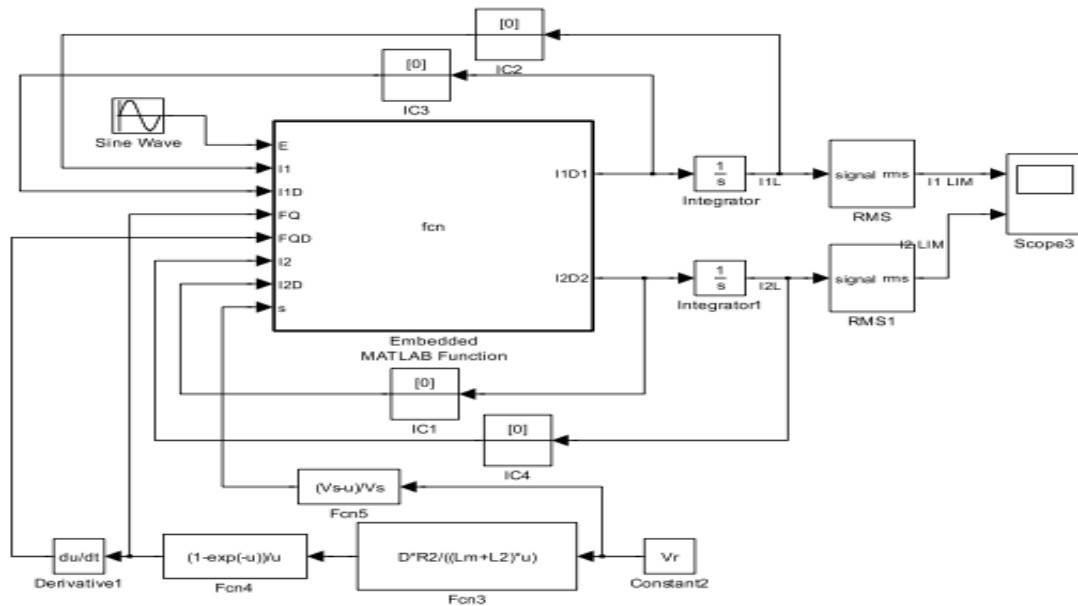
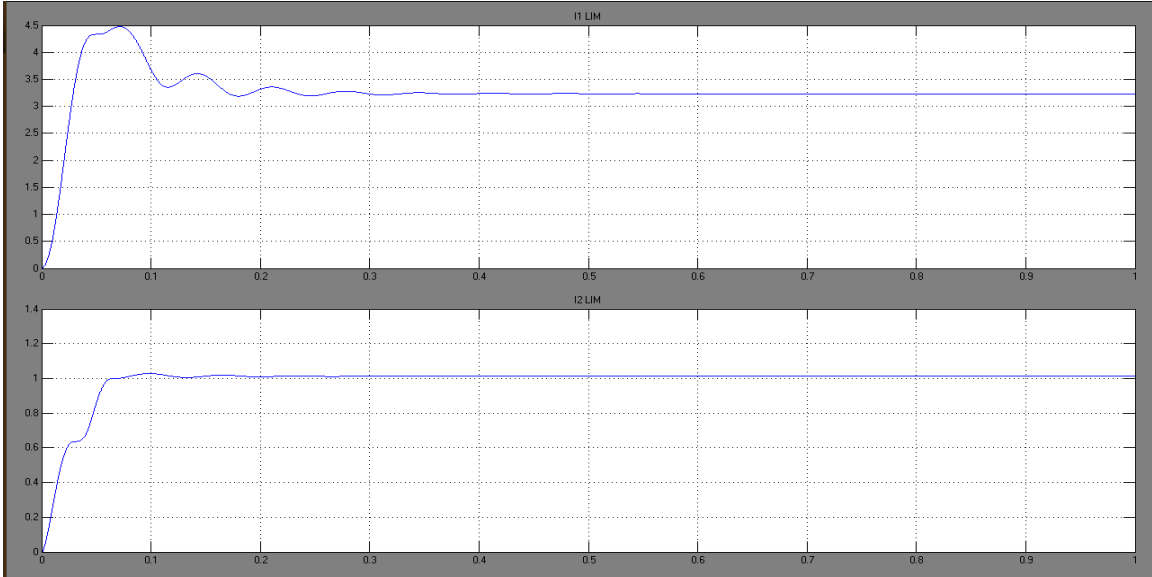
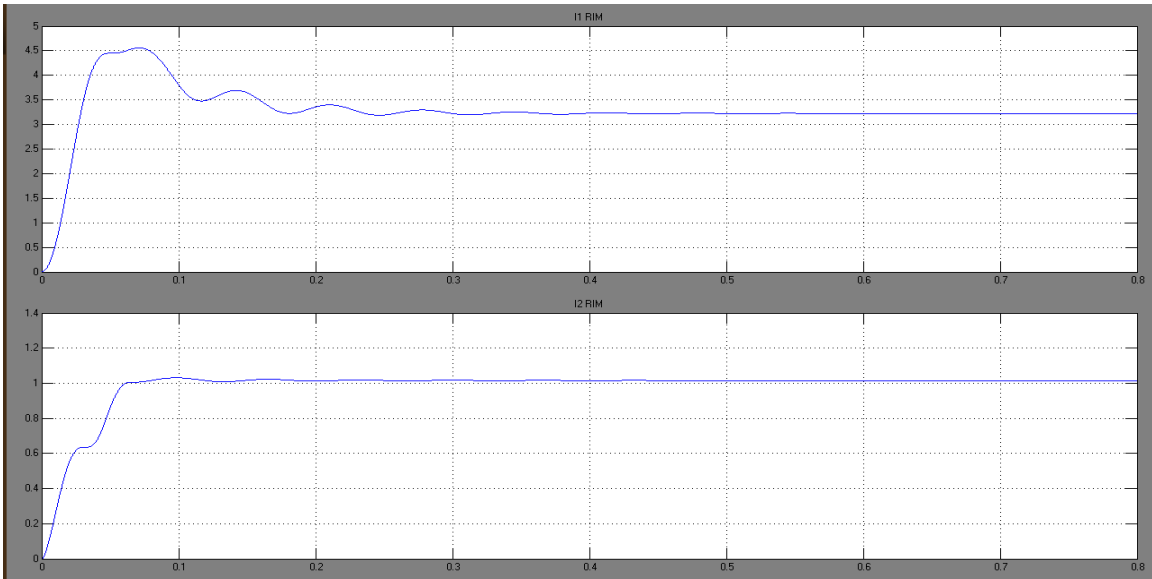


Figure 6.13. Simulation model for the equivalent LIM motor in steady state.



**Figure 6.14. RMS stator and rotor currents responses for the actual LIM.**



**Figure 6.15. RMS stator and rotor currents responses for the equivalent LIM.**

### 6.5.3 Simulation of the equivalent electromechanical system of the LIM

Table 6.15, shows all the parameters of the equivalent LIM obtain in section 6.5.1.

However some changes regarding the geometric parameters of the motor ( $\tau$  and  $D$ ) as

well as the voltage and frequency were done in order to get a more realistic model and also to match the geometric parameters with the one shown in Table 6.16.

Table 6.16, shows the corresponding parameters for the previous model from Section 5.2. The voltage amplitude, the frequency and the mass is going to be the same for both models. The Simulink models are visualized as the one in Figure 5.14.

Parameters	NAME	LIM
R1 (ohms)	Stator Resistance	1.14
R2 (ohms)	Rotor Resistance	0.626
L2 (H)	Rotor Inductance	0.006442
L1 (H)	Stator Inductance	0.004295
Lm (H)	Magnetizing Inductance	0.156
F (Hz)	Frequency	35
D (m)	Effective Length of motor	0.574
$\tau$ (m)	motor pole pitch	0.0867
Vs (m/s)	Synchronous Velocity	6.069
M (Kg)	Mass	300
V (Volts)	Phase Voltage Amplitude	300

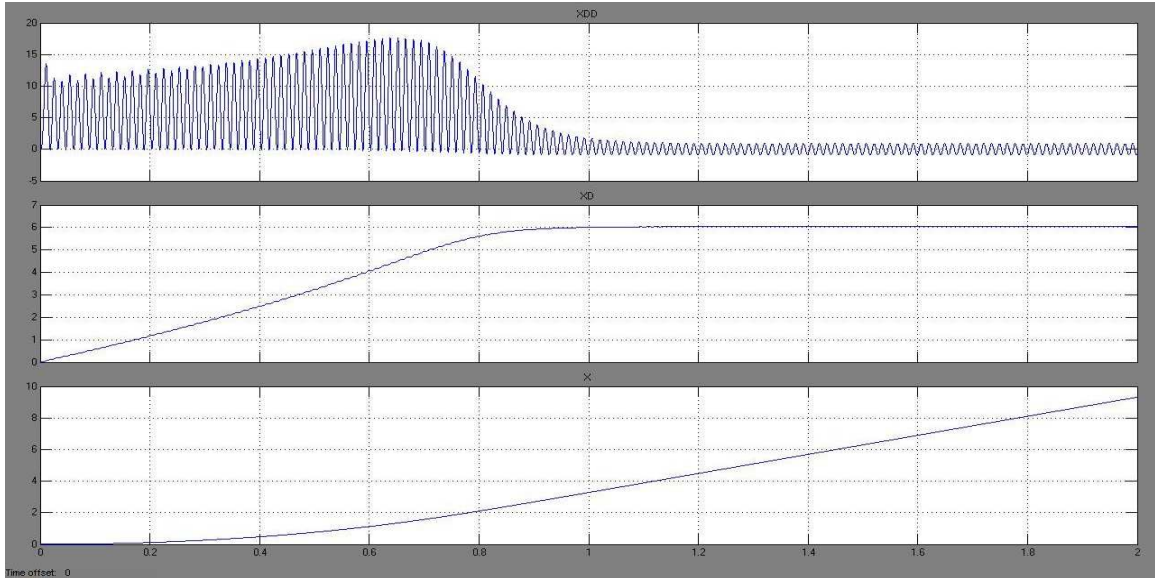
**Table 6.15. Equivalent LIM (new model).**

Parameters	NAME	LIM
R1 (ohms)	Stator Resistance	0.641
R2 (ohms)	Rotor Resistance	0.332
L2 (H)	Rotor Inductance	0.0012
L1 (H)	Stator Inductance	0.0029
Lm (H)	Magnetizing Inductance	-0.0644
F (Hz)	Frequency	35
D (m)	Effective Length of motor	0.574
$\tau$ (m)	motor pole pitch	0.0867
Vs (m/s)	Synchronous Velocity	6.069
M (Kg)	Mass	300
V (Volts)	Phase Voltage Amplitude	300

**Table 6.16. Previous model .**

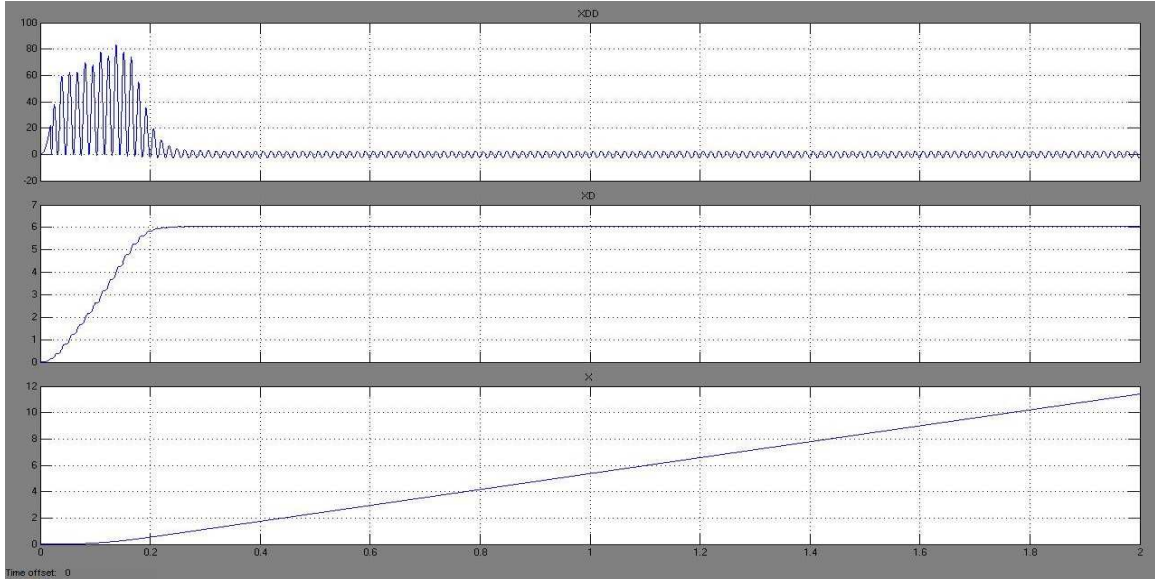
Figure 6.16, illustrates the acceleration, speed and distance response in a time interval of 2 seconds, of the secondary sheet (rotor) of the equivalent LIM, that is, the one corresponding to Table 6.15. One can see a maximum acceleration of almost  $20 \text{ m/s}^2$  at 0.7 s, time after which the acceleration starts to decay until it reaches the steady state after 1.1 s. The speed response is defined by a small “slope”, meaning that it takes a long time (1.1 s), before reaching the steady state with a speed value around 6 m/s. The

distance response show that when the system reach the steady state the secondary sheet has displaced around 4 m, and less than 10 m after 2 s.



**Figure 6.16. From top to bottom: Acceleration, speed and position of the rotor.**

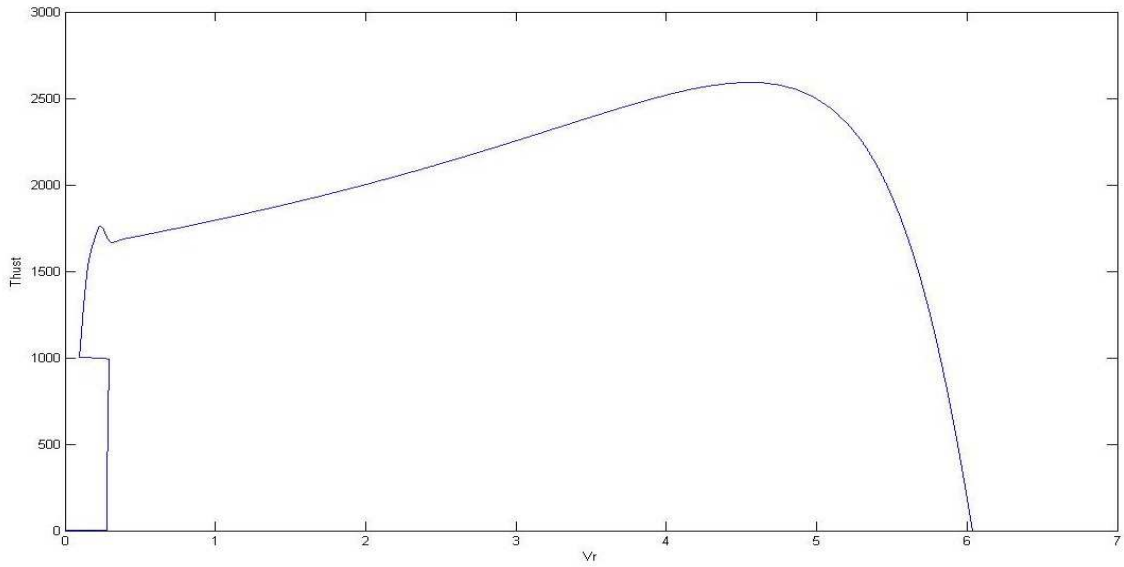
Figure 6.17, illustrates the acceleration, speed and distance response in the same time interval of 2 seconds, of the secondary sheet (rotor) of the LIM corresponding to Table 6.16. One can see a maximum acceleration of more than  $80 \text{ m/s}^2$  at 0.12 s, time after which the acceleration starts to decay until it reaches the steady state after 0.26 s. The speed response is steeper than the one from Figure 6.16, meaning that it takes less time (0.26 s), to reach the steady state speed around 6 m/s. The distance response show that when the system reach the steady state the secondary sheet has displaced less than 1 m, and almost 12 m after 2 s.



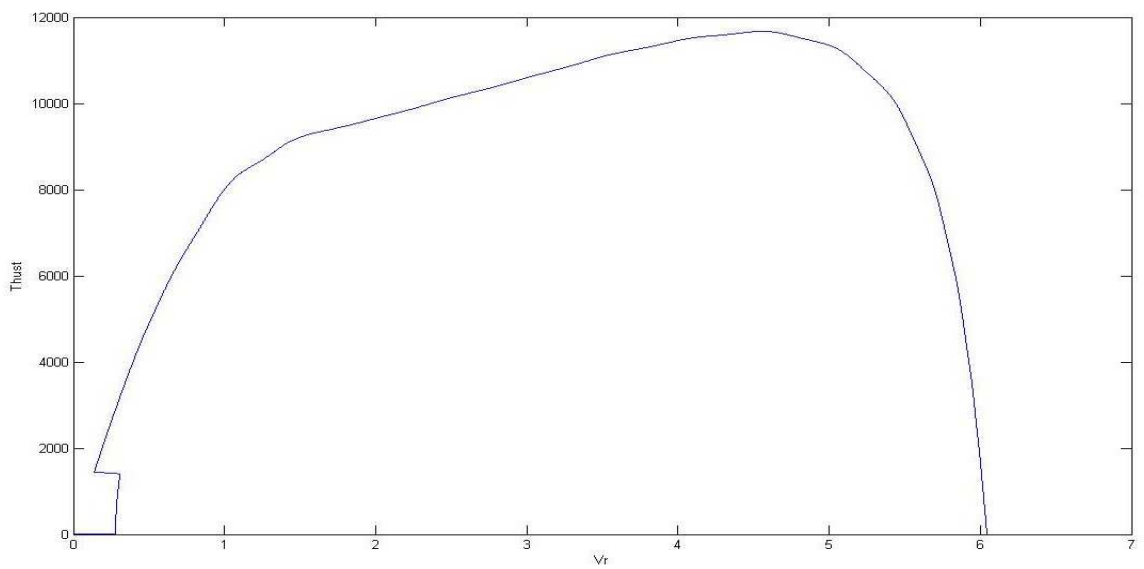
**Figure 6.17. From top to bottom: Acceleration, speed and distance responses of the previous model.**

Figure 6.18, shows the response of the thrust by changing the secondary sheet speed ( $V_r$ ) in the equivalent LIM (new model). One can notice a maximum thrust of more than 2500 N corresponding to a rotor speed ( $V_r$ ) of around 5 m/s which can be verified by observing the time at which the rotor reaches this speed and then noticing that the maximum acceleration corresponds to this same time in Figure 6.16 .

The same analysis can be made with Figure 6.19 and Figure 6.17, where the maximum thrust is less than 12000 N at a rotor speed around 4.5 m/s.



**Figure 6.18. Thrust Vs Rotor speed of the equivalent LIM (new model).**



**Figure 6.19. Thrust Vs Rotor speed of previous model.**

This analysis led to the conclusion that the LIM corresponding to Table 6.16 has a faster response than the equivalent LIM from Table 6.15 as it develops a larger thrust, allowing

the motor to obtain higher accelerations in less time which conduces to reach the steady state faster.

## 7 CONCLUSIONS

By running several tests on the Test Bench, the electrical parameters of the motor and the generator were finally found through a combination of different approaches, and also validated by a simulation model for which the RMS value of the stator current was close from the actual value measured, with an error of 3.9 % as showed in section 6.5.2.

In an attempt to define an equivalence of the parameters between the LIM and RIM, the Thevenin quantities for both per phase equivalent circuits were chosen as the criterion to be set equal for both cases, under the assumption of steady state, that is, when the system is stabilized and has been reached a constant value of rotor speed for both machines. It was also observed through the Thevenin equations that the magnetizing inductance was the predominant parameter in order to establish the equivalences between both models.

A functional simulation model based on the governing equations of the electromechanical system was developed and an evident similarity to the dynamic response of the RIM was observed, as one can see in the Thrust Vs. Rotor Speed plots (Figure 5.18), compare to the Torque Vs. Rotor Speed of the RIM, in which is also distinguishable a starting value of thrust at the initial stage, after the initial transients have passed, a maximum value of thrust for a certain rotor speed value, and from this point on, a progressive and fast decay of the thrust while the rotor speed keeps moving forward, until it finally reaches the

synchronous speed where the value of thrust will be zero, as no relative motion between the stator magnetic field and the secondary sheet is present.

The best way to cover a vast range of the rotor speed was found by defining an efficiency criterion at which the system would reach the steady state before certain time, which in this case was 2 s. This was developed as a first stage in the control of the LIM, where setting a desired speed of the rotor and reaching it rapidly were the main concerns. In order to achieve this compromise of reaching the reference speed in a small time, was found that the best way was not only by changing the frequency of the source but also the voltage amplitude. For that purpose two demultiplexer blocks were implemented in the simulation model. The first one addressed the lookup table corresponding to the range under which the speed reference of the rotor was covered outputting the optimum value of frequency. The second demultiplexer addressed the value of voltage amplitude corresponding to the speed reference of the rotor (upon defined ranges) necessary for the system to reach the desired conditions.

The most difficult part was on implementing the PI controller for which disturbing forces and sudden changes of reference speeds of the rotor (on the run) had to be overcome by the controller, as the system is highly nonlinear and can lead to instability very easy. Also was found that the conventional tuning methods for the PI controller gains didn't work as expected, so manual calibration based on trial and error was the only way to get acceptable results for limited and specific conditions. This however could be overcome by implementing advanced nonlinear control techniques which is suggested for further work.

## 8 APPENDIXES

### 8.1 Matlab Script from Section 5.4.1, page 38 (interp3.m).

```
clear all;
clc;

x=[10.40 12.14 13.87 15.61 17.34]; % Vs
y=[9.36 10.92 12.48 14.05 15.61]; % Vr
z=[100 200 300 400 500]; %Voltage
c=[221.15 218 148.5 103.2 72 884.64 872 594 414 288 1990.53 1960 1337 932.65 648
3539.6 3490 2375 1657.9 1152 5529.19 5455 3710 2575 1800
0 174 169.3 114.8 81 0 697 676.5 460.5 322 0 1570 1523 1031.5 729 0 2790
2707 1845 1285 0 4360 4230 2871 2015
0 0 138 129.6 92.4 0 0 552 519.5 369.5 0 0 1242 1169 832 0 0 2207
2072 1478.5 0 0 3450 3237 2310
0 0 0 110.8 101.4 0 0 0 442.5 405.5 0 0 0 995.5 914.5 0 0 0 1770
1620 0 0 0 2766 2536
0 0 0 0 89.9 0 0 0 0 360.7 0 0 0 0 811.5 0 0 0 0 1439 0 0
0 0 2254];
v=reshape(c,5,5,5,5); % Thrust

xi=17.34;
yi=15.61;
zi=100:10:500;

Th=interp3(x,y,z,v,xi,yi,zi);
```

```

Th1=[Th(:)]';
Thi=[89.9 360.7 811.5 1439 2254];

Vol=[interp1(Th1,zi,Thi,'spline','extrap')]';

plot(Thi,Vol,'o');
xlabel('Th');
ylabel('Vol');

```

## 8.2 Matlab Script from Section 6.4.3.3, page 93, (MotorParam.m and myfunk.m).

```

clear all;
clc;

global Ws
global Tei
global s
global n
global m
global i
global j

n=input('Specify number of sets required:');
%m=input('Specify number of measures in each set:');
f=input('Specify operation frequency f (Hz):');
%p=input('Specify number of poles p:');
p=4;
Ws=4*pi*f/p; % in [rad/sec]
Te=zeros(n,5);
Tei=zeros(n,5);
s=zeros(n,5);
Vth=zeros(n,1);
Xth=zeros(n,1);
Xr=zeros(n,1);
Rth=zeros(n,1);
Rr=zeros(n,1);

for i=1:1:n %rows
disp(['Specify set values No.' num2str(i) blanks(7) '(T in [lb-in] and
W in [RPM])'])
    for j=1:1:5 %columns

        Te(i,j)=input(['T' num2str(j) ':']); % torque [lb-in]
        Tei(i,j)=Te(i,j)*(4.448222/39.370079); % torque [N.m]
        Nm(i,j)=input(['W' num2str(j) ':']); % mechanical speed [rpm]
        Wm(i,j)=Nm(i,j)*2*pi/60; % angular velocity [rad/s]
        s(i,j)=(Ws-Wm(i,j))/Ws; % slip

    end

end
x0=[255; 1.106; 0.1; 0.1; 0.1];

```

```
options=optimset('Display', 'iter', 'MaxFunEvals', 10000, 'TolX',1e-
20);
[x, fval, exitflag, output]=fsolve(@myfunk, x0, options);
```

```
Vth(i,1)=x(1)
Xth(i,1)=x(2)
Xr(i,1)=x(3)
Rth(i,1)=x(4)
Rr(i,1)=x(5)
```

```
end
```

```
%Averages
Vtha=sum(Vth)/i
Xtha=sum(Xth)/i
Xra=sum(Xr)/i
Rtha=sum(Rth)/i
Rra=sum(Rr)/i
```

myfunk function, (myfunk.m)

```
function F=myfunk(x,Tei,Ws,s)
%function F=myfunk(x, Ws, s)

%{
Vth=x1
Xth=x2
Xr=x3
Rth=x4
Rr=x5
%}

global Ws
global Tei
global s
global n

for i=1:1:n %rows
F=[Tei(i,1)*Ws*((x(4)+x(5)/s(i,1))^2+(x(2)+x(3))^2)-
3*x(1)^2*x(5)/s(i,1);
Tei(i,2)*Ws*((x(4)+x(5)/s(i,2))^2+(x(2)+x(3))^2)-
3*x(1)^2*x(5)/s(i,2);
Tei(i,3)*Ws*((x(4)+x(5)/s(i,3))^2+(x(2)+x(3))^2)-
3*x(1)^2*x(5)/s(i,3);
Tei(i,4)*Ws*((x(4)+x(5)/s(i,4))^2+(x(2)+x(3))^2)-
3*x(1)^2*x(5)/s(i,4);
Tei(i,5)*Ws*((x(4)+x(5)/s(i,5))^2+(x(2)+x(3))^2)-
3*x(1)^2*x(5)/s(i,5)];
End
```

## 8.3 TEST BENCH PROCEDURES

### 8.3.1 Test-Bench Startup Procedure

(Roa, 2010)

#### 8.3.1.1 Special Directions for Operating Dynamometer Test Stand Site Selection

The dynamometer test stand is designed for installation inside a building. The site selected for the installation of this equipment must be free from excessive moisture. An ideal installation would be a concrete pad with a level surface on which the dynamometer would be placed. If the surface is not level, then it will be necessary to insert shims under the base of the dynamometer to avoid distortion of its frame.

#### 8.3.1.2 On-Site Balancing and Alignment

The dynamometer has been aligned at the factory. Proper alignment should be verified at the site prior to start-up.

#### 8.3.1.3 Equipment Ground

The frame of the dynamometer stand and the control panel must be solidly connected to a low resistance path to ground before energization.

#### 8.3.1.4 Wiring the Dynamometer

The dynamometer test stand must be wired in exact accordance with the wiring diagram (Horlick Manual). Prior to initial startup, verify that the electrical installation is correct. A source of power should be brought to the dynamometer motor and a separate source of power should be brought to the motor under test.

The motor under test should also be equipped with a motor start as illustrated on the electric schematic. There are no safety features to protect against faulty installation wiring.

#### 8.3.1.5 Starting/Operating the Dynamometer

After the wiring of the test stand has been checked for wiring accuracy, follow this procedure to start the system.

Position the Main Disconnect Switch to the “On” position.

Depress the “Dyno Motor Start” push button

Once the system is started, the variable frequency drive connected to the dynamometer will automatically ramp the system speed to 1800 RPM. The system speed is displayed on the torque meter.

Once the system has reached 1800 RPM, the motor under test can be started. This motor can be started either locally at the main control panel or locally at the remote motor starter.

Note: the dynamometer must be running and up to speed prior to Starting the motor under test. Under no conditions, should the Motor under test be started without the dynamometer running At 1800 rpm.

Once the motor under test is started, its torque can be tested by varying the speed of the dynamometer motor. There is a potentiometer on the front of the control enclosure that is used for speed control. As you lower the speed of the system, the torque will increase on the motor under test. The system speed should not be lowered below the slip speed of the motor under test.

Once testing is complete, the motor under test should be stopped.

Once it is verified that the motor under test is no longer running, the dynamometer motor can be stopped by depressing the “Dyno Motor Stop” push button.

When work is complete, position the Main Disconnect Switch to the “Off” position.

Danger:

Do not operate test stand unless enclosure of control cubicle and frame of motor-generator are solidly connected to ground.

Do not operate test stand with protective covers removed.

To prevent shock hazard, interrupt the line voltage supplying the test stand prior to performing trouble-shooting or maintenance procedures.

### 8.3.2 Communications Connection Procedure

(Roa, 2010)

- Acquire USB to EIA485 interface described in section 8.3.2.1.
- Install CTSofT in your PC, section 8.3.2.4.
- Check serial communication parameters using the keypad, leave the default values, section 8.3.2.2. and 8.3.2.3.
- Upload or download parameters, section 8.3.2.5.
- Monitor the Unidrive if requires, section 8.3.2.6. or 8.3.2.7.

#### 8.3.2.1 Serial Communications Introduction

The Unidrive SP has a standard 2-wire EIA485 interface (serial communications interface) which enables all drive set-up, operation and monitoring to be carried out with a PC or controller if required. Therefore, it is possible to control the drive entirely by

serial communications without the need for a SM-keypad or other control cabling. The drive supports two protocols selected by parameter configuration:

- Modbus RTU
- CT ANSI

Modbus RTU has been set as the default protocol, as it is used with the PC-tools commissioning/start-up software as provided on the CD ROM. The serial communications port of the drive is a RJ45 socket, which is isolated from the power stage and the other control terminals (see section 4.12 *Serial communications connections* on page 84 for connection and isolation details, User guide).

The communications port applies a 2 unit load to the communications network.

#### USB/EIA232 to EIA485 Communications

An external USB/EIA232 hardware interface such as a PC cannot be used directly with the 2-wire EIA485 interface of the drive. Therefore a suitable converter is required.

Suitable USB to EIA485 and EIA232 to EIA485 isolated converters are available from Control Techniques as follows:

- CT USB Comms cable (CT Part No. 4500-0096)
- CT EIA232 Comms cable (CT Part No. 4500-0087)

When using one of the above converters or any other suitable converter with the Unidrive SP, it is recommended that no terminating resistors be connected on the network. It may be necessary to 'link out' the terminating resistor within the converter depending on which type is used. The information on how to link out the terminating resistor will normally be contained in the user information supplied with the converter.

### 8.3.2.2 Configuration of Serial Communication Parameters Using the Keypad

It is recommended to leave the default parameters. However, in order to change them:

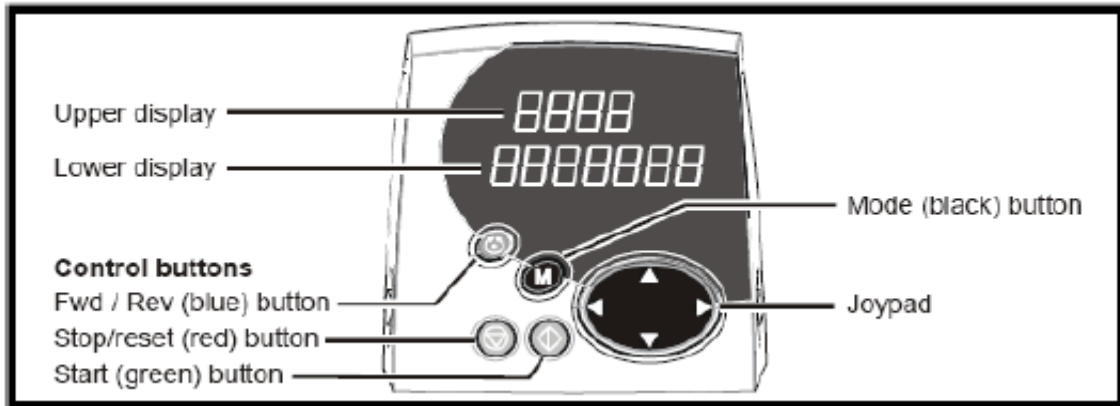


**Figure 8.1. Unidrive Display.**

Control buttons

The keypad consists of:

1. Joypad - used to navigate the parameter structure and change parameter values.
2. Mode button - used to change between the display modes – parameter view, parameter edit, status.
3. Three control buttons - used to control the drive if keypad mode is selected.
4. Help button (SM-Keypad Plus only) - displays text briefly describing the selected parameter. The Help button toggles between other display modes and parameter help mode. The up and down functions on the joypad scroll the help text to allow the whole string to be viewed. The right and left functions on the joypad have no function when help text is being viewed.

The display examples in this section show the SM-Keypad 7 segment LED display.

Saving parameters

When changing a parameter in Menu 0, the new value is saved when pressing the Mode button to return to parameter view mode from parameter edit mode.

If parameters have been changed in the advanced menus, then the change will not be saved automatically. A save function must be carried out.

Procedure:

Enter 1000\* in Pr. xx.00

Either:

- Press the red reset button

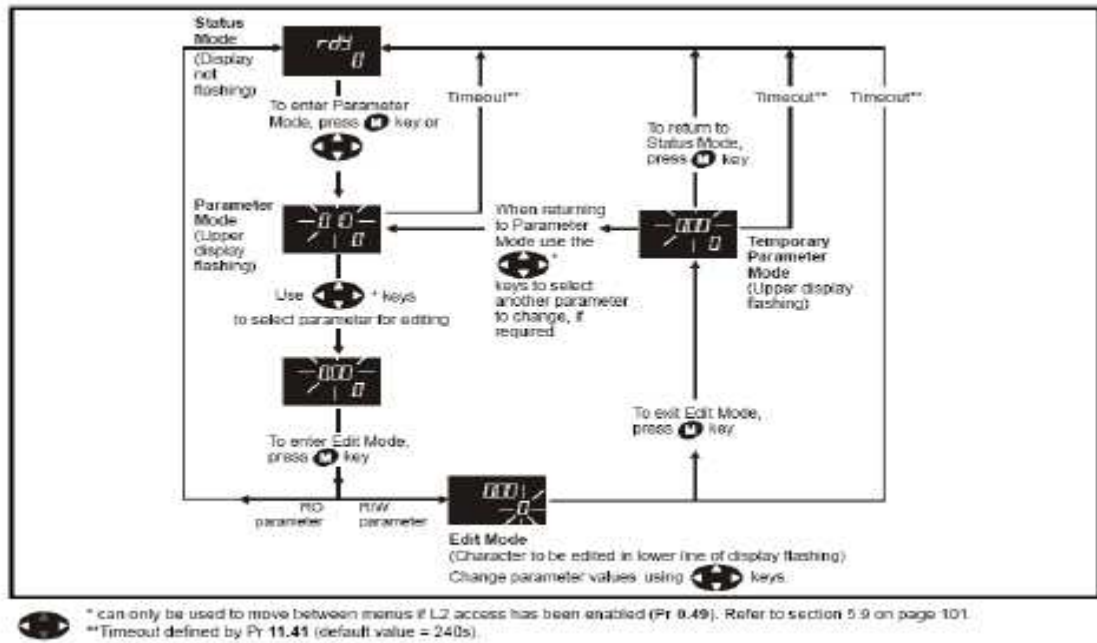


Figure 8.2. Flow chart of Unidrive menus.

- Toggle the reset digital input
- Carry out a drive reset through serial communications by setting Pr 10.38 to 100 (ensure that Pr. xx.00 returns to 0).

\*If the drive is in the under voltage trip state or is being supplied from a low

voltage DC supply, a value of 1001 must be entered into Pr xx.00 to perform a save function.

### 8.3.2.3 Serial Communications Set-Up Parameters

The following parameters need to be set according to the system requirements. In most of the cases the default parameters will work for the purpose of this project.

0.35 {11.24}		Serial mode						
RW	Txt						US	
↕		AnSI (0)			⇒	rtU (1)		
		rtU (1)						

**Table 8.1. Serial mode.**

This parameter defines the communications protocol used by the 485 comms port on the drive. This parameter can be changed via the drive keypad, via a Solutions Module or via the comms interface itself. If it is changed via the comms interface, the response to the command uses the original protocol. The master should wait at least 20ms before send a new message using the new protocol.

(Note: ANSI uses 7 data bits, 1 stop bit and even parity; Modbus RTU uses 8 data bits, 2 stops bits and no parity.)

Comms value	String	Communications mode
0	AnSI	ANSI
1	rtU	Modbus RTU protocol
2	Lcd	Modbus RTU protocol, but with an SM-Keypad Plus only

**Table 8.2. Serial Mode parameters.**

ANSIx3.28 protocol

Modbus RTU protocol, but with an SM-Keypad Plus only This setting is used for disabling communications access when the SSM-Keypad Plus is used as a hardware key.

0.36 {11.25}		Serial communications baud rate						
RW	Txt						US	
↕	300 (0), 600 (1), 1200 (2), 2400 (3), 4800 (4), 9600 (5), 19200 (6), 38400 (7), 57600 (8)*, 115200 (9)*	⇒	19200 (6)					

**Table 8.3. Serial communication baud rate.**

\* only applicable to Modbus RTU mode.

This parameter can be changed via the drive keypad, via a Solutions Module or via the comms interface itself. If it is changed via the comms interface, the response to the command uses the original baud rate. The master should wait at least 20ms before sending a new message using the new baud rate.

Note:

When using the CT EIA232 Comms cable the available baud rate is limited to 19.2k baud.

0.37 {11.23}		Serial communications address						
RW	Txt						US	
↕	0 to 247	⇒	1					

**Table 8.4. Serial communications address.**

Used to define the unique address for the drive for the serial interface. The drive is always a slave.

## Modbus RTU

When the Modbus RTU protocol is used addresses between 0 and 247 are permitted. Address 0 is used to globally address all slaves, and so this address should not be set in this parameter.

## ANSI

When the ANSI protocol is used the first digit is the group and the second digit is the address within a group. The maximum permitted group number is 9 and the maximum permitted address within a group is 9. Therefore, Pr 0.37 is limited to 99 in this mode. The value 00 is used to globally address all slaves on the system, and x0 is used to address all slaves of group x, therefore these addresses should not be set in this parameter.

### 8.3.2.4 Ctsoft

CTSoft is a Windows™ based software commissioning/start-up tool for Unidrive SP and other Control Techniques products. CTSoft can be used for commissioning/start-up and monitoring, drive parameters can be uploaded, downloaded and compared, and simple or custom menu listings can be created.

Drive menus can be displayed in standard list format or as live block diagrams.

CTSoft is able to communicate with a single drive or a network. CTSoft can be found on the CD which is supplied with the drive and is also available for download from [www.controltechniques.com](http://www.controltechniques.com) (file size approximately 25MB).

CTSoft system requirements:

- Windows 2000/XP/Vista. Windows 95/98/98SE/ME/NT4 and

- Windows 2003 server are NOT supported
- Internet Explorer V5.0 or later must be installed
- Minimum of 800x600 screen resolution with 256 colors. 1024x768 is recommended.
- 128MB RAM
- Pentium III 500MHz or better recommended.
- Adobe Acrobat Reader 5.1 or later (for parameter help).
- Microsoft.Net Frameworks 2.0
- Note that you must have administrator rights to install CTSOft.

To install CTSOft from the CD, insert the CD and the auto-run facility should start up the front-end screen from which CTSOft can be selected. Any previous copy of CTSOft should be uninstalled before proceeding with the installation (existing projects will not be lost). Included with CTSOft are the user guides for the supported drive models. When help on a particular parameter is request by the user, CTSOft links to the parameter in the relevant advanced user guide.

#### 8.3.2.5 Uploading and Downloading with CTSOft

CTSOft allows you to change, download or upload different parameters to the Unidrive. In order to upload parameters from Unidrive simply click on the “upload parameters” bottom. When uploading parameters from Unidrive it gathers all the values for each parameter on each menu (Figure 8.3).

To change or modify parameters first edit them (depending on the menu or the parameter, check page 106 of user guide for a list of basic parameters) in the subfolder “parameters” and then download them into the Unidrive.

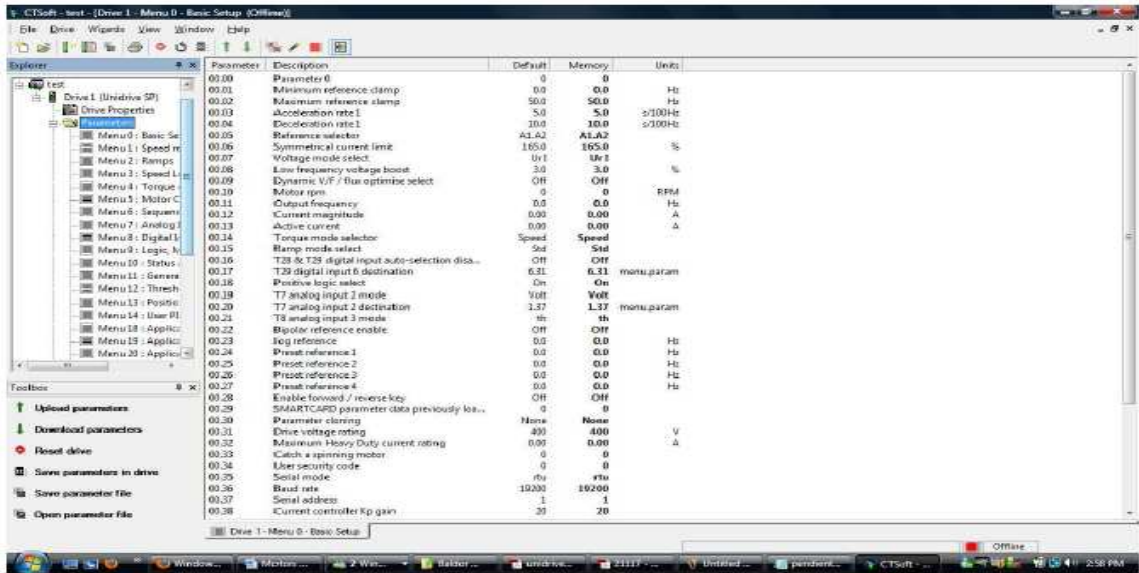


Figure 8.3. CTSOft interface.

### 8.3.2.6 Monitoring Unidrive

0.10 {5.04}		Estimated motor speed						
RO	Bit	FI				NC	PT	
OL	↕	±180,000 rpm			⇒			

Table 8.5. Estimated motor speed.

Open-loop

Pr 0.10 (5.04) indicates the value of motor speed that is estimated from the following:

0.12 Post-ramp frequency reference

0.42 Motor - no. of poles.

0.10 {3.02}		Motor speed							
RO	BI	FI				NC	PT		
VT	↕	±Speed_max rpm			⇒				

**Table 8.6. Motor speed.**

Closed-loop

Pr 0.10 (3.02) indicates the value of motor speed that is obtained from the speed feedback.

0.11 {5.01}		Drive output frequency							
RO	BI	FI				NC	PT		
OL	↕	±SPEED_FREQ_MAX Hz			⇒				
VT	↕	±1250.0 Hz			⇒				

**Table 8.7. Drive output frequency.**

Open-loop & closed loop vector

Pr 0.11 displays the frequency at the drive output.

0.11 {3.29}		Drive encoder position							
RO	Uni	FI				NC	PT		
SV	↕	0 to 65,535 1/2 <sup>16</sup> ths of a revolution			⇒				

**Table 8.8. Drive encoder position.**

### 8.3.2.7 CTScope

CTScope is a full featured software oscilloscope for viewing and analyzing changing values within the drive. The time base can be set to give high speed capture for tuning or intermittent capture for longer term trends. The interface is based on a traditional oscilloscope, making it familiar to engineers across the globe.

CTScope is free of charge and can be obtained from:

[http://www.emersonct.com/products/ac\\_drives/unidrive\\_sp\\_high\\_performance/software.a](http://www.emersonct.com/products/ac_drives/unidrive_sp_high_performance/software.a)  
spx.

### 8.3.3 Running the motors

(Roa, 2010)

- Check motor parameters using the keypad, section 8.3.3.1.
- Modify or adjust parameters accordingly, same steps than section 8.3.2.2.
- If motor parameters are not available, see auto-tuning, section 8.3.3.4.
- Check or select operational mode, section 8.3.3.2.
- Check basic requirements, section 8.3.3.3.
- Set the proper speed reference, section 8.3.3.5.
- Start the motors with the start bottom of the main panel.

#### 8.3.3.1 Motor Parameters

0.42 {5.11}		No. of motor poles						
RW	Txt						US	
OL	⇅	0 to 60 (Auto to 120 Pole)			⇒	Auto (0)		
CL	⇅				⇒	VT	Auto (0)	
						SV	6 POLE (3)	

**Table 8.9. Number of motor poles.**

Open-loop

This parameter is used in the calculation of motor speed, and in applying the correct slip compensation. When auto is selected, the number of motor poles is automatically

calculated from the rated frequency (Pr 0.47) and the rated full load rpm (Pr 0.45). The number of poles =  $120 * \text{rated frequency} / \text{rpm}$  rounded to the nearest even number.

Closed-loop vector

This parameter must be set correctly for the vector control algorithms to operate correctly. When auto is selected, the number of motor poles is automatically calculated from the rated frequency (Pr 0.47) and the rated full load rpm (Pr 0.45). The number of poles =  $120 * \text{rated frequency} / \text{rpm}$  rounded to the nearest even number.

0.43 {5.10}		Motor rated power factor					
RW	Uni						US
OL	↕	0.000 to 1.000			⇒	0.850	
VT	↕				⇒		

**Table 8.10. Motor rated power factor.**

The power factor is the true power factor of the motor, i.e. the angle between the motor voltage and current.

Open-loop

The power factor is used in conjunction with the motor rated current (Pr 0.46) to calculate the rated active current and magnetizing current of the motor. The rated active current is used extensively to control the drive, and the magnetizing current is used in vector mode Rs compensation. It is important that this parameter is set up correctly.

This parameter is obtained by the drive during a rotational autotune. If a stationary autotune is carried out, then the nameplate value should be entered in Pr 0.43.

Closed-loop vector

If the stator inductance (Pr 5.25) contains a non-zero value, the power factor used by the drive is continuously calculated and used in the vector control algorithms (this will not update Pr 0.43).

If the stator inductance is set to zero (Pr 5.25) then the power factor written in Pr 0.43 is used in conjunction with the motor rated current and other motor parameters to calculate the rated active and magnetizing currents which are used in the vector control algorithm.

This parameter is obtained by the drive during a rotational autotune. If a stationary autotune is carried out, then the nameplate value should be entered in Pr 0.43.

<b>0.43 {3.25}</b>		<b>Encoder phase angle</b>							
RW	Uni							US	
SV	↕	0.0 to 359.9°				⇒	0.0		

**Table 8.11. Encoder phase angle.**

The phase angle between the rotor flux in a servo motor and the encoder position is required for the motor to operate correctly. If the phase angle is known it can be set in this parameter by the user.

Alternatively the drive can automatically measure the phase angle by performing a phasing test (see autotune in servo mode Pr 0.40). When the test is complete the new value is written to this parameter. The encoder phase angle can be modified at any time and becomes effective immediately. This parameter has a factory default value of 0.0, but is not affected when defaults are loaded by the user.

0.44 {5.09}		Motor rated voltage					
RW	Uni				RA		US
↕		0 to AC_VOLTAGE_SET_MAX V			⇒	200V drive: 230 400V drive: EUR> 400 USA> 460 575V drive: 575 690V drive: 690	

**Table 8.12. Motor rated voltage.**

Open-loop & Closed-loop vector

Enter the value from the rating plate of the motor.

0.45 {5.08}		Motor rated full load speed (rpm)					
RW	Uni						US
OL	↕	0 to 180,000 rpm			⇒	EUR> 1,500 USA> 1,800	
VT	↕	0.00 to 40,000.00 rpm			⇒	EUR> 1,450.00 USA> 1,770.00	

**Table 8.13. Motor rated full load speed (RPM).**

Open-loop

This is the speed at which the motor would rotate when supplied with its base frequency at rated voltage, under rated load conditions (=synchronous speed - slip speed). Entering the correct value into this parameter allows the drive to increase the output frequency as a function of load in order to compensate for this speed drop.

Slip compensation is disabled if Pr 0.45 is set to 0 or to synchronous speed, or if Pr 5.27 is set to 0. If slip compensation is required this parameter should be set to the value from the rating plate of the motor, which should give the correct rpm for a hot machine. Sometimes it will be necessary to adjust this when the drive is commissioned because the nameplate value may be inaccurate.

Slip compensation will operate correctly both below base speed and within the field weakening region. Slip compensation is normally used to correct for the motor speed to

prevent speed variation with load. The rated load rpm can be set higher than synchronous speed to deliberately introduce speed droop. This can be useful to aid load sharing with mechanically coupled motors.

#### Closed loop vector

Rated load rpm is used with motor rated frequency to determine the full load slip of the motor which is used by the vector control algorithm.

Incorrect setting of this parameter can result in the following:

- Reduced efficiency of motor operation
- Reduction of maximum torque available from the motor
- Failure to reach maximum speed
- Over-current trips
- Reduced transient performance
- Inaccurate control of absolute torque in torque control modes

The nameplate value is normally the value for a hot machine, however, some adjustment may be required when the drive is commissioned if the nameplate value is inaccurate.

The rated full load rpm can be optimized by the drive (For further information, refer to section 8.1.3 Closed loop vector motor control on page 135, user guide).

0.46 {5.07}		Motor rated current					
RW	Uni				RA		US
↕		0 to Rated_current_max A			⇒	Drive rated current [11.32]	

**Table 8.14. Motor rated current.**

Enter the name-plate value for the motor rated current.

0.47 {5.06}		Rated frequency					
RW	Uni					US	
OL	⇅	0 to 3,000.0Hz			⇒	EUR> 50.0, USA> 60.0	
VT	⇅	0 to 1,250.0Hz			⇒	EUR> 50.0, USA> 60.0	

**Table 8.15. Rated frequency.**

Open-loop & Closed-loop vector

Enter the value from the rating plate of the motor.

### 8.3.3.2 Operating-Mode Selection

0.48 {11.31}		Operating mode selector					
RW	Txt	NC			PT		
⇅		1 to 4			⇒	OL	1
						VT	2
						SV	3

**Table 8.16. Operating mode selector.**

The settings for Pr 0.48 are as follows:

Setting		Operating mode
OPEn LP	1	Open-loop
CL VECT	2	Closed-loop vector
SerVO	3	Servo
rEgEn	4	Regen

**Table 8.17. Operating mode selector settings.**

This parameter defines the drive operating mode. Pr xx.00 must be set to 1253 (European defaults) or 1254 (USA defaults) before this parameter can be changed. When the drive is reset to implement any change in this parameter, the default settings of all parameters will be set according to the drive operating mode selected and saved in memory.

### 8.3.3.3 Quick Start Connections

#### 8.3.3.3.1 Basic Requirements

This section shows the basic connections which must be made for the drive to run in the required mode. For minimal parameter settings to run in each mode please see the relevant part of section 7.3 Quick Start commissioning/start-up, page 122 (user guide (Control Techniques, 2007)).

Drive control method	Requirements
Terminal mode	Drive Enable Speed reference Run forward or run reverse command
Keypad mode	Drive Enable
Serial communications	Drive Enable Serial communications link

**Table 8.18. Min. connection requirements for each control mode.**

Operating mode	Requirements
Open loop mode	Induction motor
Closed loop vector - RFC mode	Induction motor
Closed loop vector mode	Induction motor with speed feedback
Closed loop servo mode	Permanent magnet motor with speed and position feedback

**Table 8.19. Min. connection requirements for each mode of operation.**

Speed feedback

Suitable devices are:

- Incremental encoder (A, B or F, D with or without Z)
- Incremental encoder with forward and reverse outputs (F, R with or without Z)

- SINCOS encoder (with, or without Stegmann Hiperface, EnDat or SSI communications protocols)
- EnDat absolute encoder

### 8.3.3.4 Autotune

0.40 {5.12}		Autotune								
RW	Uni									
OL	↕	0 to 2				⇒	0			
VT	↕	0 to 4				⇒	0			
SV	↕	0 to 6				⇒	0			

**Table 8.20. Autotune.**

#### Open-Loop

There are two autotune tests available in open loop mode, a stationary and a rotating test. A rotating autotune should be used whenever possible, so the measured value of power factor of the motor is used by the drive.

- The stationary autotune can be used when the motor is loaded and it is not possible to remove the load from the motor shaft.
- A rotating autotune first performs a stationary autotune, before rotating the motor at 2/3 base speed in the forward direction for several seconds. The motor must be free from load for the rotating autotune.

To perform an autotune, set Pr **0.40** to 1 for a stationary test or 2 for a rotating test, and provide the drive with both an enable signal (on terminal 31) and a run signal (on terminal 26 or 27).

Following the completion of an autotune test the drive will go into the inhibit state. The drive must be placed into a controlled disable condition before the drive can be made to

run at the required reference. The drive can be put in to a controlled disable condition by removing the SAFE TORQUE OFF (SECURE DISABLE) signal from terminal 31, setting the drive enable parameter Pr **6.15** to OFF (0) or disabling the drive via the control word (Pr **6.42** & Pr **6.43**). For further information refer to section *Pr 0.40 {5.12} Autotune* on page 130 user guide (Control Techniques, 2007).

#### Closed-loop

There are three autotune tests available in closed loop vector mode, a stationary test, a rotating test and an inertia measurement test. A stationary autotune will give moderate performance whereas a rotating autotune will give improved performance as it measures the actual values of the motor parameters required by the drive. An inertia measurement test should be performed separately to a stationary or rotating autotune.

- The stationary autotune can be used when the motor is loaded and it is not possible to remove the load from the motor shaft.
- A rotating autotune first performs a stationary autotune, before rotating the motor at  $2/3$  base speed in the forward direction for approximately 30 seconds. The motor must be free from load for the rotating autotune.
- The inertia measurement test can measure the total inertia of the load and the motor. This is used to set the speed loop gains (see *Speed loop gains*, user guide) and to provide torque feed forwards when required during acceleration. During the inertia measurement test the motor speed changes from  $1/3$  to  $2/3$  rated speed in the forward direction several times.

The motor can be loaded with a constant torque load and still give an accurate result, however, non-linear loads and loads that change with speed will cause measurement errors.

To perform an autotune, set Pr **0.40** to 1 for a stationary test, 2 for a rotating test, or 3 for an inertia measurement test and provide the drive with both an enable signal (on terminal 31) and a run signal (on terminal 26 or 27).

Following the completion of an autotune test the drive will go into the inhibit state. The drive must be placed into a controlled disable condition before the drive can be made to run at the required reference. The drive can be put in to a controlled disable condition by removing the SAFE TORQUE OFF (SECURE DISABLE) signal from terminal 31, setting the drive enable parameter Pr **6.15** to OFF (0) or disabling the drive via the control word (Pr **6.42** & Pr **6.43**).

Setting Pr **0.40** to 4 will cause the drive to calculate the current loop gains based on the previously measured values of motor resistance and inductance. The drive does apply any voltage to the motor during this test. The drive will change Pr **0.40** back to 0 as soon as the calculations are complete (approximately 500ms). For further information refer to section *Pr 0.40 {5.12} Autotune* on page 133, user guide (Control Techniques, 2007).

### 8.3.3.5 Speed Reference

#### 8.3.3.5.1 Speed Limits

Open-loop

Set Pr 0.01 at the required minimum output frequency of the drive for both directions of rotation. The drive speed reference is scaled between Pr 0.01 and Pr 0.02. [0.01] is a nominal value; slip compensation may cause the actual frequency to be higher.

0.01 {1.07}		Minimum reference clamp								
RW	BI						PT	US		
OL	↕	±3,000.0Hz				⇒	0.0			
CL	↕	±SPEED_LIMIT_MAX Hz/rpm				⇒	0.0			

**Table 8.21. Minimum reference clamp.**

When the drive is jogging, [0.01] has no effect.

Closed-loop

Set Pr 0.01 at the required minimum motor speed for both directions of rotation. The drive speed reference is scaled between Pr 0.01 and Pr 0.02.

0.02 {1.06}		Maximum reference clamp								
RW	Uni							US		
OL	↕	0 to 3,000.0Hz				⇒	EUR> 50.0 USA> 60.0			
CL	↕	SPEED_LIMIT_MAX Hz/rpm	⇒	VT	EUR> 1,500.0 USA> 1,800.0					
				SV	3,000.0					

**Table 8.22. Maximum reference clamp.**

The drive has additional over-speed protection.

Open-loop

Set Pr 0.02 at the required maximum output frequency for both directions of rotation. The drive speed reference is scaled between Pr 0.01 and Pr 0.02. [0.02] is a nominal value; slip compensation may cause the actual frequency to be higher.

Closed-loop

Set Pr 0.02 at the required maximum motor speed for both directions of rotation. The drive speed reference is scaled between Pr 0.01 and Pr 0.02.

For operating at high speeds see section 8.6 High speed operation on page 141, user guide.

### 8.3.3.5.2 Reaching the Speed.

#### Open-loop

When the drive is enabled with Pr 0.33 = 0, the output frequency starts at zero and ramps to the required reference. When the drive is enabled when Pr 0.33 has a non-zero value, the drive performs a start-up test to determine the motor speed and then sets the initial output frequency to the synchronous frequency of the motor. Restrictions may be placed on the frequencies detected by the drive as follows:

<b>0.33 {6.09}</b>		<b>Catch a spinning motor</b>							
RW	Uni							US	
OL	↕	0 to 3				⇒	0		

Table 8.23. Catch a spinning motor.

Pr 0.33	Function
0	Disabled
1	Detect all frequencies
2	Detect positive frequencies only
3	Detect negative frequencies only

Table 8.24. Catch a spinning motor settings.

<b>0.33 {5.16}</b>		<b>Rated rpm autotune</b>					
RW	Uni						US
VT	↕	0 to 2			⇒	0	

**Table 8.25. Rated rpm autotune.**

Closed-loop vector

The motor rated full load rpm parameter (Pr 0.45) in conjunction with the motor rated frequency parameter (Pr 0.46) defines the full load slip of the motor. The slip is used in the motor model for closed-loop vector control.

The full load slip of the motor varies with rotor resistance which can vary significantly with motor temperature. When Pr 0.33 is set to 1 or 2, the drive can automatically sense if the value of slip defined by Pr 0.45 and Pr 0.46 has been set incorrectly or has varied with motor temperature. If the value is incorrect parameter Pr 0.45 is automatically adjusted. The adjusted value in Pr 0.45 is not saved at power-down. If the new value is required at the next power-up it must be saved by the user.

Automatic optimization is only enabled when the speed is above 12.5% of rated speed, and when the load on the motor load rises above 62.5% rated load.

Optimization is disabled again if the load falls below 50% of rated load.

For best optimization results the correct values of stator resistance (Pr 5.17), transient inductance (Pr 5.24), stator inductance (Pr 5.25) and saturation breakpoints (Pr 5.29, Pr 5.30) should be stored in the relevant parameters.

These values can be obtained by the drive during an autotune (see Pr 0.40 for further details).

Rated rpm auto-tune is not available if the drive is not using external position/speed feedback.

The gain of the optimizer, and hence the speed with which it converges, can be set at a normal low level when Pr 0.33 is set to 1. If this parameter is set to 2 the gain is increased by a factor of 16 to give faster convergence.

## 9 BIBLIOGRAPHY

Ang, K.H. (2005). *PID control system analysis, design, and technology*. IEEE Transactions on Control Systems Technology 13(4):pp. 559-576.

Boucheta, A. (2010). *Adaptive backstepping controller for linear induction motor position control*. *COMPEL : The International Journal for Computation and Mathematics in Electrical and Electronic Engineering*, Vol. 29, No. 3, pp. 789 - 810, Emerald Group Publishing Limited.

Chapman, S. (1999). *Electric Machinery Fundamentals*. New York: McGraw-Hill.

Control Techniques. (2007). *User Guide Unidrive Models size 0 to 6*. Emerson Industrial Automation.

Doyle, M. *Electromagnetic Aircraft Launch System - EMALS*. Naval Air Warfare Center, Aircraft Division, Lakehurst, NJ 08733.

Duncan, J. (1983). *Linear induction motor – equivalent circuit model*. *IEE Proc. Electric Power applications*, Vol. 130, No. 1, pp. 51 – 57.

Meeker, D. *Indirect Vector Control of a Redundant Linear Induction Motor for Aircraft Launch*. NAVAIR Public Release 08-642.

Nowak, L. (2001). *Movement simulation in 3D eddy current transient problem*. *COMPEL : The International Journal for Computation and Mathematics in Electrical and Electronic Engineering*, Vol. 20, No. 1, 2001, pp. 293 – 302, MCB University Pres

Ogata, K. (2002). *Modern Control Engineering*. New Jersey: Prentice Hall.

Pai, R. (1988). *A complete equivalent circuit of a linear induction motor with sheet secondary. IEEE Trans. Magnetics*, Vol. 24, No. 1, Jan. 1988, pp. 639 – 654.

Roa, C. (2010). *Electric Motor Control System with Application to Marine Propulsion*. MSc Thesis Dissertation, Department of Ocean and Mechanical Engineering, Florida Atlantic University, Florida.

Xiros, N. (2010). *Nonlinear Modeling of Linear Induction Machines for Analysis and Control of Novel Electric Warship Subsystems*.